Investigating the host range of *Neoromicia capensis* coronavirus *in vitro*

by

Andrea Kotzé

Thesis presented in fulfilment of the requirements for the degree of Master of Sciences in the Faculty of Medicine and Health Science at Stellenbosch University

Supervisor: Prof. Wolfgang Preiser

Co-supervisor: Dr Tasnim Suliman

April 2019

Declaration

By submitting this thesis electronically, I declare that the entirety of the work contained therein is my own, original work, that I am the sole author thereof (save to the extent explicitly otherwise stated), that reproduction and publication thereof by Stellenbosch University will not infringe any third party rights and that I have not previously in its entirety or in part submitted it for obtaining any qualification.

Date: April 2019

Abstract

Coronaviruses are known to cause disease in humans and animals. Two important human coronaviruses that have caused epidemics are severe acute respiratory syndrome coronavirus (SARS-CoV) and Middle East respiratory syndrome coronavirus (MERS-CoV). These coronaviruses originated in animals and were introduced into the human population through zoonotic transmission.

Neoromicia capensis coronavirus (NeoCoV), a bat coronavirus that was discovered in the South African bat species *Neoromicia capensis*, is 85.5% genetically identical to MERS-CoV. It is believed that NeoCoV is an ancestor of MERS-CoV; however, the potential for NeoCoV to emerge as a potential zoonotic agent has not yet been investigated. This study investigated the host range of NeoCoV in order to assess its potential to cross the species barrier from bats to other mammals.

This study attempted to isolate NeoCoV in cell culture to investigate its behaviour *in vitro*. The host range of NeoCoV was further explored by developing viral pseudoparticles that expressed the spike proteins of NeoCoV, MERS-CoV or SARS-CoV. These pseudoparticles were used to infect various cell lines of mammalian origin to determine which animal species NeoCoV may be able to infect and if its host range has any similarities to that of MERS- and/or SARS-CoV.

Attempts were made to isolate NeoCoV in cell culture by inoculating host-derived cells with NeoCoV-positive bat faecal homogenate. Attempts were proven unsuccessful by a highly sensitive quantitative reverse transcription polymerase chain reaction assay.

Infecting cell lines with pseudoparticles bearing either the NeoCoV, MERS- or SARS-CoV spike protein revealed that NeoCoV could possibly utilise *N. capensis* kidney cells for replication, and not the lungs or trachea. Infection of *Pipistrellus pipistrellus* kidney cells with the three different pseudotypes yielded low levels of infection, suggesting that this cell line is less susceptible to infection by the three viruses. None of the pseudotypes generated were able to infect a kidney cell line derived from *Camelus dromedarius*, a known host of MERS-CoV, indicating that camel kidney cells are likely not the site of MERS-CoV replication. Results from pseudoparticle infection experiments suggest that NeoCoV would have the ability to infect Vero cells, which originate from African green monkey kidneys, with the same efficiency as MERS- and SARS-CoV.

Since pseudoparticles bearing the spike protein of NeoCoV have the ability to infect Vero cells, NeoCoV might have the ability to cross the species barrier from its natural host to non-human

primates such as *Cercopithecus aethiops*. As the human population encroaches on wildlife habitats, the transmission of viruses capable of crossing the species barrier becomes an increasing risk to public health.

Opsomming

Coronavirusse veroorsaak siektes in mense en diere. Twee prominente menslike coronavirusse, erge akute respiratoriese sindroomcoronavirus (SARS-CoV) en Midde-Ooste respiratoriese sindroomcoronavirus (MERS-CoV), het epidemies in mense veroorsaak. Hierdie virusse is van diergashere afkomstig en het die menslike bevolking deur zoönotiese oordrag binnegedring.

Neoromicia capensis-coronavirus (NeoCoV), 'n vlermuiscoronavirus wat in die Suid-Afrikaanse vlermuisspesie *Neoromicia capensis* ontdek is, is 85.5% geneties identies aan MERS-CoV. Daar word vermoed dat NeoCoV 'n voorouer van MERS-CoV is; NeoCoV se potensiaal om as zoönotiese agent op te tree, is egter nog nie ondersoek nie. Hierdie studie het die gasheeromvang van NeoCoV ondersoek in 'n poging om die virus se potensiaal om die grens van vlermuise na ander soogdiere oor te steek, te evalueer.

Die studie het gepoog om NeoCoV in selkultuur te isoleer om die gedrag van die virus *in vitro* te bestudeer. Die gasheeromvang van NeoCoV is verder ondersoek deur virale pseudopartikels wat die uitsteekselproteïene van NeoCoV, MERS-CoV of SARS-CoV op hul oppervlak uitdruk, te ontwikkel. Hierdie pseudopartikels is gebruik om verskeie sellyne van soogdieroorsprong te infekteer om vas te stel of NeoCoV oor die vermoë om hierdie selle binne te gaan, beskik, en of die virus se gasheeromvang enige ooreenkomste met dié van MERS- en/of SARS-CoV toon.

Daar is gepoog om NeoCoV in selkultuur te isoleer deur selle afkomstig van die gasheer met NeoCoV-positiewe vlermuisontlastingshomogenaat te inokuleer. Pogings is deur 'n hoogs sensitiewe kwantitatiewe trutranskripsie-polimerasekettingreaksie-toets onsuksesvol bewys.

Die infektering van sellyne met pseudopartikels wat die NeoCoV-, MERS-CoV of SARS-CoV-uitsteekselproteïen uitdruk, het geopenbaar dat NeoCoV moontlik *N. capensis*-nierselle, en nie die longe of trachea nie, vir replisering gebruik. Infektering van *Pipistrellus pipistrellus*-nierselle met die drie pseudotipes het lae vlakke van infeksie gelewer, wat suggereer dat die sellyn minder vatbaar vir infeksie deur die drie virusse is. Geeneen van die gegenereerde pseudotipes kon 'n sellyn wat afkomstig is van *Camelus dromedarius*, 'n bevestigde MERS-CoV-gasheer, infekteer nie, wat aandui dat kameelnierselle waarskynlik nie die repliseringsetel van MERS-CoV is nie. Pseudopartikelinfekteringsresultate dui daarop dat NeoCoV die vermoë het om Vero-selle, wat van Afrikaanse groenaapnier afkomstig is, met dieselfde doeltreffendheid as MERS- en SARS-CoV te infekteer.

Aangesien pseudopartikels wat die uitsteekselproteïene van NeoCoV uitdruk die vermoë het om Vero-selle te infekteer, mag NeoCoV moontlik oor die vermoë om die spesiegrens van sy

natuurlike gasheer na nie-menslike primate soos *Cercopithecus aethiops* oor te steek, beskik. Soos die menslike bevolking inbreuk maak op diere se habitat, word die oordrag van virusse wat die spesiegrens kan oorsteek ‘n groter risiko vir openbare gesondheid.

Acknowledgements

Thank you to my supervisor, Prof. Wolfgang Preiser, and my co-supervisor, Dr Tasnim Suliman, for their guidance throughout my project.

Thank you to Prof. Gert van Zyl, Dr Richard Glashoff, Dr Ndapewa Ithete, Dr Nadine Cronjé, Mrs Karlien Barnard and Ms Bronwyn Kleinhans for assistance regarding laboratory work and/or theoretical aspects of my project. Furthermore, to Dr Nadine Cronjé for the effort she took to assist me in editing my thesis. Thank you to Dr Markus Hoffmann of the German Primate Center (Göttingen, Germany) for providing protocols regarding the pseudoparticle aspect of my project, and for giving suggestions on the optimisation of protocols, providing extra information on technical aspects and for input in the writing of my thesis.

I thank Dr Markus Hoffmann and Prof. Dr Georg Herrler of the University of Veterinary Medicine Hannover (Hannover, Germany) for providing the stock used in pseudoparticle propagation.

Thank you to Prof. Dr Christian Drosten and his research group at Charité University Hospital for providing the BHK-21 (G43), CaKi, PipNi, Vero E6 and Vero EMK cells, empty plasmid and plasmids carrying the VSV-G, MERS-S, NCV-S and SARS-S inserts.

I extend my gratitude towards the Poliomyelitis Research Foundation for providing funding for my postgraduate studies and funding for my project. Furthermore, to the National Health Laboratory Service Research Trust, Harry Crossley Foundation, National Research Foundation and German Research Foundation for funding this project.

Thank you to Mr Jan de Wit and Mrs Michelle Tango for technical assistance and moral support.

I extend my appreciation to Dr Corena de Beer for providing moral support and always having the students of the Division of Medical Virology's best interests at heart.

Thank you to the students at the Division of Medical Virology for their constant support and motivation. A special thanks to Bronwyn Kleinhans, Danielle Cupido, Jamie Saayman, Shannon Kiewitz, Olivette Varathan, Gadean Brecht, Karlien Barnard and Ansia van Coller for their encouragement and sound advice.

I extend my gratitude towards my parents, brother, extended family and friends. This would not have been possible without their constant support, love and encouragement.

Lastly, thank you to my Lord and Saviour, who gave me the strength and courage to make it this far.

Table of Contents

List of Abbreviations

ACE2	Angiotensin-converting enzyme 2
Arg tag	Polyarginine tag
BCoV	Bovine coronavirus
BHK	Baby hamster kidney
BLAST	Basic Local Alignment Search Tool
bp	Base pair
CAF	Central Analytical Facility
CaKi	Camel kidney
cDNA	Complementary deoxyribonucleic acid
CHO	Chinese hamster ovaries
CPE	Cytopathic effect
DAPI	4’,6-diamidino-2-phenylindole, dihydrochloride
DEPC-treated	Diethylpyrocarbonate-treated
DMEM	Dulbecco's Modified Eagle Medium
DMSO	Dimethyl sulfoxide
DNA	Deoxyribonucleic acid
dNTP	Deoxyribonucleotide triphosphate
DPP4	Dipeptidyl peptidase 4
E protein	Envelope protein
EV	Empty vector
FBS	Foetal bovine serum
FECV	Feline enteric coronavirus
FIPV	Feline infectious peritonitis virus
GFP	Green fluorescent protein
h.p.i.	Hours post-infection
HCoV	Human coronavirus
HEK	Human embryonic kidney
His tag	Polyhistidine tag
IBV	Infectious bronchitis virus
IDT	Integrated DNA Technologies
IPTG	Isopropyl β-D-1-thiogalactopyranoside
LB	Lysogeny broth

M protein	Membrane protein
MDBK	Madin-Darby bovine kidney
MDCK	Madin-Darby canine kidney
MERS-CoV	Middle East respiratory syndrome coronavirus
MHV	Mouse hepatitis virus
MOI	Multiplicity of infection
mRNA	Messenger ribonucleic acid
N protein	Nucleocapsid protein
NCBI	National Center for Biotechnology Information
NCK	*Neoromicia capensis* kidney
NCL	*Neoromicia capensis* lung
NCT	*Neoromicia capensis* trachea
NEAA	Non-essential amino acids
NeoCoV	*Neoromicia capensis* coronavirus
ORF	Open reading frame
PBS	Phosphate buffered saline
PCR	Polymerase chain reaction
PEDV	Porcine epidemic diarrhoea virus
PK	Porcine kidney
ppEV	Pseudoparticles bearing no surface antigens
ppMERS-S	Pseudoparticles bearing MERS-CoV spike protein
ppNCV-S	Pseudoparticles bearing NeoCoV spike protein
ppSARS-S	Pseudoparticles bearing SARS-CoV spike protein
ppVSV-G	Pseudoparticles bearing VSV-G
RBD	Receptor binding domain
RdRp	RNA-dependent RNA polymerase
RNA	Ribonucleic acid
RT	Reverse transcription
RT-PCR	Reverse transcription polymerase chain reaction
RT-qPCR	Quantitative reverse transcription polymerase chain reaction
S protein	Spike protein
S1	Subunit 1
S2	Subunit 2
SARS-CoV	Severe acute respiratory syndrome coronavirus

SB	Sodium boric acid
SEAP	Secreted alkaline phosphatase
TCV	Turkey coronavirus
TGEV	Transmissible gastroenteritis coronavirus
Trypsin-EDTA	Trypsin-ethylenediaminetetraacetic acid
UK	United Kingdom
USA	United States of America
VSV	Vesicular stomatitis virus
VSV-G	Vesicular stomatitis virus glycoprotein
VTM	Viral transport medium
X-gal	5-bromo-4-chloro-3-indolyl-D-galactopyranoside

List of Figures

List of Tables

CHAPTER 1

1 Introduction

1.1 Background

1.1.1 Coronaviruses

1.1.1.1 Coronaviruses in humans and animals

Coronaviruses have been known to infect humans and other mammals on a large scale (Masters, 2006; Banerjee *et al.*, 2018). Various epidemics caused by coronaviruses, such as that of Middle East respiratory syndrome coronavirus (MERS-CoV) (Zaki *et al.*, 2012) and severe acute respiratory syndrome coronavirus (SARS-CoV) (Drosten *et al.*, 2003), have been observed over the years. Both of these virus outbreaks have been linked to zoonotic transmission events, i.e. events where diseases are transmitted from animal hosts to humans.

Neoromicia capensis coronavirus (NeoCoV) was discovered in the Cape serotine bat, *Neoromicia capensis*, in South Africa in 2013 (Ithete *et al.*, 2013; Corman *et al.*, 2014). Phylogenetic analysis of the viral genome revealed that it is 85.5% identical to MERS-CoV. MERS-CoV-related viruses have since been detected in other samples from the same bat species (Cronjé, 2017). The relatedness of these viruses leads to the assumption that NeoCoV might be an ancestral virus of MERS-CoV (Corman *et al.*, 2014).

1.1.1.2 Coronavirus spike protein

The coronavirus genome encodes four major proteins, namely the spike (S), envelope (E), membrane (M) and nucleocapsid (N) proteins (Masters, 2006). The S protein is responsible for the binding to, and fusion with, host cells (Masters, 2006). The S protein consists of subunits 1 (S1) and 2 (S2) (Masters, 2006). S1 contains the receptor binding domain (RBD) and is responsible for the binding of the viral particle to host cell receptors, whereas S2 enables the fusion of viral particles with the host cell. As this protein is responsible for viral entry into host cells, its structure is of significance when describing the host range of coronaviruses.

1.1.2 Pseudoparticles

Pseudoparticles are replication-deficient viral particles that bear the surface antigen(s) of other viruses (Tani *et al.*, 2012). Pseudoparticles are used in instances where it is not possible to study the surface antigen of interest when expressed by the virus of origin due to safety concerns and/or difficulties with isolating or propagating the virus itself in order to investigate its behaviour in cell culture further (Tani *et al.*, 2012).

1.1.3 Rationale

The NeoCoV genome shares 85.5% homology with that of MERS-CoV (Ithete *et al.*, 2013; Corman *et al.*, 2014). Since the host-switching abilities of NeoCoV remain unknown, similarities between the host ranges of NeoCoV and MERS-CoV have not yet been explored. Therefore, strategies to determine which cell lines are susceptible to NeoCoV need to be developed.

The ability of a virus to infect a cell is highly dependent on its receptor (de Haan & Rottier, 2005; Masters, 2006; Hoffmann *et al.*, 2013). The receptor for MERS-CoV was identified as dipeptidyl peptidase 4 (DPP4) (Raj *et al.*, 2013), an enzyme involved in the metabolism of glucose (Vlieger & De Meester, 2018). This receptor is expressed by many cell lines, such as Vero cells (Zaki *et al.*, 2012; Raj *et al.*, 2014), *P. pipistrellus* kidney cells (Cui *et al.*, 2013; Raj *et al.*, 2014), and *C. dromedarius* umbilical cord cells (Eckerle *et al.*, 2014). The NeoCoV S1 protein is only 45% identical to that of MERS-CoV, but their S2 proteins bear a similarity of 87% on the amino acid level (Corman *et al.*, 2014). These similarities led to the hypothesis that the viruses should be able to infect cell lines originating from the same species and could possibly utilise the same receptor.

Angiotensin-converting enzyme 2 (ACE2) was identified as the receptor for SARS-CoV (Li *et al.*, 2003), which is expressed in cells originating from human kidneys (Warner *et al.*, 2005; Eckerle *et al.*, 2013), human hearts (Boehm & Nabel, 2002; Warner *et al.*, 2005) and African green monkey kidneys (Wang *et al.*, 2004).This enzyme is associated with blood pressure regulation (Danilczyk *et al.*, 2004). With S1 and S2 of NeoCoV and the more distantly related SARS-CoV sharing 20% and 42% similarity on the amino acid level, respectively, it is unlikely that these two viruses utilise the same receptor. However, determining whether NeoCoV and SARS-CoV are able to infect the same cell lines would provide a greater comprehension of the infectivity of NeoCoV.

If NeoCoV had the ability to infect cell lines susceptible to MERS-CoV and/or SARS-CoV, there might be a possibility that NeoCoV might utilise the animal species from which the cell lines originate as intermediate hosts in the process of emergence. Knowledge of the host range of NeoCoV can be used to determine which other mammalian species NeoCoV could infect, where it may have the opportunity to adapt or recombine and possibly emerge as an agent able to infect humans.

Isolation of NeoCoV in cell culture would provide a basis on which to study the characteristics of this virus *in vitro*. Furthermore, isolation of NeoCoV would aid in determining which receptors are

utilised by the virus, advancing the current knowledge on which cells would be susceptible to infection by NeoCoV. Access to NeoCoV-positive bat faecal samples and host-derived cell lines provide advantageous conditions for the establishment of an isolation protocol for NeoCoV.

Since isolating bat coronaviruses in cell culture remains a major challenge (Banerjee *et al*., 2018), a need exists to find an approach that does not involve the use of isolated NeoCoV to test the ability of the virus to infect different cell lines. Another problem to be expected when working with the virus itself is that different cell lines might require the use of different infection protocols. The process of developing cell line-specific isolation protocols can be time-consuming and expensive. Furthermore, there is a biological risk involved in working with MERS-CoV and SARS-CoV directly (World Health Organization, 2003; Lim *et al*., 2004; Tani *et al.*, 2012).

To circumvent the aforementioned challenges, the use of viral pseudoparticles bearing the surface antigens of viruses of interest has been proposed. Using viral pseudoparticles ensure that approximately equal titres of virus can be generated in order to standardise infection of cell lines. Additionally, pseudoparticles express reporter genes that simpliy the detection of infection, making the use of expensive and time-consuming procedures such as viral detection by reverse transcription (RT) polymerase chain reaction (PCR) (RT-PCR) or quantitative RT-PCR (RT-qPCR) unnecessary. Viral pseudoparticles could be used to infect different cell lines to test their susceptibility to MERS-CoV, NeoCoV and SARS-CoV, with reporter proteins present in the particles providing a simple method of detecting infection.

1.1.4 Strategy for studying viral entry *in vitro*

Developing a protocol for the isolation of NeoCoV would be an ideal method to study its viral behaviour *in vitro*. Once NeoCoV has successfully been cultured on an appropriate cell line, the protocol can be used to propagate virus to be tested on other cell lines.

Another approach to study viral entry was the use of viruses that mimic the binding and entry of NeoCoV and two human coronaviruses, SARS-CoV and MERS-CoV, in different types of cell cultures, and to compare cell susceptibility among the three viruses. To achieve this, a range of pseudotyped viruses was developed.

A recombinant vesicular stomatitis virus (VSV) with the gene of its own envelope glycoprotein (VSV-G) removed, developed by Hoffmann *et al.* (2013), was used to express the envelope genes of heterologous viruses. A replication-deficient VSV lacking the VSV-G gene, hereafter referred to as VSV*ΔG-Luc, has been made available to our laboratory by collaborators at the Charité University Hospital (Berlin, Germany). This system contains genes for the expression of

green fluorescent protein (GFP) and firefly luciferase (Luc). The VSV*ΔG-Luc system is only able to initiate cell entry but cannot replicate and cause infection and is able to report successful infection of cell lines by expression of GFP.

In order to produce pseudoparticles bearing proteins of interest using this system, baby hamster kidney (BHK) cells, strain BHK-21 (G43), were transfected with plasmids containing the genes for the MERS-CoV-, NeoCoV- or SARS-CoV S proteins, resulting in expression of the respective S proteins on the cell surfaces. The VSV*ΔG-Luc stock was then used to infect these S-expressing cells, resulting in the budding of pseudoparticles carrying the respective coronavirus S proteins. The resulting pseudoparticles were tested on different cell lines to determine which cells are susceptible to infection by the aforementioned viruses.

1.1.5 Aims and objectives

This study aimed to investigate the host range of NeoCoV *in vitro*. Establishing a protocol for the isolation of NeoCoV in cell culture and producing pseudoparticles were extensions of this aim.

The objectives for this study were:

- To culture NeoCoV in cell culture using a cell line derived from its host, *N. capensis*.
- To propagate and rescue replication-deficient viral pseudoparticles bearing the S proteins of MERS-CoV, NeoCoV or SARS-CoV.
    - To transfect BHK-21 (G43) cells with pCG1 vectors carrying the S protein inserts of MERS-CoV, NeoCoV and SARS-CoV.
    - To generate pseudoparticles bearing the S proteins of MERS-CoV, NeoCoV and SARS-CoV.
    - To infect mammalian cell lines derived from *Camelus dromedarius*, *N. capensis*, *Pipistrellus pipistrellus* and *Cercopithecus aethiops* with the generated pseudotyped viruses to investigate the range of cells susceptible to infection with NeoCoV.

1.2 Literature review

1.2.1 Coronaviruses

Coronaviruses belong to the family *Coronaviridae*, which belong to the order *Nidovirales* (Navas-Martín & Weiss, 2004; Masters, 2006). Even though this family of viruses is morphologically distinguishable from other viruses of the order *Nidovirales*, sequencing is required to distinguish between different viruses from the *Coronaviridae* family itself (Masters, 2006).

1.2.1.1 Molecular biology

Viruses of the family *Coronaviridae* are enveloped and have single-stranded, positive-sense ribonucleic acid (RNA) genomes. These genomes are approximately 30 000 bases in size; the largest known RNA genomes in existence (Navas-Martín & Weiss, 2004; Masters, 2006).

The open reading frame (ORF) 1a and ORF1b are found at the 5'-end of the genome and make up roughly two-thirds of the entire genome as seen in Figure 1.1. These proteins are post-translationally cleaved into the viral protease and non-structural proteins involved in replication (Lai *et al.*, 1994). The last third of the genome that is located at the 3'-end is transcribed into structural proteins (Lai *et al*., 1994). These structural proteins include the S, E, M and N proteins (Navas-Martín & Weiss, 2004; Masters, 2006).

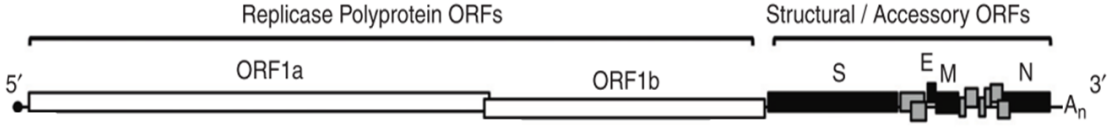

Figure 1.1. A diagram of a typical coronavirus genome. This illustrates the first two-thirds of the genome encoding for the replicase genes and the last third of the genome encoding for the structural proteins spike (S), envelope (E), membrane (M) and nucleocapsid (N) (Smith & Denison, 2012) (permission number for use of image: 4410691200986).

The S proteins are located on the envelope of coronaviruses. They are club-shaped proteins that protrude from the virion's surface. These proteins attach to host cells to facilitate fusion of virions with host cells (Masters, 2006). The E protein forms part of the virion membrane (Masters, 2006). According to Fischer and Sansom (2002), this protein aids in the formation of ion channels in the membrane to regulate the virion pH, which, when lowered, enables the viral genome to move from the virion to the nucleus of the host cell. The E protein also facilitates virion budding in some members of the coronavirus family, such as mouse hepatitis virus (MHV) and infectious bronchitis virus (IBV) (Raamsman *et al.*, 2000; Machamer & Youn, 2006). The M

protein of coronaviruses is a glycoprotein. It is integrated into the lipid bilayer that forms the viral membrane. This protein is responsible for the spherical shape of the virions and offers structural support and stability (Masters, 2006). The N proteins of coronaviruses are wound around the viral genome to compact it and are helically symmetrical (Kennedy & Johnson-Lussenburg, 1975). This is not a common feature in positive-sense RNA viruses, which usually have icosahedral nucleocapsids (Kennedy & Johnson-Lussenburg, 1975; Masters, 2006).

1.2.1.2 Replication cycle

Coronavirus S proteins bind to receptors on the surfaces of host cells at the start of their life cycle (de Haan & Rottier, 2005). The coronavirus S protein consists of two subunits: S1 and S2 (de Haan & Rottier, 2005; Masters, 2006; Cavanagh *et al.*, 2007; Hoffmann *et al*., 2013). S1 mediates the binding of the viral particle to receptors on the host cell surface. S2 is responsible for the fusion of the virion with the host cell. Seeing as the compatibility of the S protein with the receptors on the host cell surface is essential for viral entry, the genetic composition and three-dimensional structure of the coronaviral S protein plays a significant role in the tropism of coronaviruses (de Haan & Rottier, 2005; Masters, 2006; Hoffmann *et al*., 2013).

The coronavirus envelope disintegrates once the viral particle binds to the host cell surface and the RNA is released into the host cell's cytoplasm (de Haan & Rottier, 2005; Masters, 2006). The replicase genes are translated to form a replication-transcription complex that aids in the replication of the viral genome and translation of the structural proteins S, E, M and N. Proteins S, E, M and N attach to the endoplasmic reticulum and Golgi complex to initiate virion assembly, after which the virions are exocytosed to become mature virions (La Monica *et al*., 1992; Navas-Martín & Weiss, 2004; de Haan & Rottier, 2005; Masters, 2006).

During the replication process, which is depicted in Figure 1.2, a negative-sense RNA intermediate is formed to act as template. The positive-sense genome itself acts as messenger RNA (mRNA) for the translation of structural and accessory proteins (La Monica *et al*., 1992; Navas-Martín & Weiss, 2004; de Haan & Rottier, 2005; Masters, 2006; Corman *et al*., 2014; Corman *et al*., 2015). The polycistronic genome, in which one strand of mRNA encodes more than one protein, provides a platform for the genes to be translated and/or replicated simultaneously but separately.

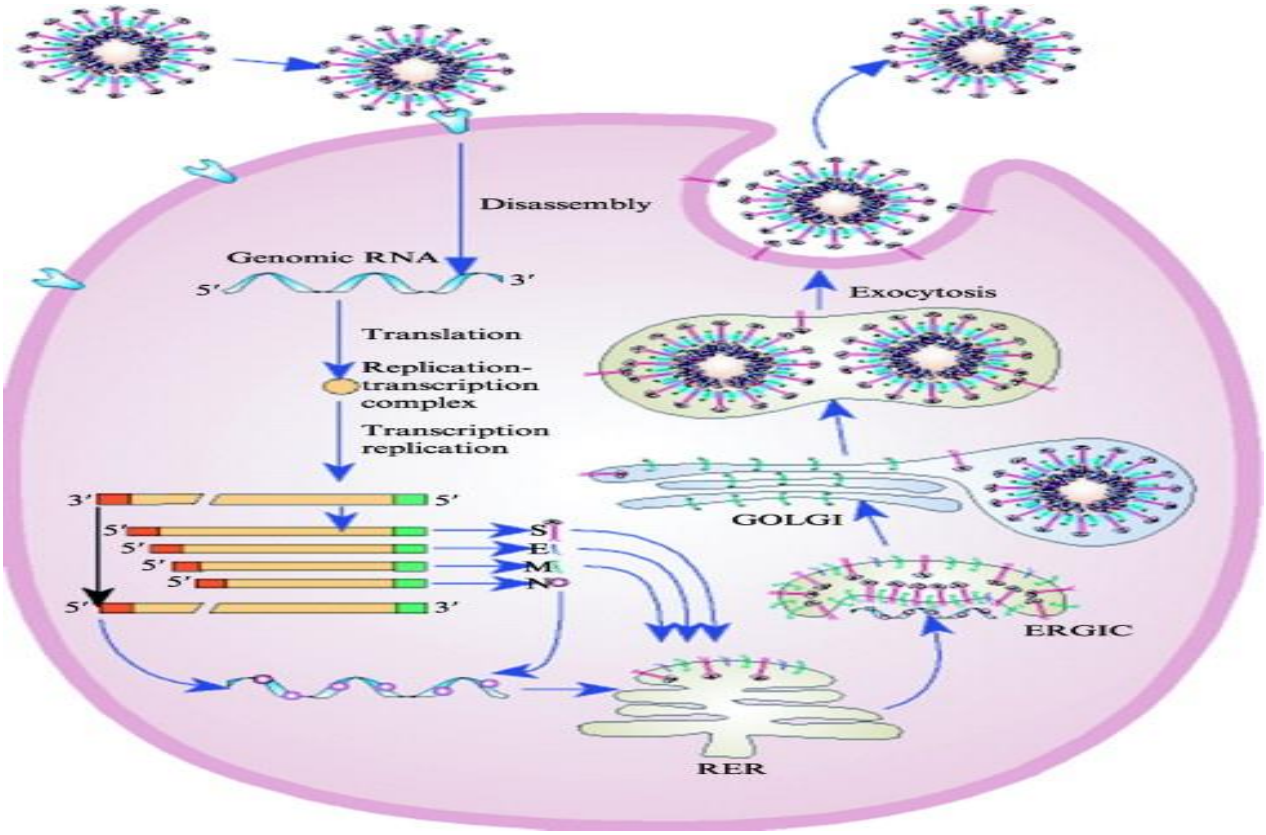

Figure 1.2. The replication cycle of a coronavirus. The virion binds to receptors on the host cell surface, enters the cell and disassembles. The viral genome replicates and structural proteins are translated. Thereafter, particles are assembled and exocytosed (de Haan & Rottier, 2005) (permission number for use of image: 4410690675754).

1.2.1.3 Human and animal coronaviruses

Different coronavirus species have been known to infect humans, other mammals and avian species (de Haan & Rottier, 2005; Masters, 2006; Banerjee *et al.*, 2018) and typically infect the respiratory and digestive systems (de Haan & Rottier, 2005; Masters, 2006). Coronavirus infections can be of an acute or chronic nature, resulting in symptoms such as coughs, a sore throat, chills, fever, and other flu-like symptoms (Masters, 2006).

1.2.1.3.1 Non-zoonotic animal coronaviruses

Mammals are often found to harbour coronaviruses that are not transmissible to humans. Some of these non-zoonotic animal coronaviruses include transmissible gastroenteritis coronavirus (TGEV), bovine coronavirus (BCoV), feline coronavirus, turkey coronavirus (TCV), ferret enteric coronavirus and pantropic canine coronavirus.

TGEV is a pathogen of pigs. It was first described by Doyle and Hutchings (1946). TGEV causes diarrhoea in pigs and is often fatal for piglets.

BCoV is found in cattle and other ruminants such as Sambar deer (*Cervus unicolor)* and waterbuck (*Kobus ellipsiprymnus*) (Saif & Heckert, 1990; Tsunemitsu *et al.*, 1995). BCoV causes respiratory and enteric infections in ruminants (Saif & Heckert, 1990; Tsunemitsu *et al.*, 1995).

Feline coronavirus exists as two pathotypes, namely feline enteric coronavirus (FECV) and feline infectious peritonitis virus (FIPV) (Rottier *et al.*, 2005). FECV and FIPV manifests as two different diseases in felines (Rottier *et al.*, 2005). Both of these manifestations cause infection of epithelial cells in the gastrointestinal tract, from where it can spread through viraemia (Herrewegh *et al.*, 1995; Sharif *et al.*, 2011; Desmarets *et al.*, 2016).

TCV causes inflammation of the intestinal tract of turkeys (Adams & Hofstad, 1971). This results in inflammation of the intestines, with symptoms such as diarrhoea and dehydration. TCV often has a high fatality rate, especially in young individuals.

Ferret enteric coronavirus is the causative agent of a disease that spreads between young ferrets and is frequently transmitted from young individuals to adults (Williams *et al.*, 2000; Wise *et al*., 2006). The virus causes inflammation of the mucous membranes of ferrets. The disease results in dehydration, usually caused by vomiting and diarrhoea.

Pantropic canine coronavirus, described by Erles *et al*. (2003), causes canine infectious respiratory disease. As the name implies, many different tissue types are susceptible to infection by pantropic canine coronavirus. The virus can also manifest as a neurologic condition, resulting in lowered coordination and, in more severe cases, seizures.

1.2.1.3.2 Coronavirus diseases in humans

Human coronaviruses are transmitted in various ways, among others through microdroplet transmission, fomites and faecal-oral routes (Graham *et al*., 2013; Raj *et al*., 2014; Baseler *et al*., 2016; Scully & Samaranayake, 2016).

Mild coronavirus infection in humans can include symptoms such as fever, chills, muscular pain, shortness of breath, coughs, sore throat and runny nose, general feeling of physical discomfort caused by immunosuppression, and other common cold-like symptoms (Graham *et al*., 2013; Raj *et al*., 2014; Baseler *et al*., 2016; Scully & Samaranayake, 2016). In severe infections, renal failure and pneumonia have been reported (Baseler *et al*., 2016). In some cases, patients have

been asymptomatic despite being infected with a coronavirus (Raj *et al*., 2014; Baseler *et al*., 2016).

There are currently six coronaviruses known to cause disease in humans (Centers for Disease Control and Prevention, 2017). These viruses are human coronaviruses (HCoV) 229E, HCoV-OC43, HCoV-NL63, HCoV-HKU1, SARS-CoV and MERS-CoV (Centers for Disease Control and Prevention, 2017).

HCoV-229E was originally isolated by Hamre and Procknow (1966). The virus belongs to the alphacoronavirus genus and causes infection in the upper respiratory tract (Hamre & Procknow, 1966; Vabret *et al.*, 2003). It is one of the causative agents of the common cold, but can also result in more severe diseases such as pneumonia (Vabret *et al.*, 2003). HCoV-229E is believed to be of bat origin (Graham *et al.*, 2013).

HCoV-OC43, originally described by McIntosh *et al.* (1967), is a betacoronavirus that causes upper respiratory tract infections (Vabret *et al.*, 2003). The virus is also associated with the manifestation of the common cold and can lead to the development of pneumonia or bronchitis in more severe cases (Vabret *et al.*, 2003).

Van der Hoek *et al.* (2004) identified HCoV-NL63 as the causative agent of bronchiolitis in an infant; thus discovering the fourth disease-causing HCoV. This virus belongs to the genus alphacoronaviruses and causes respiratory tract infections in humans, leading to mild infections. It can also result in diseases such as pneumonia and bronchiolitis, especially in immunocompromised individuals (van der Hoek *et al.*, 2004; Chiu *et al.*, 2005). According to Graham *et al.* (2013), HCoV-NL63 also originates from bats.

HCoV-HKU1 was first described by Woo *et al.* (2005). It is a betacoronavirus that causes infection of the respiratory tract. HCoV-HKU1-infection can result in diseases such as the common cold, pneumonia and bronchitis (Kanwar *et al.*, 2017).

SARS-CoV (Drosten *et al.*, 2003) and MERS-CoV (Zaki *et al.*, 2012) are two of the most pathogenic human coronaviruses discovered to date. Both of these viruses have been found to originate from animal hosts (Guan *et al.*, 2003; Lau *et al.*, 2005; Li *et al.*, 2005, Yuan *et al.*, 2010; Perera *et al.*, 2013; Reusken *et al.*, 2013; Haagmans *et al.*, 2014; Nowotny & Kolodziejek, 2014; Yang *et al.*, 2016) and are described in more detail in subsequent sections (refer to sections 1.2.1.3.4 and 1.2.1.3.5).

1.2.1.3.3 Zoonotic transmission of coronaviruses from animals to humans

Zoonosis is the term used to describe a disease that can be transmitted from animals to humans (The Oxford English Dictionary, 2018). Viral zoonoses and the emergence of novel infectious viruses are often associated with RNA viruses due to their high mutation rates that cause variants to develop that can 'jump' from one host species to another (Scully & Samaranayake, 2016). Host-switching can also facilitate faster spread of diseases as the infections can spread between humans and animals and in the human population itself once it has adapted to its new host system (Otter *et al*., 2016).

Some coronavirus outbreaks in the human population have resulted in the discovery of related viruses in other mammals, such as the discovery of MERS-CoV-like viruses in bats (Annan *et al.*, 2013; Ithete *et al.*, 2013; Corman *et al.*, 2014; Lau *et al.*, 2018a) and MERS-CoV itself in camels (Perera *et al.*, 2013; Reusken *et al.*, 2013; Haagmans *et al.*, 2014). SARS-CoV-like viruses have also been found in bats (Lau *et al.*, 2005; Li *et al*., 2005, Yuan *et al.*, 2010) and civets (Guan *et al.*, 2003; Lau *et al.*, 2005). Phylogenetic analysis of the genomes of these viruses has shown close relatedness between human and animal-derived coronavirus sequences and has led to the notion that some coronavirus outbreaks are the result of zoonotic transmission events (Guan *et al.*, 2003; Lau *et al.*, 2005; Li *et al.*, 2005; Yuan *et al.*, 2010; Annan *et al.*, 2013; Ithete *et al.*, 2013; Perera *et al.*, 2013; Reusken *et al.*, 2013; Corman *et al.*, 2014; Haagmans *et al.*, 2014; Lau *et al.*, 2018a).

The host range of coronaviruses is largely determined by their surface proteins' ability to bind to host cell surface receptors. Coronavirus S proteins consist of two subunits, S1 and S2. These subunits play an important role in host-switching, seeing as the ability of the virus to adapt its S protein subunits to bind to different receptors determine whether it can 'jump' from one host to another (Hoffmann *et al.*, 2013).

There is a variety of coronaviruses that can infect vertebrates. These viruses can cause diseases that affect the respiratory, gastrointestinal and central nervous systems (Shi *et al*., 2016). Coronaviruses have been proven to infect various hosts, such as civets, camels and bats (Masters, 2006; Smith & Denison, 2012; Coleman & Frieman, 2014; Corman *et al*., 2014, Moratelli & Calisher, 2015, Banerjee *et al.*, 2018). There is evidence that suggests transmission of coronavirus from animals to humans occurs (Guan *et al.*, 2003; Reusken *et al.*, 2013; Nowotny & Kolodziejek, 2014). This is a public health risk in instances where humans are in

close contact with animals, as is the case with domesticated and farm animals (Coleman & Frieman, 2014).

Bats are known to host a wide variety of viruses and they are suspected to host viruses that can adapt to infect human populations, either directly or through intermediate hosts (Calisher *et al.*, 2006). Human viruses that originated from bats include rabies virus (Dato *et al.*, 2016), henipavirus (Pernet *et al.*, 2014), Menangle virus (Barr *et al.*, 2012) and Ebola virus (Leroy *et al.*, 2009). Some bat species, such as *Hipposideros caffer ruber* of Ghanaian origin (Pfefferle *et al*., 2009) and several North American bat species (Huynh *et al*., 2012), have been found to host coronaviruses that are related to known human coronaviruses, indicating that bats might have played a role in the emergence of these viruses in humans. This is cause for concern, since some bats nest close to human populations and can travel great distances, thus having the means to spread viruses widely through zoonotic transmission. Once a human has been infected and the virus has adapted to facilitate human transmission, the virus can be spread rapidly in the human population, leading to an outbreak.

1.2.1.3.4 Severe acute respiratory syndrome coronavirus

A coronavirus named SARS-CoV caused an outbreak of severe respiratory disease in China in 2003 (Drosten *et al.*, 2003; World Health Organization, 2003). The disease spread to 37 countries and resulted in 8 273 cases and 775 deaths (Drosten *et al*., 2003; Navas-Martín & Weiss, 2004; Graham *et al*., 2013; Coleman & Frieman, 2014; Corman *et al*., 2014). SARS-CoV was predominantly spread through droplet transmission, but was also linked to transmission through fomites (Otter *et al*., 2016). Some patients with SARS-CoV infections showed symptoms such as fever, migraines, cough, and general discomfort, whilst more serious infections caused symptoms ranging from pneumonia and respiratory failure to liver or heart failure (Berger *et al.*, 2004; Navas-Martín & Weiss, 2004).

The receptor for SARS-CoV was identified by Li *et al.* (2003) as ACE2. This receptor is found on numerous cell types, including those from human kidneys (Warner *et al.*, 2005; Eckerle *et al.*, 2013), human hearts (Boehm & Nabel, 2002; Warner *et al.*, 2005), African green monkey kidneys (Wang *et al.*, 2004), Madin-Darby canine kidney (MDCK) cells (Warner *et al.*, 2005), Chinese hamster (*Cricetulus griseus*) ovaries (CHO) (Warner *et al*., 2005), human colons, human embryonic kidney (HEK) cells, human endometrial adenocarcinoma cells, human alveolar adenocarcinoma cells, human cervical cancer cells, and feline (*Felis catus*) lungs (Mossel *et al.*, 2005). This suggests that all the aforementioned cell lines may be susceptible to

infection with SARS-CoV; however, it has not been possible for researchers to successfully infect all of these cells with SARS-CoV in cell culture (Mossel *et al.*, 2005).

One of the first SARS-CoV patients is believed to have contracted the disease from civets (*Paguma larvata*) and raccoon dogs (*Nyctereutes procyonoides*) through zoonotic transmission. Horseshoe bats (*Rhinolophus sinicus*) have also been found to carry antibodies against SARS-CoV and indicate yet another zoonotic source of this disease (Breiman *et al.*, 2003; Graham *et al*., 2013; Coleman & Frieman, 2014). Furthermore, a SARS-CoV progenitor more closely related to the virus than any other discovered in animal hosts before was discovered in Chinese horseshoe bats (Yang *et al.*, 2016). It is speculated that the virus 'jumped' from horseshoe bats to civets and raccoon dogs and from there to humans, likely undergoing genetic adaption with each host-switch (Graham *et al*., 2013). The virus might have been transmitted from the bats to the civets through a faecal-oral route when nesting close together, which could then have been transmitted to humans when they handled the civets or ate undercooked civet meat (Graham *et al.*, 2013).

1.2.1.3.5 Middle East respiratory syndrome coronavirus

An outbreak of MERS-CoV originated in the Arabian Peninsula in 2012 and is still on-going (Zaki *et al.*, 2012; World Health Organization, 2018). To date, the virus has spread to 27 countries and has resulted in 2 260 cases and 803 deaths (World Health Organization, 2018). MERS-CoV infects the lower respiratory tract of humans (Scully & Samaranayake, 2016). Infected individuals usually present with symptoms such as fever, chills, migraines, coughs, sore throats, muscular pain, nausea, and chest pain when breathing. More severe symptoms include pneumonia and renal failure (Baseler *et al*., 2016).

Raj *et al.* (2013) identified DPP4 as the functional receptor for MERS-CoV. A myriad of cells express this receptor, among others African green monkey kidney cells (Zaki *et al.*, 2012; Raj *et al.*, 2014), human liver cells (Raj *et al.*, 2014), *P. pipistrellus* kidney cells (Cui *et al.*, 2013; Raj *et al.*, 2014), human bronchial and lung tissue cells (Chan *et al.*, 2013) equine (*Equus caballus*) kidney cells (Meyer *et al*., 2015), ferret (*Mustela putorius furo*) kidney cells (Raj *et al.*, 2014), rhesus macaque *(Macaca mulatta*) kidney cells, human lung adenocarcinoma cells, human epithelial colorectal adenocarcinoma cells and HEK cells (Shirato *et al.*, 2013). Furthermore, goat (*Capra hircus*) lung cells, alpaca (*Llama pacos*) kidney cells, dromedary camel (*C. dromedarius*) umbilical cord cells, sheep (*Ovis aries*) kidney cells, cattle (*Bos taurus*) kidney and lung cells, bank vole (*Myodes glareolus*) trachea cells and lesser white-toothed shrew (*Crocidura*

suaveolens) lung cells also express DPP4 (Eckerle *et al.*, 2014). Although many of these cells have been inoculated with MERS-CoV *in vitro*, not all of these cells have shown susceptibility to the virus in cell culture.

Some evidence suggests that bats have transmitted ancestral variants of MERS-CoV to dromedary camels through an intermediate host(s) (Coleman & Frieman, 2014; Corman *et al*., 2014). MERS-CoV has been found in many populations of dromedary camels and thus implicates these animals as a reservoir host for the virus (Reusken *et al*., 2013; Coleman & Frieman, 2014; Corman *et al*., 2014; van den Brand *et al.*, 2015). The 'jump' from camels to an intermediate host or directly to humans likely required some genetic changes to adapt for human infection and transmission (de Wit & Munster, 2013; Reusken *et al*., 2016). Humans were possibly initially infected with the virus when working with camels (Coleman & Frieman, 2014; Corman *et al*., 2014; Raj *et al*., 2014; Baseler *et al*., 2016).

Some bat species have been shown to carry coronaviruses that are closely related to MERS-CoV (de Groot *et al.*, 2013; Ithete *et al.*, 2013; Memish *et al.*, 2013; Corman *et al.*, 2014; Banik *et al*., 2015; Anthony *et al.*, 2017; Cronjé, 2017; Moreno *et al.*, 2017; Lau *et al.*, 2018b). Upon the discovery of MERS-CoV, it was found that MERS-CoV was related to two bat coronaviruses, namely *Tylonycteris* bat coronavirus HKU4 (Ty-BatCoV HKU4) and *Pipistrellus* bat coronavirus HKU5 (Pi-BatCoV HKU5) (Wang *et al.*, 2014; Yang *et al.*, 2014), which were discovered in China. This indicated that bats might harbour the ancestral viruses from which MERS-CoV developed by means of mutations and other genomic modifications in other reservoir hosts (Wang *et al.*, 2014; Yang *et al.*, 2014; Lau *et al.*, 2018a).

Several studies have detected MERS-related coronaviruses in African bats (Corman *et al.*, 2014; Anthony *et al.*, 2017; Cronjé, 2017). Anthony *et al*. (2017) discovered a coronavirus, PREDICT/PDF-2180, in the bat species *Pipistrellus hesperidus* that is related to MERS-CoV in Uganda. The S protein of PREDICT/PDF-2180 was genetically distinct from that of MERS-CoV, with which it shared only 46% homology on the amino acid level (Anthony *et al.*, 2017). It was discovered that this disparity between the S proteins makes it impossible for PREDICT/PDF-2180 to bind to human DPP4. This was confirmed by protein modelling (refer to section 1.2.1.4), during which the S protein structure of PREDICT/PDF-2180 was predicted and visualised *in silico* with specialised software to determine whether it shared similarities with the MERS-CoV S protein on a phenotypic level (Anthony *et al.*, 2017). Furthermore, the study constructed full-length infectious clones of the MERS-CoV genome, replacing the RBD of MERS-CoV with that

of PREDICT/PDF-2180 and transfecting cells with these clones. Cells produced recombinant viruses which were harvested and used to infect Vero cells, but no replicating virus could be detected through RT-PCR, leading to the conclusion that PREDICT/PDR-2180 does not have the ability to utilise human DPP4 (Anthony *et al.*, 2017). This virus is therefore not believed to pose a zoonotic threat (Anthony *et al.*, 2017).

Human MERS-CoV itself has not been found in bats; however, the RBD of a closely related bat coronavirus, namely HKU4, can bind human DPP4, albeit with a lower affinity than that of MERS-CoV (Wang *et al.*, 2014). More recently, Lau *et al*. (2018b) discovered the RBD of another bat coronavirus strain, Hp-BatCoV HKU25, originating from *Hypsugo pulveratus*, can bind to human DPP4 for viral entry by replacing the MERS-CoV RBD with that of the novel strain. Lau *et al.* (2018b) also developed pseudoparticles bearing the S protein of Hp-BatCoV HKU25 to confirm that the virus is able to utilise human DPP4. The pseudoparticles were able to enter human cells, but with a lower efficiency than MERS-CoV. Taking this into account, it is speculated that MERS-CoV reached the human population after a series of genetic changes that was possibly brought about by multiple host-switching and recombination events, during which the S protein adapted to enter human cells (de Wit & Munster, 2013; Corman *et al*., 2014; Banik *et al*., 2015; van den Brand *et al.*, 2015; Shi *et al*., 2016; Lau *et al.*, 2018b).

MERS-CoV is transmitted by droplets through the respiratory route in the human population (Raj *et al*., 2014; Baseler *et al*., 2016; Otter *et al*., 2016). The disease can also be contracted from fomites. Figure 1.3 demonstrates the speculated transmission routes through which MERS-CoV can spread between populations. It is believed that bats infected camels with MERS-CoV-related viruses, from where it adapted and was transmitted to humans in the form of MERS-CoV (Milne-Price *et al.*, 2014). As different strains of MERS-CoV have been detected in patients that contracted the disease in the same region, it is possible that MERS-CoV-related viruses can also be transmitted from bats to other unknown intermediate hosts where slightly different mutations occur (Cotten *et al.*, 2013; Milne-Price *et al.*, 2014). Once contracted by humans, MERS-CoV can also spread in the population on occasion; however, human-to-human transmission has not often been reported (Milne-Price *et al.*, 2014; Baseler *et al.*, 2016).

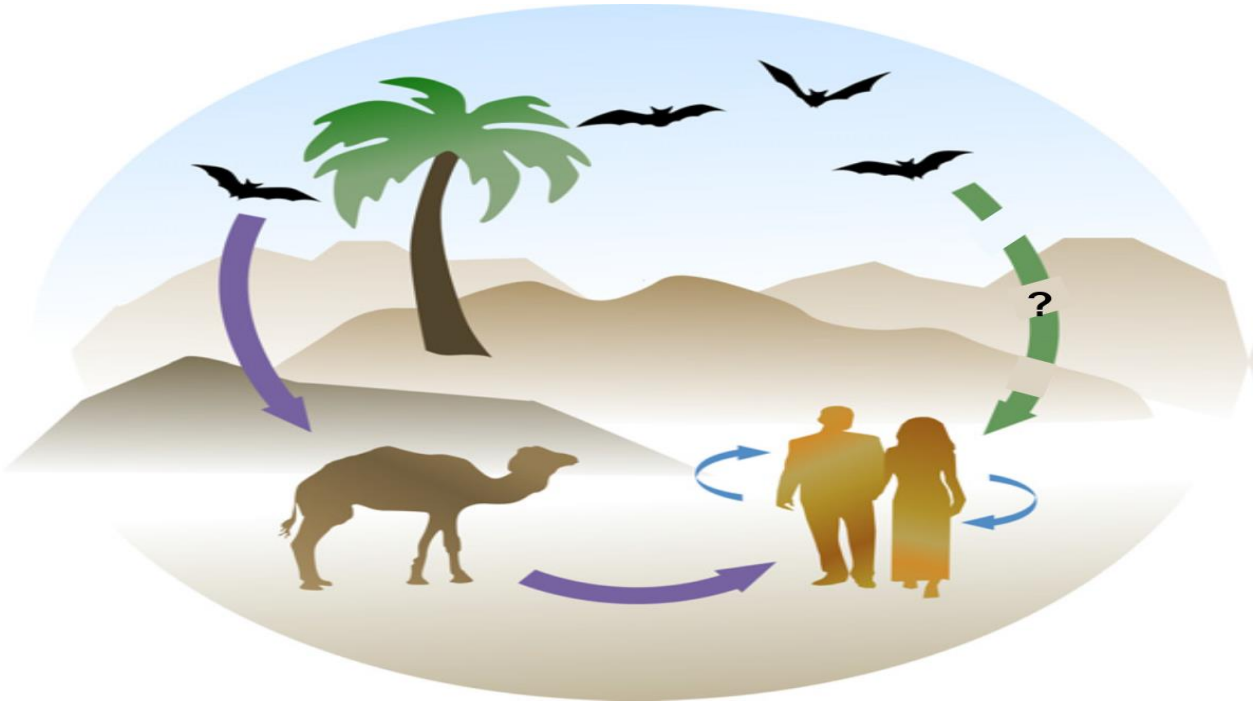

Figure 1.3. The supposed transmission cycle of MERS-CoV. It has been speculated that ancestral viruses to MERS-CoV were transmitted from bats to camels, where genetic changes and host adaptation leads to the emergence of MERS-CoV, a virus that has acquired the ability to infect humans. Other routes of transmission from bats to humans remain unknown. Human-to-human transmission occurs occasionally (adapted from Milne-Price *et al*., 2014) (permission number for use of image: 4410530025102).

1.2.1.3.6 *Neoromicia capensis* coronavirus

NeoCoV was discovered in the South African bat species *Neoromicia capensis* (Ithete *et al*., 2013; Corman *et al*., 2014) and has since been detected by other studies (Cronjé, 2017; Geldenhuys *et al.*, 2018). NeoCoV is 85.5% genetically identical to MERS-CoV, meaning that, by definition, it belongs to the same virus species as MERS-CoV (de Groot *et al*., 2012). From this information it is inferred that NeoCoV is an ancestral virus to MERS-CoV (Corman *et al.*, 2014).

The S1 subunit of NeoCoV is 45% similar to that of MERS-CoV and its S2 subunit is 87% identical to that of MERS-CoV (Ithete *et al*., 2013; Corman *et al*., 2014). The discrepancy between the S subunits indicates that NeoCoV is not the direct ancestor of MERS-CoV (Lau *et al.*, 2018a). It also denotes that NeoCoV and MERS-CoV do not use the same cellular receptors and might not be able to infect the same cell types and/or hosts, which infers that NeoCoV would not have the ability to infect human cells (Lau *et al.*, 2018a). This is further supported by

the fact that the S proteins of NeoCoV and PREDICT/PDF-2180, which cannot enter human cells, share 94% homology on an amino acid level (Anthony *et al.*, 2017).

The emergence of MERS-CoV is possibly the result of mutations and recombination events that NeoCoV and other ancestral viruses underwent by being transmitted from bats to different hosts such as camels and possibly other mammals that live in close contact with humans, from where it is finally transmitted to humans (Ithete *et al*., 2013; Corman *et al*., 2014, Geldenhuys *et al.*, 2018; Lau *et al.*, 2018a). To better understand the host-switching and recombination events that gave rise to MERS-CoV, it is necessary to develop tools with which to study the different ways in which NeoCoV and MERS-CoV can infect cells. Isolating NeoCoV in cell culture would provide a manner in which NeoCoV infectivity and behaviour can be studied. However, as bat coronavirus isolation proves a challenge (Govorkova *et al.*, 1996; Lednicky & Wyatt, 2012; Ge *et al.*, 2013; Wei *et al.*, 2017; Banerjee *et al.*, 2018; Lau *et al.*, 2018b), other approaches to study NeoCoV *in vitro* also need to be developed as a means of overcoming the issue of isolation.

1.2.1.4 Viral receptors

Various factors play a role in viral host tropism and cell susceptibility to viral infection. Among others, viruses require a direct contact with host cells in order to cause infection as well as an intracellular environment that allows for viral replication (i.e. the presence of viral promoters and enzymes involved in viral replication within host cells) (Baron *et al.*, 1996). Receptors expressed on cell surfaces play a crucial role in viral host tropism (Baron *et al.*, 1996; Masters, 2006; Milne-Price *et al.*, 2014). If a cell line expresses a receptor that allows the binding of a coronavirus, the cell line is susceptible to viral entry, after which infection can manifest.

As mentioned previously, the coronavirus S protein is responsible for binding to and entry of host cells, provided that the cells of interest express the virus-specific receptors (Masters, 2006; Milne-Price *et al.*, 2014). In the case of emerging viruses, the receptors to which these viruses attach are not always known. It is therefore not possible to determine whether the viruses can bind to cells with known receptors. Furthermore, this makes it impossible to determine which cell lines, mammalian species and organs are susceptible to infection by the emerging viruses of interest.

Novel three-dimensional protein modelling methods exist to aid in predicting the molecular structure of an RBD *in silico*. These methods aid in determining whether the RBD of a protein will be able to bind to receptors based on the gene sequence encoding the protein. Furthermore, the methods also aid in determining which receptors the virus can utilise. Predicting the three

dimensional structure of a protein based on sequencing data is usually done by firstly comparing the RBD sequence to that of RBDs with known structures that are available in the protein data bank using specialised bioinformatics software (Moreno *et al.*, 2017). Features of the secondary protein structure are then identified with the aid of algorithms available on web servers such as ENDscript 2 or SWISS-MODEL, after which the predicted structure can be compared to that of a virus of which the receptor has been identified by means of superimposition (Moreno *et al.*, 2017; Lau *et al.*, 2018b). If there are major similarities between the RBDs of the two viruses, it indicates that the virus of interest would be able to utilise the same receptor (Anthony *et al.*, 2017; Moreno *et al.*, 2017; Lau *et al.*, 2018b). However, these studies do not provide information for viruses that are not closely related to viruses of which receptors have already been identified, nor does it prove that the virus of interest will be able to enter cells and establish an infection.

In order to increase the feasibility of determining the host cell receptors for a specific virus that proves difficult to isolate in cell culture, methods to circumvent this issue have been established. Binding assays, in which envelope proteins of the virus of interest are expressed through baculovirus vectors, harvested and used to detect binding between the protein and receptors of interest, have been developed. However, these assays do not provide any information on how viral entry takes place (Tani *et al.*, 2012).

Another approach that has been developed is the use of viral pseudoparticles (Tani *et al.*, 2012). Pseudotyped systems allow for studying the binding and entry of harmful viruses without the requirement of stringent biosafety measures and are combined with uncomplicated methods for detecting viral entry (Tani *et al.*, 2012).

1.2.2 Pseudotyped virus systems

Pseudoparticles (also known as pseudotyped viruses or virus-like particles) are viral particles that have been modified to mimic a certain aspect of another virus (Cronin *et al.*, 2005; Tani *et al.*, 2012). Pseudotyped viruses entail the use of experimental systems in which a viral particle expresses the envelope gene(s) of other viruses (Cronin *et al.*, 2005; Tani *et al.,* 2012).

There are two main reasons for using pseudoparticles instead of the actual virus of interest. Firstly, there are many viruses that, although attempted, have not been successfully isolated and cultivated in cell culture; as a result there is no virus available to use directly for the testing of host cell susceptibility or to investigate virus-cell interactions (Bartosch *et al.*, 2003; Tani *et al.*, 2012). Secondly, the use of pseudoparticles lessens the danger of exposure to hazardous

agents in experimental settings; since they do not contain the virus of interest's genome, the risk of viral replication and/or mutation is eliminated (Cosset *et al.*, 2009; Tani *et al.*, 2012).

Pseudoparticles are usually constructed to bear the surface proteins of another virus (Tani *et al.*, 2012). This is done in order to determine which host cell receptors are susceptible to binding to viruses of interest or the effect that viral binding and/or entry have on host cells (Tani *et al.*, 2012). Pseudoparticles have been used in determining host cell susceptibility to certain viruses and/or interactions between the two (Aiken, 1997; Wool-Lewis & Bates, 1998; Wang *et al.*, 2004; Hanika *et al.*, 2005; Hoffmann *et al.*, 2013; Wang *et al.*, 2016; Lau *et al.*, 2018b), as well as to test samples for the presence of antibodies against specific viruses (Beels *et al.*, 2008; Perera *et al.*, 2013; Qiu *et al.*, 2013), and also in the development of vaccines (Desjardins *et al*., 2009; Garrone *et al.*, 2011; Schultz *et al.*, 2012; Bolz *et al*., 2016; Wang *et al.*, 2018).

There are different methods of constructing pseudoparticles. One of the most widely used methods involves the use of a modified VSVΔG system that can be used to express foreign proteins. Another popular method to produce pseudoparticles is the use of plasmids carrying gene sequences which result in the formation of pseudoparticles when transcribed.

Constructing a pseudotyped system such as the VSV*ΔG system usually involves the removal of the envelope protein gene from the genome of the virus to be used as the pseudoparticle and replacing it with a reporter gene such as luciferase, GFP or secreted alkaline phosphatase (SEAP) (Wool-Lewis & Bates, 1998; Tani *et al.*, 2012). VSV is typically used for this method by removing the VSV-G gene from the viral genome, resulting in the formation of VSV*ΔG (Berger Rentsch & Zimmer, 2011; Tani *et al.*, 2012; Hoffmann *et al.*, 2013). These VSV*ΔG particles cannot replicate to form infectious particles, as it will produce particles that do not possess an envelope protein that can attach to host cells (Hoffmann, 2017). However, a stock of these particles can be generated through a process of trans-complementation (Hoffmann, 2017).

Trans-complementation involves transfecting cells with plasmids containing VSV-G or using a cell line that can be induced to express VSV-G (such as BHK-21 [G43]) and infecting it with VSV*ΔG, resulting in the propagation of VSV*ΔG that expresses VSV-G but does not contain the gene itself (Hoffmann, 2017). These pseudoparticles can be used to infect cells expressing the foreign surface antigen of interest, usually generated by transfection with plasmids carrying the gene(s) of interest. After transfection with plasmids and subsequent infection with VSV*ΔG, pseudoparticles that contain the reporter gene and express the desired surface antigen on their surfaces are released from the cells (Berger Rentsch & Zimmer, 2011; Tani *et al.*, 2012;

Hoffmann *et al.*, 2013). The process of pseudoparticle production using the VSV*ΔG system is diagrammatically explained in Figure 1.4. The newly-formed pseudoparticles can then be harvested and used in the experimental procedures mentioned previously, the reporter gene(s) aiding in visualising whether infection was successful (Hoffmann *et al.*, 2013).

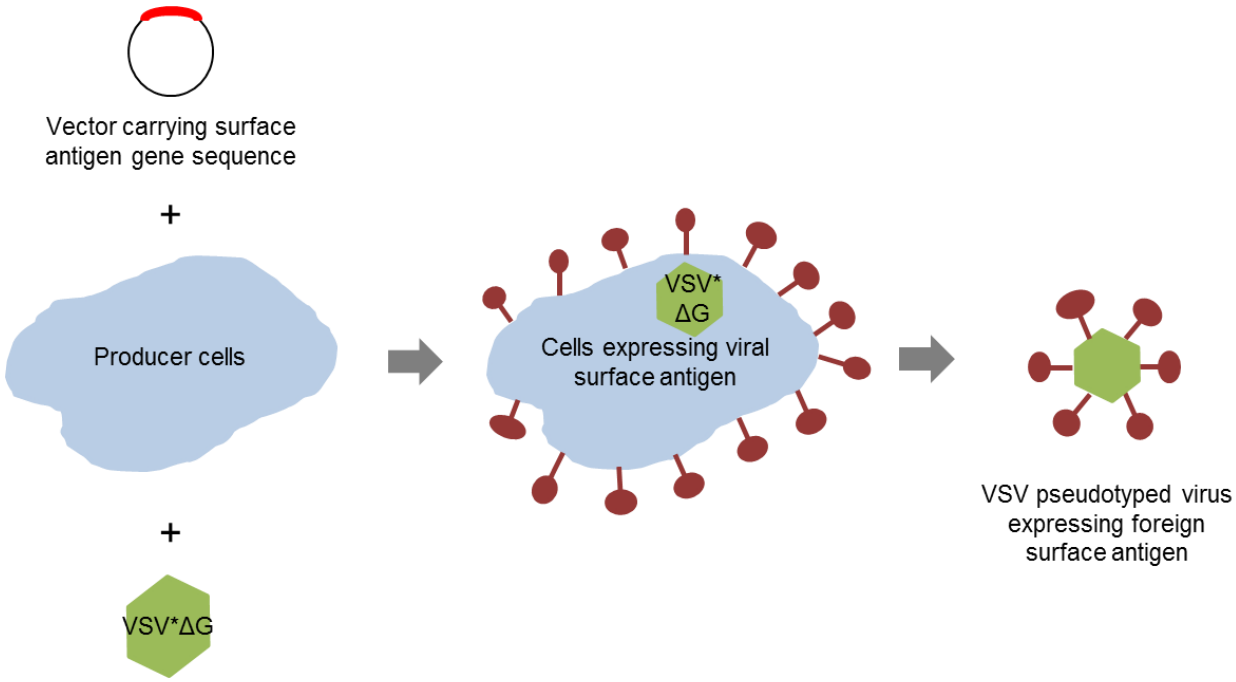

Figure 1.4. Pseudoparticle production using the VSV*ΔG system. Cells used for the production of pseudoparticles are transfected with plasmids carrying the surface antigen of interest's gene sequence. After transfection, cells are infected with the VSV*ΔG pseudoparticles and when the pseudoparticles bud from the cells, which are expressing the foreign surface antigen, the particles carry the surface antigen.

The propagation of pseudoparticles can also be achieved through the use of various plasmids carrying the genes required (Wool-Lewis & Bates, 1998; Giroglou *et al.*, 2004; Simmons *et al.*, 2004; Belouzard *et al.*, 2009; Wang *et al.*, 2016; Lau *et al.*, 2018b; Wang *et al.*, 2018). The triple plasmid transfection assay involves transfecting cells with three plasmids in order to produce pseudoparticles (Wool-Lewis & Bates, 1998; Giroglou *et al.*, 2004; Simmons *et al.*, 2004; Belouzard *et al.*, 2009; Wang *et al.*, 2016; Lau *et al.*, 2018b; Wang *et al.*, 2018). One plasmid contains the group-specific antigen and polymerase gene sequences of a retrovirus such as human immunodeficiency virus or murine leukemia virus, a second plasmid carries the gene sequence for a reporter gene and another vector has the gene sequence of the surface protein(s) of interest (Wool-Lewis & Bates, 1998; Giroglou *et al.*, 2004; Simmons *et al.*, 2004; Belouzard *et al.*, 2009; Wang *et al.*, 2016; Lau *et al.*, 2018b; Wang *et al.*, 2018). The transfected cells express the desired surface protein(s), pseudoparticles carrying the reporter proteins

assemble within the cells with the aid of the retroviral proteins and bud from cells bearing the desired surface protein(s) (Wool-Lewis & Bates, 1998; Giroglou *et al.*, 2004; Simmons *et al.*, 2004; Belouzard *et al.*, 2009; Wang *et al.*, 2016; Lau *et al.*, 2018b; Wang *et al.*, 2018).

Another method to construct strictly plasmid-based pseudoparticles involves the transfection of cells with a plasmid(s) carrying the genetic sequences for the structural proteins of the virus of interest (Mortola & Roy, 2004). Reporter genes can be included in the plasmids for *in vitro* visualisation purposes. Viral capsids are assembled and released, making it possible to harvest the pseudoparticles that resemble the virus of interest, but does not contain any genetic material (Mortola & Roy, 2004).

Wang *et al.* (2016) made use of a lentivirus-based pseudotyped system in order to produce pseudoparticles expressing the S proteins of SARS-CoV, MHV, HCoV-229E, HCoV-OC43, IBV, BCoV, porcine epidemic diarrhoea virus (PEDV) or TGEV. These pseudoparticles were used to test the susceptibility of HEK (strain 293), African green monkey kidney (Vero-CCL-81), human liver (Huh-7), porcine kidney (PK) (strain 15) and feline kidney (CCL94) cells by monitoring the viruses' infectivity for each cell type. It was found that pseudoparticles bearing the S protein of SARS-CoV were able to infect only HEK-293 cells (Wang *et al.*, 2016). HEK-293 cells were also susceptible to infection by pseudoparticles expressing the S proteins of HCoV-OC43, IBV, BCoV, PEDV and TGEV (Wang *et al.*, 2016). Furthermore, it was found that pseudotyped viruses bearing the PEDV- and TGEV S proteins were able to infect Vero-CCL-81, Huh-7 and PK-15 cells, but CCL94 cells were only susceptible to infection by TGEV-S-bearing pseudoparticles (Wang *et al.*, 2016).

In 1998, Wool-Lewis and Bates constructed pseudoparticles expressing the glycoprotein of the Ebola viruses using a murine leukemia virus-based system. The pseudoparticles were used to test the susceptibility of various cell lines, including HEK-293, Swiss albino mouse embryo fibroblasts (NIH 3T3), human cervical carcinoma (HeLa), Vero, MDCK, Madin-Darby bovine kidney (MDBK), PK-15, human B cell precursor leukemia (Nalm-6), human B lymphoblast (Daudi), human T lymphocyte (HUT-78) and mouse B lymphocyte (WEHI) cells. It was found that the pseudoparticles were not able to infect any of the lymphoid cells, an observation that concurs with the literature (Wool-Lewis & Bates, 1998). Pseudoparticles were successful in entering all other tested cell lines, including cells that have never been successfully infected *in vivo*, such as fibroblasts originating from Swiss albino mice embryos. This suggests that Ebola

viruses are able to enter these cells, but that the spread of infection is inhibited by host immune systems (Wool-Lewis & Bates, 1998).

The current study was based on work previously done by Hoffmann *et al.* (2013). The research group produced pseudoparticles expressing the surface proteins of SARS-CoV, Marburg virus, Sendai virus, bovine respiratory syncytial virus and influenza virus strains H1N1, H7N7 and H9N2. Various cell lines, including *Rousettus aegyptiacus* kidney (RoNi/7), *Hypsignathus monstrosus* kidney (HypNi/1.1), *Epomops buettikoferi* kidney (EpoNi/22.1), *Rhinolophus alcyone* lung (RhiLu/1.1), *Carollia perspicillata* lung (CpLu) and *Tadarida brasiliensis* lung (Tb 1 Lu) cells were inoculated with the pseudoparticles. Infection was monitored with fluorescence microscopy detecting GFP expression or measuring luciferase activity. None of the cell lines were susceptible to infection with pseudoparticles bearing the SARS-CoV S protein. Furthermore, it was found that all cells lines were susceptible to infection with Marburg virus, Sendai virus and bovine respiratory syncytial virus. Infection of Ro/Ni/7, HypNi/1.1, EpoNi/22.1 and CpLu cells with the three influenza viruses resulted in high numbers of infected cells, whereas fewer infected cells were observed when infecting RhiLu/1.1 and Tb 1 Lu cells.

The characterisation of viral proteins responsible for binding to and fusing with host cells, and the investigation of host tropism, play significant roles in the detection and possible prevention of viral spread. Investigating the host ranges of emerging viruses and understanding the factors that contribute to zoonotic emergence is beneficial to possible future outbreak preparedness.

CHAPTER 2

2 Materials & Methods

2.1 Ethics

Ethical clearance was obtained for the testing of bat faecal samples for coronaviruses from Stellenbosch University's Research Ethics Committee: Animal Care and Use (Protocol number SU-ACUD16-00008). The letter of ethics approval can be found in Addendum A.

2.2 Materials

A comprehensive list of the consumables, equipment and software used is provided in Table B.1 in Addendum B. Table 2.1 provides a list of all the kits and reagents used in this study.

Table 2.1. List of kits and reagents used.

Kit/reagent	Catalogue number	Company	Country
Reagents for general use			
Dulbecco's Phosphate Buffered Saline	L0615-500	Biowest	France
BioWhittaker Dulbecco's Phosphate Buffered Saline	BE17-512F	Lonza Group	Switzerland
BioWhittaker Phosphate Buffered Saline	BE17-516Q	Lonza Group	Switzerland
Dulbecco's Phosphate Buffered Saline	D8537-500ML	Sigma-Aldrich	United States of America (USA)
Gibco Dulbecco's Phosphate Buffered Saline	14190-094	Thermo Fisher Scientific	USA
BioWhittaker Phosphate Buffered Saline (10×)	BE17-517Q	Lonza Group	Switzerland
Ethyl alcohol, pure	E7023-500ML	Sigma-Aldrich	USA
Kits and reagents for molecular methods			
NucleoSpin RNA Virus kit	740956.250	Macherey-Nagel	Germany
Maxima Reverse Transcriptase kit	EP0743	Thermo Fisher Scientific	USA
dNTP Mix	BIO-39029	Bioline	United Kingdom (UK)
RiboLock RNase	EO0381	Thermo Fisher Scientific	USA

Inhibitor			
Maxima Hot Start *Taq* DNA Polymerase kit	EP0601	Thermo Fisher Scientific	USA
One*Taq* Hot Start DNA Polymerase kit	M0481	New England Biolabs	USA
TopVision Agarose Tablets	R2801	Thermo Fisher Scientific	USA
Sodium hydroxide pellets	AB006498.500	Merck	USA
Boric acid	AC000165.500	Merck	USA
Pronasafe Nucleic Acid Staining solution (20 000×)	CK130	Laboratorios CONDA	Spain
GeneRuler 1kb DNA Ladder	SM0311	Thermo Fisher Scientific	USA
6× DNA Loading Dye	R0611	Thermo Fisher Scientific	USA
NucleoSpin Gel and PCR Clean-up kit	740609.250	Macherey-Nagel	Germany
BigDye Terminator v3.1 Cycle Sequencing kit	4336917	Thermo Fisher Scientific	USA
BigDye Xterminator Purification kit	4376487	Thermo Fisher Scientific	USA
InsTAclone PCR Cloning kit	K1214	Thermo Fisher Scientific	USA
Mix & Go Competent Cells - Strain JM109	T3005	Zymo Research	USA
LB Broth	61748	Fluka BioChemika	Switzerland
Agar	A7002-1KG	Sigma-Aldrich	USA
Ampicillin Sodium	A0104	Melford Biolaboratories Ltd.	UK
IPTG	I6758-5G	Sigma-Aldrich	USA
X-Gal	R0404	Thermo Fisher Scientific	USA
One Shot Top 10 Chemically Competent Cells	C404010	Thermo Fisher Scientific	USA
SOC Medium	S2630	Melford Laboratories Ltd.	UK
GeneJET Plasmid	K0503	Thermo Fisher Scientific	USA

Miniprep kit			
GeneJET Plasmid Midiprep kit	K0482	Thermo Fisher Scientific	USA
Eco*RI*	R0101M	New England Biolabs	USA
MinElute PCR Purification kit (250)	28006	Qiagen	Germany
TranscriptAid T7 High Yield Transcription kit	K0441	Thermo Fisher Scientific	USA
Invitrogen PureLink RNA Mini kit	12183018A	Thermo Fisher Scientific	USA
β-Mercaptoethanol, Molecular Biology Grade	44-420-3250ML	Calbiochem™	USA
Qubit RNA HS Assay kit	Q32852	Thermo Fisher Scientific	USA
SensiFAST Probe No-ROX One-Step kit	BIO-76005	Bioline	UK
Kits and reagents for cell culture			
DMEM High Glucose	L0102-500	Biowest	France
BioWhittaker DMEM	BE12-614F	Lonza Group	Switzerland
Penicillin-Streptomycin Solution 100×	L0022-100	Biowest	France
BioWhittaker Pen-Strep	BW17-602E	Lonza Group	Switzerland
Gibco Pen Strep	15140-122	Thermo Fisher Scientific	USA
BioWhittaker NEAA 100×	BE13-114E	Lonza Group	Switzerland
BioWhittaker Na pyruvate (100 mM solution)	BE13-115E	Lonza Group	Switzerland
BioWhittaker L-glutamine	BE17-605F	Lonza Group	Switzerland
Gibco L-glutamine 200mM (100×)	25030-032	Thermo Fisher Scientific	USA
Fetal Bovine Serum	S181Y-50	Biowest	France
Gibco Fetal Bovine Serum	10499-044	Thermo Fisher Scientific	USA
Trypsin-EDTA 1× in PBS	L0940-500	Biowest	France
BioWhittaker Trypsin 10× (diluted to 1×)	BE02-007E	Lonza Group	Switzerland

Gibco Trypsin/EDTA solution (1×)	R-001-100	Thermo Fisher Scientific	USA
Accutase	L0950-100	Biowest	France
Dimethyl Sulfoxide	D8418-50ML	Sigma-Aldrich	USA
100mg Amphotericin B - solubilized	A9528-100MG	Sigma-Aldrich	USA
Gibco OptiPRO Serum-Free Medium	12309-050	Thermo Fisher Scientific	USA
Mifepristone	M8046-100MG	Sigma-Aldrich	USA
Formaldehyde Solution (40% w/v)	N/A	BDH Laboratory Supplies Limited	UK
Formaldehyde Solution	SAAR2436020LP	Merck	USA
Invitrogen Lipofectamine 2000	11668-027	Thermo Fisher Scientific	USA
DAPI (4',6-diamidino-2-phenylindole, dihydrochloride)	D1306	Thermo Fisher Scientific	USA
ProLong Gold antifade reagent	P10144	Thermo Fisher Scientific	USA

Bat faecal samples that were screened for coronaviruses were previously collected as part of a bigger research project by collaborators at the University of KwaZulu-Natal. These collaborators, under the guidance of Prof. M. Schoeman, are trained zoologists and ecologists who sourced these samples with the relevant permits. Details on these samples can be found in Table C.1 in Addendum C.

The primer and probe sequences used for reverse transcription, PCR and RT-qPCR assays are listed in Table 2.2.

Table 2.2. Primers and probe used in reverse transcription, PCR and RT-qPCR assays.

Primers used for reverse transcription			
Primer name	**Catalogue number**	**Company**	**Country**
Random hexamer primers	BIO-38028	Bioline	UK
Primers used in coronavirus screening PCR			
Primer name		**Primer sequence (5' - 3')**	
PCAs4		CACACAACACCTTCATCAGATAGAATCATCA	
Gr1Sp	Gr1Sp_F1	TTCTTTGCACAGAAGGGTGATGC	

	Gr1Sp_F2	CTTTGCACAAAAAGGTGATGCWGC
RGU_2c**Error! ookmark not defined.**	RGU_2c_F1	TTYGCDCAAGATGGAMATGCTGC
	RGU_2c_F2	TTYGCDCAAGATGGTMATGCTGC
SP3080 F1		CTTCTTCTTTGCTCAGGATGGCAATGCTGC
SP3374 F3		CTATAACTCAAATGAATCTTAAGTATGC
Primers used in *Mycoplasma* screening		
Primer name		**Primer sequence (5' - 3')**
Myco-5-1		CGCCTGAGTAGTACGTTCGC
Myco-5-2-1		CGCCTGAGTAGTACGTACGC
Myco-5-2-2		TGCCTGAGTAGTACATTCGC
Myco-5-2-3		TGCCTGGGTAGTACATTCGC
Myco-5-5		CGCCTGGGTAGTACATTCGC
Myco-5-6		CGCCTGAGTAGTATGCTCGC
Myco-3-1		GCGGTGTGTACAAGACCCGA
Myco-3-2		GCGGTGTGTACAAAACCCGA
Myco-3-3		GCGGTGTGTACAAACCCCGA
Primers used in sequencing PCR of cloning products		
Primer name		**Primer sequence (5' - 3')**
M13 Forward		GTAAAACGACGGCCAG
M13 Reverse		CAGGAAACAGCTATGAC
T7 promoter primer		TAATACGACTCACTATAGGG
Primers used in RT-qPCR		
Primer name		**Primer sequence (5' - 3')**
2c_RdRp_qPCR_F		GTGYGCTCAAGTGYTWAGTGARTATGT
2c_RdRp_qPCR_R		CCATTAGCRCYCATAAGTGCACTAACA
Probe used in RT-qPCR		
Probe name		**Probe sequence (5' - 3')**
2c_RdRp_qPCR_P		FAM-GCWTAYGCC/ZEN/AATAGTGTYTTTAACAT/3IABkFQ

All PCR primers, RT-qPCR primers and the RT-qPCR probe were purchased from Integrated DNA Technologies (IDT) (USA). The primers used for sequencing of cloned products were included in the InsTAclone PCR Cloning kit.

Primer PCAs4 was used as reverse primer in all screening PCR reactions. Both of the Gr1Sp and RGU_2c primers were used in equimolar dilutions in the screening PCRs.

Gr1Sp primers were designed to detect alphacoronaviruses; RGU_2c primers were designed for the detection of MERS-related betacoronaviruses; and SP3080 F1 and SP3374 F3 were designed for the detection of SARS-related betacoronaviruses. The Gr1Sp, SP3080 F1 and SP3374 F3 primers were designed by Drexler *et al.* (2010); RGU_2c primers were designed by Dr N. Ithete (Cronjé, 2017). Primer PCAs4 was originally designed by de Souza Luna *et al*. (2007) and has subsequently been used as the reverse primer for other coronavirus screening PCRs.

The primers and probe for the RT-qPCR targeting MERS-related betacoronaviruses were designed by Dr N. Ithete.

The primers used in the screening for *Mycoplasma* contamination were designed by Wirth *et al.* (1994) for the detection of *M. orale*, *M. arginini*, *M. hyorhinis*, *M. fermentans*, *M. hyopneumoniae*, *M. salivarium*, *M. gallisepticum*, *M. pneumoniae*, *M. hominis*, *M. bovis*, *M. californicum*, *M. bovigenitalium*, *M. bovoculi*, *M. mycoides*, *M. bovirhinis*, *M. alkalescens*, *M. canadense*, *M. synoviae*, *M. verecundum*, *M. gatae*, *M. meleagridis*, *M. gallinarum*, *M. iowae*, *M. pullorum*, *M. gallinaceum*, *M. gallopavonis*, *M. arthridis*, *Acholeplasma laidlawii* and *A. axanthum*. Equimolar dilutions with a final concentration of 10 µM of each primer were made of the forward primers (designated Myco-5) and of the reverse primers (designated Myco-3), respectively.

A gBlocks Gene Fragment (IDT) of a region of the *M. bovis* genome (GenBank accession number: CP002188) (positions 321 910 to 322 530) was purchased from IDT and used as a positive control when screening for *Mycoplasma* contamination.

The pCG1 plasmids containing inserts of interest for use in the preparation of pseudoparticles were obtained from collaborators at the Charité University Hospital in Berlin, Germany. The inserts and designated names of these plasmids can be found in Table 2.3.

Table 2.3. Plasmids used for pseudoparticle preparation.

Insert	**Designated name of plasmid with insert**
VSV-G	pCG1-VSV-G
No insert (empty vector [EV])	pCG1-EV
MERS-CoV S protein	pCG1-MERS-S
NeoCoV S protein	pCG1-NCV-S
SARS-CoV S protein	pCG1-SARS-S

Plasmid pCG1-VSV-G was used to generate a positive control, while pCG1-EV was used for production of a negative control. The other three plasmids aided in producing pseudoparticles expressing the three coronaviruses' S proteins.

2.3 Methods

2.3.1 Molecular methods

2.3.1.1 Screening of bat faecal samples for NeoCoV

2.3.1.1.1 Homogenisation of bat faecal samples

Bat faecal samples collected from different bat species in 2017 and stored in viral transport medium (VTM) (consisting of Dulbecco's Modified Eagle Medium [DMEM] supplemented with 1% v/v amphotericin B and 1% v/v penicillin-streptomycin) were homogenised according to the protocol described by Dr N. Cronjé (2017). This was achieved by adding one faecal pellet (weight ≈ 30 mg) from each sample (see Table C.1 in Addendum C) to separate 2 ml microcentrifuge tubes each containing five 2.4 mm metal beads and 1 ml phosphate buffered saline (PBS). The microcentrifuge tubes were placed in the TissueLyser LT and oscillated for five minutes at 50 Hz. After oscillation, the microcentrifuge tubes were centrifuged at 12 000 × *g* for two minutes and the supernatants transferred to sterile microcentrifuge tubes. The homogenates were stored at -80°C.

2.3.1.1.2 Extraction of viral RNA from homogenised bat faecal samples and cell culture supernatant

RNA was extracted from homogenised bat faecal samples (section 2.3.1.1.1) and from supernatant removed from cell cultures inoculated with virus-positive homogenate (refer to section 2.3.3) using the NucleoSpin RNA Virus kit. The manufacturer's protocol was followed. Briefly, 150 µl of homogenised sample or cell culture supernatant was mixed with 600 µl buffer RAV1 containing 1% v/v carrier RNA and incubated at 56°C. Thereafter, 600 µl ethanol (96% v/v) was added to the mixture, followed by loading up to 700 µl of sample mixture to a provided NucleoSpin RNA Virus Column in a collection tube. The column was centrifuged at 8 000 × *g* for one minute, the flow-through discarded and the centrifugation repeated after loading the remaining sample mixture onto the column. Washing steps were performed by adding 500 µl wash buffer RAW and 600 µl wash buffer RAV3 onto the column in subsequent steps, centrifuging the column at 8 000 × *g* for one minute after each loading step. After discarding the flow-through, 200 µl wash buffer RAV3 was added to the column, followed by centrifugation at 11 000 × *g* for five minutes. Flow-through was discarded, after which the column was centrifuged

for an additional two minutes at 11 000 × *g*. The column was placed in a 1.5 ml microcentrifuge tube and 50 µl nuclease-free water pre-heated to 70°C was added to the column and incubated at room temperature for one minute. The tube with the column was centrifuged at 11 000 × *g* for one minute and eluted RNA was stored at -80°C.

2.3.1.1.3 Reverse transcription

Complementary deoxyribonucleic acid (cDNA) strands was generated using RNA extracted from bat faecal samples as templates (section 2.3.1.1.2). The cDNA was subsequently used in the screening PCR reactions.

The Maxima Reverse Transcriptase kit was used and the reactions were prepared and incubated as shown in Tables 2.4 and 2.5.

Table 2.4. Preparation of the first reaction mixture for reverse transcription reactions.

First reaction mixture	
Component	**Volume (µl)**
RNA template	10.0
Random hexamer primer (10 µM)	1.5
Deoxyribonucleotide triphosphate (dNTP) mix (10 mM each)	1.0
Nuclease-free water	2.0
Total	**14.5**

Reactions were incubated at 65°C for five minutes, after which they were chilled on ice for one minute. Thereafter, the second reaction mixture, as seen in Table 2.5, was added to each reaction and reactions were incubated according to the parameters in Table 2.5.

Table 2.5. Preparation of the second reaction mixture and incubation of reverse transcription reactions.

Second reaction mixture	
Component	**Volume (µl)**
5× RT Buffer	4.0
RiboLock RNase inhibitor (40 U/µl)	0.5
Maxima Reverse Transcriptase (200 U/µl)	1.0
Total	**5.5**
Incubation	
Temperature (°C)	**Time (minutes)**
25	10
50	30
85	5
4	∞

Products of reverse transcription were stored at -20°C until further use.

2.3.1.1.4 Amplification of cDNA

The cDNA obtained through reverse transcription (section 2.3.1.1.3) was screened using a PCR targeting a region of roughly 900 base pairs (bp) of the RNA-dependent RNA polymerase (RdRp) gene of certain alphacoronaviruses, MERS-related betacoronaviruses and SARS-related betacoronaviruses. Four different primer sets (Table 2.2) (Drexler *et al.*, 2010; Cronjé, 2017) were used for screening; i.e. four reactions were prepared for each sample that was screened, each using a different set of primers. The PCRs will hereafter be referred to as PCR Gr1Sp, PCR RGU_2c, PCR SP3080 F1 and PCR SP3374 F3. The reverse primer (PCAs4) binds to the NeoCoV genome (GenBank accession number: KC869678) from positions 15 689 to 15 719. The Maxima Hot Start *Taq* DNA Polymerase kit was used and reactions were prepared as described in Table 2.6.

Table 2.6. Reaction mixture for PCR reactions.

Component	Volume (µl)
10× Hot Start PCR Buffer	2.5
dNTP mix (10 mM each)	0.5
Forward primer 1 (10 µM)	1.25
Forward primer 2 (where applicable) (10 µM)	1.25
Reverse primer (10 µM)	1.25
$MgCl_2$ (25 mM)	1.5
cDNA template	2.5
Maxima Hot Start *Taq* DNA Polymerase (5 U/µl)	0.125
Nuclease-free water	to 25.0
Total	**25.0**

Thermal cycling of these reactions was done according to the parameters described in Table 2.7. Thermal cycling was done at maximum ramp speed. Ten touchdown cycles, decreasing by 1°C in each annealing step, were followed for the first stage of the PCR thermal cycling.

Table 2.7. Thermal cycling parameters for PCR reactions.

Temperature (°C)	Time	
95	4 minutes	
95	20 seconds	×10 touchdown cycles (-1°C)
60	50 seconds	
72	1 minute	
95	20 seconds	×50 cycles
54	50 seconds	
72	1 minute	
72	5 minutes	
4	∞	

Products of amplification were stored at -20°C until further use.

2.3.1.2 Screening cell cultures for *Mycoplasma* contamination

Mycoplasma contamination poses a threat to cell cultures, resulting in unreliable results when transfecting and infecting cells (Rottem & Barile, 1993; Uphoff & Drexler, 2002a; Uphoff & Drexler, 2004). Aliquots of supernatants were taken off cell cultures prior to transfection and infection experiments (refer to sections 2.3.3 – 2.3.4) and stored at -20°C until required. These

aliquots were subsequently used for screening for *Mycoplasma* contamination using a method described by Uphoff and Drexler (2002a; 2004), which detects a 500 bp fragment of the *Mycoplasma* genome by PCR. This was achieved by using the One*Taq* Hot Start DNA Polymerase kit according to the manufacturer's instructions.

Supernatant was removed from cell cultures prior to transfection/infection, heated to 95°C for five minutes to lyse cells and centrifuged at 16 000 × *g* for two minutes to remove cell debris. Thereafter, 2 µl of the supernatant was added to the reaction mixtures to act as template. Reaction mixtures were prepared according to the method described in Table 2.8. The 620 bp gBlocks Gene Fragment of the *M. bovis* genome was used as positive control, of which 5 µl with a concentration of 10 ng/µl was used as template.

Table 2.8. Reaction mixtures for *Mycoplasma* screening PCR reactions.

Component	Volume (µl)
5× One*Taq* Standard Reaction Buffer	5.0
dNTPs (10 mM each)	0.5
Forward primer mix (10 µM each)	0.5
Reverse primer mix (10 µM each)	0.5
One*Taq* Hot Start DNA Polymerase (5 U/µl)	0.125
Template DNA	1-1000 ng
Nuclease-free water	to 25.0
Total	**25.0**

Thermal cycling of the reactions was then performed according to the parameters described in Table 2.9.

Table 2.9. Thermal cycling parameters for *Mycoplasma* screening PCR reactions.

Temperature (°C)	Time	
94	30 seconds	
94	30 seconds	
50	30 seconds	×5 cycles
68	35 seconds	
94	15 seconds	
56	15 seconds	×30 cycles
68	30 seconds	
68	10 minutes	
4	∞	

2.3.1.3 Agarose gel electrophoresis and visualisation of amplified products

Agarose gel electrophoresis was performed to visualise DNA amplified by PCR. This was done by adding TopVision Agarose tablets to 1× sodium boric acid (SB) buffer prepared as described by Brody and Kern (2004) at a concentration of 1% w/v. After dissolving the agarose tablet, the mixture was boiled and swirled to mix thoroughly. After cooling slightly, Pronasafe Nucleic Acid Staining solution (20 000×) was added to the mixture at a concentration of 7% v/v. This was poured in a gel tray and allowed to set before submerging in 1× SB buffer in an electrophoresis tank.

Samples were loaded into the wells after mixing 1 µl 6× loading dye with 4.5 µl PCR product. Furthermore, 3 µl GeneRuler 1kb DNA Ladder was mixed with 1 µl 6× loading dye and added to the gel as a reference sizing marker. Electrophoresis was carried out for 40 minutes at 90 volts. Gels were visualised using the UVITec Gel Documentation System operated by UVIproChemi software. Amplified products of the desired sizes, as can be seen in Table 2.10, were processed further in order to obtain genomic sequences of the amplified products.

Table 2.10. Desired sizes of amplified DNA for all PCRs.

PCR	Desired product size (bp)
PCR Gr1Sp	974
PCR RGU_2c	974
PCR SP3080 F1	974
PCR SP3374 F3	682
Mycoplasma screening PCR	500

2.3.1.4 Purification of PCR products

The NucleoSpin Gel and PCR Clean-up kit was used to purify the desired PCR products as determined by agarose gel electrophoresis (section 2.3.1.3). Products were purified according to the manufacturer's protocol. The complete PCR product was mixed with double the volume of binding buffer NTI and loaded onto a provided NucleoSpin Gel and PCR Clean-up Column in a collection tube. The column was centrifuged at 11 000 × *g* for 30 seconds. The flow-through was discarded and 700 µl wash buffer NT3 was added to the column. The column was centrifuged at 11 000 × *g* for one minute, flow-through was discarded and the washing step was repeated. The column was centrifuged at 11 000 × *g* for one minute after the second washing step, after which the column was placed in a 1.5 ml microcentrifuge tube. The column was incubated with 20 µl

elution buffer NE for one minute and centrifuged at 11 000 × *g* for one minute. Eluted products were stored at -20°C until further use.

2.3.1.5 Spectrophotometric analysis

The concentration of genomic material in purified samples was determined with the NanoDrop ND-1000 Spectrophotometer V3.1.0 before use in subsequent reactions. ND-1000 V3.1.0 software was used to analyse and capture data. First, the optical surfaces of the instrument were wiped down with ethanol and distilled water, after which 1 µl nuclease-free water was loaded onto the instrument to initialise it. After initialisation, optical surfaces were cleaned with ethanol and distilled water; thereafter, 1 µl of the substance used for elution of the specific sample was loaded onto the instrument and a blank measurement was taken. The optical surfaces were cleaned with ethanol and water, after which the concentration of genomic material of each sample was measured. This was achieved by loading 1 µl of sample onto the instrument and taking a measurement using the ND-1000 V3.1.0 software. Optical surfaces were cleaned with ethanol and water after each measurement.

2.3.1.6 Sequencing PCR and analysis

Purified DNA fragments obtained through PCR, as well as purified plasmids (refer to section 2.3.1.10) and cultures yielding products during *Mycoplasma* screening (section 2.3.1.2), were sequenced by the Sanger method using the BigDye Terminator v3.1 Cycle Sequencing kit according to the manufacturer's protocol. Reaction mixtures were prepared as described in Table 2.11.

Table 2.11. Reaction mixture for sequencing reactions.

Component	Volume (µl)
Nuclease-free water	2
BigDye Terminator v1.1, v3.1 5× Sequencing Buffer	3
BigDye Terminator v3.1 Cycle Sequencing RR-100	1
DNA template (10 ng/µL)	2
Primer (2.5 µM)	2
Total	**10**

Separate reactions were prepared with each of the primers used to amplify each sample. Thus, two reactions, one with a forward primer and another with a reverse primer, were prepared for samples amplified with PCRs SP3080 F1 and SP3374 F3, and three were prepared for products of PCRs Gr1Sp and RGU_2c to accommodate the second forward primer. For the sequencing of

plasmids, a forward and a reverse primer were selected based on the binding sites available on the plasmid; i.e. the M13 primers were used when sequencing pTZ57R/T, whereas the M13 forward primer and the T7 promoter primer were used when sequencing pCG1.

The reactions underwent thermal cycling at the parameters detailed in Table 2.12, setting the thermal cycler to maximum ramp speed.

Table 2.12. Thermal cycling parameters for sequencing reactions.

Temperature (°C)	Time	
96	1 minute	
95	10 seconds	×30 cycles
54	5 seconds	
60	4 minutes	
4	∞	

After thermal cycling, reactions were purified using the BigDye Xterminator Purification kit. Briefly, 45 µl of SAM Solution and 10 µl Xterminator Solution Buffer was added to each reaction before vortexing for 30 minutes. Thereafter, the DNA fragments were sent to Stellenbosch University's Central Analytical Facility (CAF) for sequencing electrophoresis. The sequencing data files were analysed and contiguous sequences were assembled with the molecular biology analysis tool Geneious R10 bioinformatics software. Genomic similarity was determined by using the Basic Local Alignment Search Tool (BLAST) online tool developed by the National Center for Biotechnology Information (NCBI) (USA) (available online at https://blast.ncbi.nlm.nih.gov/Blast.cgi).

Sequences obtained from sequencing of the PCR products were used to identify a NeoCoV-related sample to be used in attempts at isolating NeoCoV in cell culture (refer to section 2.3.3). Sequencing of the plasmids was performed to confirm the presence of the desired inserts.

2.3.1.7 Ligation

In order to generate *in vitro* transcribed RNA positive controls for RT-qPCR, a purified PCR product obtained from a NeoCoV-screening positive sample (purified PCR RGU_2c product of sample 23) was cloned into pTZ57R/T vector (Figure 2.1) using the InsTAclone PCR cloning kit according to the manufacturer's protocol. The reaction was prepared according to the guidelines in Table 2.13.

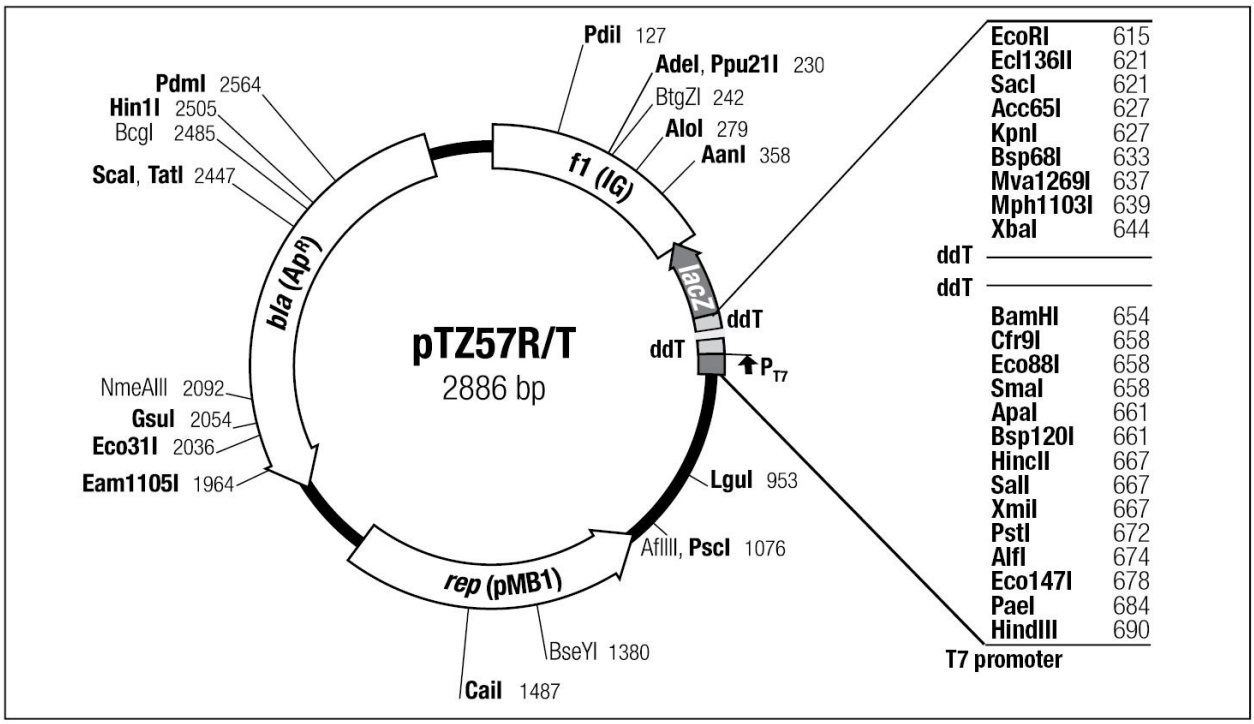

Figure 2.1. pTZ57R/T vector map indicating restriction sites, genes and cloning region (Thermo Fisher Scientific, 2016).

Table 2.13. Reaction mixture for ligation reaction.

Component	Volume (µl)
Nuclease-free water	to 30
Vector pTZ57R/T (55 ng/µl)	3
5× Ligation Buffer	6
DNA fragment (17 ng/100 bp)	166 ng
T4 DNA Ligase	1
Total	**30**

The reaction was incubated at the parameters developed by Dr R. Fisher (2016) described in Table 2.14.

Table 2.14. Incubation parameters for ligation reaction.

Temperature (°C)	Time
25	2 hours
4	16 hours
75	5 minutes
4	∞

Products were stored at -20°C after incubation.

2.3.1.8 Bacterial transformation of plasmids

Agar was prepared before transformation experiments. This was done by adding 7.5 g agar to 500 ml distilled water and autoclaving it. Once the agar mixture had reached ~50°C, 0.05 mg/ml ampicillin was added to the mixture. The mixture was then poured onto agar plates, 25 ml agar per plate, and stored at 4°C until needed.

2.3.1.8.1 Transformation using *Mix & Go* Competent Cells

Mix & Go Competent Cells (Strain JM109) were transformed with the pTZ57R/T clone containing the NeoCoV RdRp region insert according to the manufacturer's instructions. Briefly, 1.25 µl of ligation product prepared through the method described in section 2.3.1.7 was mixed with 25 µl competent cells and incubated on ice for five minutes. Thereafter, the cells were spread on a pre-warmed agar plate along with 40 µl isopropyl β-D-1-thiogalactopyranoside (IPTG) (1 mM) and 16 µl 5-bromo-4-chloro-3-indolyl -D-galactopyranoside (X-gal) (2% w/v). The plate was incubated overnight at 37°C.

The pTZ57R/T plasmid facilitates blue-white colony screening as a visual means to assess successful transformation. Colonies containing inserts were white in colour due to blue-white screening, which is observed when an insert disrupts the *lacZ* gene on the plasmid. If the *lacZ* gene was still intact, the colony would be able to utilise the X-gal on the plate, leading to the formation of a blue colour. Therefore, the formation of a blue colony would mean that ligation was unsuccessful, and a white colony that ligation was successful.

2.3.1.8.2 Transformation using One Shot Top 10 Chemically Competent Cells

One Shot Top 10 Chemically Competent Cells were transformed with the plasmids to be used in the preparation of the pseudoparticles (Table 2.3; refer to section 2.3.4.2.1). The manufacturer's protocol was followed. Briefly, a vial of cells was thawed on ice for each of the plasmids and 1 µl of plasmid DNA was mixed with the cells in the corresponding vial. Cells were incubated on ice for 30 minutes, after which cells were heat-shocked at 42°C for 30 seconds. Cells were subsequently incubated on ice for two minutes and 250 µl of SOC Medium was added to each vial. Vials were incubated at 37°C, shaking at 225 rpm for one hour. Cells were then spread on pre-warmed agar plates along with 40 µl IPTG (1 mM) and 16 µl X-gal (2% w/v). Plates were incubated at 37°C overnight.

The plasmid pCG1 contains the *lacZ* gene. Blue-white colony screening, as described in section 2.3.1.8.1, was used for the selection of competent cells transformed with plasmids that contain

inserts. A blue colony was selected in the case of plasmid pCG1-EV, as the plasmid did not contain an insert.

2.3.1.9 Preparation of liquid cultures of transformed colonies

Lysogeny broth (LB) medium was prepared by adding 10 g LB broth and 7.5 g agar to 500 ml distilled water and autoclaving the mixture. Thereafter, 0.05 mg/ml ampicillin was added to the LB medium and the medium was inoculated with positive colonies detected through blue-white screening. A positive colony obtained in section 2.3.1.8.1 was used to inoculate 5 ml LB medium; positive colonies obtained in section 2.3.1.8.2 were used to inoculate 200 ml LB medium each. Different volumes were used for these two procedures as only a small amount of plasmids carrying the NeoCoV RdRp fragment was required, whereas larger amounts of pCG1 vectors with inserts were required for the subsequent procedures. The liquid cultures were incubated at 37°C overnight, shaking at a speed of 225 rpm.

2.3.1.10 Purification of plasmid DNA

2.3.1.10.1 Purification of plasmids carrying NeoCoV RdRp fragment

Since the transformed cells containing the cloned PCR product of interest was cultured in a volume less than 10 ml, the GeneJET Plasmid Miniprep kit was used to purify the plasmid DNA that was produced through liquid culture (section 2.3.1.9). The manufacturer's protocol was followed. Firstly, the liquid culture was centrifuged at 4 000 × *g* for five minutes and the supernatant was removed. Cells were resuspended in 250 µl resuspension solution and mixed by pipetting, after which 250 µl lysis solution was added to lyse cells. The contents of the tube were mixed by inversion and 350 µl neutralisation solution was added to the sample and mixed. The tube was centrifuged at 12 000 × *g* for five minutes, after which the supernatant was transferred to a provided GeneJet Spin Column in a collection tube. The column was centrifuged at 12 000 × *g* for one minute. The membrane was washed by adding 500 µl wash solution and centrifuging for one minute at 12 000 × *g*. The washing step was repeated once, after which the empty tube was centrifuged for one minute at 12 000 × *g*. The column was transferred to a 1.5 ml microcentrifuge tube, 50 µl elution buffer was added to the column and incubated at room temperature for two minutes. The column was centrifuged at 12 000 × *g* for two minutes and the products were stored at -20°C after sequencing to confirm the presence of the desired insert.

2.3.1.10.2 Purification of pCG1 vectors

As the cells transformed with pCG1 vectors were cultured in volumes of more than 50 ml, the GeneJET Plasmid Midiprep kit was used to purify the plasmid DNA that was obtained through

liquid culture (section 2.3.1.9). The manufacturer's protocol was followed by dividing each liquid culture into aliquots of 50 ml each. Cells were harvested by centrifuging the liquid cultures at 4 000 × *g* for 15 minutes and removing the supernatants. Cells were resuspended in 2 ml resuspension solution containing 4% v/v RNase A. Subsequently, 2 ml lysis solution was added to each tube and mixed by inverting, followed by addition of 2 ml neutralisation solution. After thoroughly mixing the contents of each tube separately, 0.5 ml endotoxin binding solution was added to each aliquot, mixed and incubated at room temperature for five minutes. After incubation, 3 ml ethanol (96% v/v) was added to each suspension and centrifuged at 4 000 × *g* for 50 minutes to remove cell debris. Supernatants were transferred to new centrifugation tubes and 3 ml ethanol (96% v/v) was added to each tube containing supernatant and mixed by inversion. Samples were loaded onto provided columns in collection tubes 5 ml at a time until the entire sample had been loaded. After each loading step, columns were centrifuged at 2 000 × *g* for three minutes, discarding flow-through afterwards. Washing steps were performed by adding 4 ml washing solution I to each column and centrifuging at 3 000 × *g* for two minutes. Flow-through was discarded and the second washing step was done by adding 4 ml washing solution II and centrifuging at 3 000 × *g* for two minutes. Flow-through was discarded and the second washing step repeated once. Columns were then centrifuged at 3 000 × *g* for five minutes, after which columns were placed in 15 ml centrifuge tubes. Plasmid DNA was eluted by adding 0.35 ml elution buffer to columns, incubating tubes at room temperature for two minutes and centrifuging for five minutes at 4 000 × *g*. Products were stored at -20°C after sequencing to confirm the presence of the desired inserts.

2.3.1.11 RT-qPCR

2.3.1.11.1 Preparation of *in vitro* transcribed RNA standard

Purified plasmid DNA containing the NeoCoV RdRp fragment (sections 2.3.1.7 - 2.3.1.10.1) was linearised by digestion with restriction enzyme *Eco*RI in order to prepare the circular plasmid DNA for *in vitro* transcription. A reaction mixture was prepared as described in Table 2.15.

Table 2.15. Reaction mixture for *Eco*RI digestion of plasmid DNA.

Component	Volume (µl)
Nuclease-free water	to 100
New England BioLabs 10× *Eco*RI Reaction Buffer	10
Purified DNA template (2 µg)	2 µg
New England BioLabs *Eco*RI (10 U/µl)	2
Total	**100**

The reaction was incubated according to the parameters described in Table 2.16.

Table 2.16. Incubation parameters for *Eco*RI digestion of plasmid DNA.

Temperature (°C)	Time (minutes)
37	60
65	20
4	∞

The product was then purified using the MinElute PCR Purification kit according to the manufacturer's protocol. Briefly, 300 µl adsorption buffer ERC was added to the *Eco*RI-digested product. The mixture was loaded onto a provided MinElute column in a microcentrifuge tube. The column was centrifuged at 17 900 × *g* for one minute. After discarding the flow-through, 750 µl wash buffer PE was added to the column and the column was centrifuged for one minute at 17 900 × *g*. The column was centrifuged again at 17 900 × *g* for one minute after discarding the flow-through. The column was transferred to a 1.5 ml microcentrifuge tube and 10 µl elution buffer EB was loaded onto the column, allowing it to incubate for one minute at room temperature. The column was centrifuged for one minute at 17 900 × *g*.

The purified product was *in vitro* transcribed using the TranscriptAid T7 High Yield Transcription kit according to the manufacturer's instructions. The mixture in Table 2.17 was prepared, after which it was incubated at 37°C for two hours.

Table 2.17. Reaction mixture for *in vitro* transcription reaction.

Component	Volume (µl)
Diethylpyrocarbonate-treated (DEPC-treated) water	to 20
5× TranscriptAid Reaction Buffer	4
ATP/CTP/GTP/UTP mix	8
Template DNA	1 µg
TranscriptAid Enzyme Mix	2
Total	**20**

The *in vitro* transcribed product was digested with DNase I to remove residual DNA and obtain a product consisting of only RNA. This was achieved by adding 4 units of DNase I to the reaction and incubating it at 37°C for 15 minutes.

The RNA was purified with the Invitrogen PureLink RNA Mini kit by following the manufacturer's protocol. The DNase I-digested product was mixed with 22 µl lysis buffer and 96% v/v ethanol each. This mixture was loaded onto a provided Spin Cartridge in a collection tube and

centrifuged at 12 000 × *g* for 15 seconds. The flow-through was discarded and 500 µl wash buffer II was added to the cartridge. The cartridge was centrifuged at 12 000 × *g* for 15 seconds and the flow-through was discarded. The washing step was repeated once. The empty cartridge was centrifuged for one minute at 12 000 × *g*. The cartridge was transferred to a 1.5 ml microcentrifuge tube and 30 µl nuclease-free water was added to the cartridge. The cartridge was incubated at room temperature and centrifuged at 12 000 × *g* for two minutes. The product was stored at -80°C.

Purified RNA was quantified using the Qubit RNA HS Assay kit and Qubit 2.0 Fluorometer according to the manufacturer's instructions. A working solution was prepared by adding Qubit RNA HS Reagent to Qubit RNA HS Buffer at a ratio of 1:200. Two tubes were prepared for the Qubit RNA standards by adding 190 µl working solution to each tube and adding 10 µl of each standard (Standard #1 and Standard #2) to the corresponding tubes. The tube for sample RNA was prepared by adding 198 µl working solution and 2 µl sample RNA to a tube. All tubes were vortexed briefly and incubated at room temperature for two minutes. The option for measuring the concentration of RNA standards was selected on the Qubit 2.0 Fluorometer, the tube for Standard #1 was inserted in the instrument and a reading was taken. The step was repeated for Standard #2. The option for measuring the concentration of sample RNA was selected, the sample tube was inserted in the instrument and a reading was given and captured. The reading given by the instrument in ng/ml was converted to copy numbers by importing data on the reading and fragment size into a conversion equation on the EndMemo website (available online at http://www.endmemo.com/bio/dnacopynum.php). The RNA was diluted to a concentration of 1×10^8 RNA copies/ml, aliquoted and stored at -80°C.

2.3.1.11.2 Performing RT-qPCR reactions

The SensiFAST Probe No-ROX One-Step kit was used to quantitatively measure the presence of NeoCoV genomic material in the supernatants removed from inoculated cell cultures and the bat faecal homogenate used for inoculation (refer to section 2.3.3). This was done in order to determine the concentration of NeoCoV in the inoculum used and whether viral replication took place in cell culture. The assay is able to detect a minimum of 1×10^5 viral RNA copies/ml.

The mixture described in Table 2.18 was prepared for each sample. The standard *in vitro* transcribed RNA prepared in section 2.3.1.11.1 was serially diluted from 1×10^6 RNA copies/ml to 1×10^2 RNA copies/ml, generating five standards for inclusion in each assay. Three reactions were prepared per standard, as well as for each of the samples, being RNA extracted from cell

culture supernatant and RNA extracted from sample 23; two reactions were prepared for the negative control, which contained DEPC-treated water instead of sample RNA.

Table 2.18. Reaction mixture for RT-qPCR reactions.

Component	Volume (µl)
2× SensiFAST Probe No-ROX One-Step Mix	5.0
Forward primer (10 µM)	0.4
Reverse primer (10 µM)	0.4
Probe (10 µM)	0.1
Reverse Transcriptase	0.1
RiboSafe RNase Inhibitor	0.2
DEPC-treated water	1.8
RNA template	2.0
Total	**10.0**

Thermal cycling was performed on the CFX Connect Real-Time PCR Detection System according to the parameters described in Table 2.19. CFX Manager Software was used to capture the data.

Table 2.19. Thermal cycling parameters for RT-qPCR reactions.

Temperature (°C)	Time	
45	20 minutes	
95	2 minutes	
95	5 seconds	×40 cycles
60	20 seconds	
4	∞	

2.3.2 Cell culture

Several mammalian cell lines, namely BHK-21 (G43), CaKi (camel kidney), NCK (*N. capensis* kidney), NCL (*N. capensis* lung), NCT *(N. capensis* trachea), PipNi, Vero E6 and Vero EMK cells, of which the species of origin were previously confirmed through cytochrome b sequence analysis, were cultured for this study. Pictures of these cell lines can be found in Figure D.1 in Addendum D. A detailed list with information on aspects such as the origins and maintenance of these cells is provided in Table 2.20.

Table 2.20. Cell lines used in this study.

Cell line	Country of origin	Obtained from	Organ of origin (species of origin)	% foetal bovine serum (FBS) used
BHK-21 (G43)	Germany	Collaborators at Charité University Hospital	Baby golden hamster kidney fibroblast (*Mesocricetus auratus*)	5
CaKi	Germany	Collaborators at Charité University Hospital	Dromedary camel kidney (*C. dromedarius*)	5
NCK	South Africa	Produced in-house (Stellenbosch University)	Cape serotine bat kidney (*N. capensis*)	5
NCL	South Africa	Produced in-house (Stellenbosch University)	Cape serotine bat lung (*N. capensis*)	10
NCT	South Africa	Produced in-house (Stellenbosch University)	Cape serotine bat trachea (*N. capensis*)	10
PipNi	Germany	Collaborators at Charité University Hospital	Common pipistrelle bat kidney (*P. pipistrellus*)	2
Vero E6	USA	Collaborators at Charité University Hospital	African green monkey kidney (*C. aethiops*)	5
Vero EMK	N/A	Collaborators at Charité University Hospital	Embryonic African green monkey kidney (*C. aethiops*)	5

2.3.2.1 Maintenance of cell lines

Cells were cultured with DMEM supplemented with 1% v/v penicillin-streptomycin, 1% v/v non-essential amino acids (NEAA), 1% v/v sodium pyruvate, 1% v/v L-glutamine and 2% - 10% v/v FBS, hereafter referred to as ‘supplemented DMEM’.

Cells were incubated at 37°C in a humidified incubator with 5% CO_2. Cell growth was monitored daily using a light microscope. Cells that had not reached >90% confluence three to four days after passaging (i.e. transferring cells to a new cell culture vessel) were washed with PBS and fresh supplemented DMEM was added to the cells to maintain them until they had reached >90% confluence and could be passaged. Confluence refers to the percentage of a cell culture

vessel that is covered by cells, e.g. when half the surface of a cell culture vessel is covered with adherent cells, the cells are 50% confluent.

Cryogenically frozen cell stocks were cultured and propagated as required by following a protocol designed to remove preservatives such as dimethyl sulfoxide (DMSO) that were used in the cryopreservation process. After thawing a vial containing 1 ml of cells, the contents were added to 4 ml PBS, gently resuspended and centrifuged at 1 000 × *g* for three minutes. The supernatant was discarded and the pellet resuspended in 5 ml PBS. The mixture was then centrifuged again at 1 000 × *g* for four minutes, after which the supernatant was removed and the pellet was resuspended in 5 ml supplemented DMEM. This was then added to a T25 flask and incubated at the aforementioned conditions.

Cells were passaged to new flasks/plates once the cells were >90% confluent. Passaging was done by aspirating the media from the flask and washing the adherent cells with PBS (three wash steps when using 1× trypsin-ethylenediaminetetraacetic acid [trypsin-EDTA]; one wash step when using Accutase). Cells were then detached from the flask using 1× trypsin-EDTA or Accutase (depending on availability) and incubating it at 37°C with 5% CO_2 for ten minutes. Supplemented DMEM was then added to the flask to inactivate the cell detachment medium and cells were seeded in a new cell culture vessel at the desired concentration. Desired concentrations were determined based on what purpose the newly-passaged cells would serve after adherence. Cells were then incubated at 37°C with 5% CO_2. Table 2.21 indicates the ratios of reagents used for the passaging and seeding of the cells:

Table 2.21. Reagents used for passaging and seeding of cells to culture vessels of different sizes.

Process	**Reagent**	**Flask size**			**Plate size**	
		T25	**T75**	**T175**	**6-well**	**12-well**
		Volume (ml)				
Wash	PBS	3	7	21	1/well	0.5/well
Detachment	1× trypsin-EDTA	1	3	7	1/well	N/A
	Accutase	1	3	7	1/well	N/A
Resuspension	Supplemented DMEM	4	7	21	Dependant on desired cell concentration	Dependant on desired cell concentration
Seeding (total volume)	Supplemented DMEM	5	18	25	2/well	1/well

2.3.2.2 Cell counting using a haemocytometer

Cells that had to be seeded at specific concentrations, either for use in virus isolation experiments (refer to section 2.3.3) or for pseudoparticle propagation and preparation (refer to sections 2.3.4.1 – 2.3.4.2), were counted using a haemocytometer to determine the concentration of the resuspended cell suspension. A confluent monolayer of cells in a T75 flask was detached using 1× trypsin-EDTA or Accutase and resuspended in an appropriate amount of supplemented DMEM (section 2.3.2.1). The resuspended cell solution was then diluted in PBS at a ratio of 1:9 and mixed thoroughly. Thereafter, 10 µl of the cell suspension was added to a clean haemocytometer with a coverslip. Once the cell solution had spread to fill the entire Neubauer chamber, the section of the haemocytometer that is divided into a grid for simplified counting, the slide was viewed using a light microscope and all cells within each of the four sets of 16 squares were counted. Taking into account the dilution factor of 10 and the conversion factor of 10^4, the cell concentration was determined as follows:

Average number of cells per large square × 10^5

Thereafter, cells were seeded to plates in the desired dilution using the equation:

$C_1V_1 = C_2V_2$

where C = concentration and V = volume.

2.3.2.3 Cryopreservation of cells

In some cases, cell stocks were made for future use by freezing cells that had been cultured. This was done by detaching adherent cells once they had reached >90% confluence and resuspending them in the appropriate amount of DMEM (section 2.3.2.1). The resuspended cells were centrifuged at 3 000 × *g* for five minutes, after which the supernatant was removed and the pellet resuspended in supplemented DMEM lacking penicillin-streptomycin with 10% v/v DMSO added. Typically, four vials of cells were prepared in 1 ml aliquots from a T75 flask during the cryopreservation process. The aliquots were placed in a Mr. Frosty Freezing Container pre-cooled to 4°C containing isopropyl alcohol, designed to prevent rapid cooling that could damage cells. The container was kept at -80°C overnight, after which the aliquots were transferred to a liquid nitrogen tank for long-term storage.

2.3.3 Virus isolation

Four attempts were made at isolating NeoCoV in cell culture, all using bat faecal homogenate obtained from sample 23 (Addendum C). Sample 23 originates from an *N. capensis* bat and was

confirmed NeoCoV-positive using the two-step screening RT-PCR and sequencing as described in sections 2.3.1.1 and 2.3.1.6, respectively. The isolation attempts differed mainly in inoculum preparation and passaging of the inoculated cells or supernatant.

NCK cells were used for the attempted isolation of coronavirus from the bat faecal sample. The cells were seeded in a 6-well plate at a concentration of 2.00×10^5 cells/ml on the day prior to infection using supplemented DMEM with an FBS concentration of 5% v/v. The inoculum was prepared by homogenising a bat faecal pellet from sample 23 with the method described in section 2.3.1.1.1.

2.3.3.1 First and second attempts at isolating NeoCoV

For the first two attempts (attempts 1 and 2), the inocula were prepared by mixing 450 µl homogenate with 300 µl PBS, filtering with a 0.2 µm filter and diluting in either 1.25 ml supplemented DMEM with 2% v/v FBS and 1% v/v amphotericin B or 1.25 ml OptiPRO Serum-Free Medium, respectively.

Cell supernatant was discarded and cells were washed once with PBS. Thereafter, 2 ml of the inoculum was added to separate wells of the 6-well plate, after which the plate was incubated at 37°C with 5% CO_2 for one hour. The inoculum was removed and supplemented DMEM with 2% v/v FBS v/v and 1% v/v amphotericin B was added to each well. Cells were incubated at 37°C with 5% CO_2.

Cells were monitored daily for cytopathic effect (CPE) using a light microscope and 250 µl of supernatant was removed per well at time points 24, 48, 72 and 144 hours post-infection (h.p.i.) and stored at -80°C until it could be screened for evidence of replicating virus with the RT-qPCR assay. An additional 250 µl supplemented DMEM with 2% v/v FBS and 1% v/v amphotericin B was added to each well after removal of the supernatant. At 144 h.p.i. the cells were passaged to a new 6-well plate, after which the process of supernatant aliquot removal, storage and replacement took place at time points 24, 48, 72, 96 and 168 hours after passaging of the cells.

2.3.3.2 Third and fourth attempts at isolating NeoCoV

For the third and fourth attempts (attempts 3 and 4), filtered homogenate was added to either 1.8 ml supplemented DMEM with 2% v/v FBS and 1% v/v amphotericin B or 1.8 ml OptiPRO Serum-Free Medium, respectively, at a ratio of 1:9 and added to the cells. Cells were incubated with the inocula for one hour at 37°C with 5% CO_2. Supernatants were then removed and replaced with DMEM with 2% v/v FBS v/v and 1% v/v amphotericin B and incubated at 37°C with 5% CO_2.

Cells were monitored daily for CPE and the removal, storage and replacement of supernatant was done as described for attempts 1 and 2 (section 2.3.3.1) at time points 24, 48, 72, 92 and 144 h.p.i. At 144 h.p.i., blind passaging was done by transferring 200 µl of the supernatant into a new cell culture vessel. Blind passaging refers to the process of transferring supernatant that might be virus-positive, but which has not been confirmed virus-positive through any molecular tests, to fresh cells. Supernatant was removed, stored and replaced at time points 24 and 48 hours after passaging. At time point 48 hours after virus passage, 500 µl of supernatant was removed and stored at -80°C. Subsequently, 200 µl of this stored supernatant was used to inoculate new cells in 1.8 ml supplemented DMEM. Supernatant (250 µl) was removed 24 h.p.i. and stored at -80°C.

2.3.4 Pseudoparticle production and infection

2.3.4.1 Propagation of recombinant VSV for pseudotyping

Genetically modified VSV-G-trans-complemented VSV particles without the ability to replicate (hereafter referred to as VSV*ΔG-Luc + VSV-G) were produced for future use in preparing pseudoparticles that express different surface proteins according to a method described by Hoffmann (2017). BHK-21 (G43) cells, which are able to be induced to express VSV-G for trans-complementation to take place (Hanika *et al.*, 2005; Hoffmann, 2017), were seeded in two T75 flasks at a concentration of 1.50×10^5 cells/ml to be 70% to 80% confluent within 24 hours of seeding. The supernatant was removed and cells were washed once with PBS. Subsequently, 15 ml supplemented DMEM with 10^{-8} M mifepristone was added to cells to induce the expression of VSV-G, after which they were incubated at 37°C with 5% CO_2 for six hours. The cell supernatant was then discarded and cells were washed once with PBS. A volume of 10 ml supplemented DMEM containing VSV*ΔG-Luc + VSV-G (provided by collaborators from Charité University Hospital) at a ratio of 1:999 was added to the cells, after which they were incubated at 37°C with 5% CO_2 for one hour. The cell supernatant was then discarded. Cells were washed thrice with PBS and 15 ml supplemented DMEM with 10^{-8} M mifepristone was added to the cells, which were then incubated overnight at 37°C with 5% CO_2.

Cells were monitored for CPE under a light microscope 18 to 20 h.p.i. Once >50% of cells showed signs of CPE, cell culture supernatant was removed from flasks, added to centrifugation tubes and centrifuged at 1 000 × *g* at 4°C for ten minutes to remove cell debris present in the supernatant. After centrifugation, the supernatant was aliquoted into new tubes and stored at -80°C.

2.3.4.2 Preparation of pseudoparticles expressing various surface proteins

Pseudoparticles expressing MERS-CoV- (ppMERS-S), NeoCoV- (ppNCV-S) and SARS-CoV- (ppSARS-S) S proteins were produced in order to determine whether MERS-CoV, NeoCoV and SARS-CoV can infect a selection of different cell lines selected for this study. Pseudoparticles expressing no foreign surface proteins (ppEV) and pseudoparticles expressing VSV-G (ppVSV-G) were also produced to act as negative and positive controls, respectively, according to the method described by Hoffmann (2017).

2.3.4.2.1 Transfection of cells

BHK-21 (G43) cells were seeded into five T25 flasks at a concentration of 10^5 cells/ml to reach ~70% confluence at the time of transfection (~24 hours after seeding). Cell supernatant was discarded and cells were washed thrice with PBS. Thereafter, 4.5 ml supplemented DMEM with an FBS concentration of 3% v/v was added to each flask.

Five individual transfection solutions were prepared, each containing 500 µl DMEM and 12 µl Invitrogen Lipofectamine 2000. Subsequently, 6 µg plasmid DNA, either pCG1, pCG1-VSV-G, pCG1-MERS-S, pCG1-NCV-S or pCG1-SARS-S (Table 2.3), was added to one of the mixtures and incubated at room temperature for 40 minutes.

The transfection solutions were added to the respective T25 flasks and incubated at 37°C with 5% CO_2 for six hours. Cell supernatant was then discarded, cells were washed twice with PBS and supplemented DMEM was added to each flask. Cells were incubated at 37°C with 5% CO_2 overnight.

2.3.4.2.2 Infection with VSV*ΔG-Luc + VSV-G

Cell supernatant was discarded following overnight incubation and cells were washed twice with PBS. Subsequently, 3.5 ml DMEM containing a 1:9 ratio of VSV*ΔG-Luc + VSV-G (section 2.3.4.1) to DMEM was added to each transfected T25 flask (VSV*ΔG-Luc + VSV-G needed to be applied at a multiplicity of infection [MOI] of at least 3; i.e. three particles needed to be added for every cell present in the sample). The flasks were incubated under slight agitation at room temperature for half an hour, after which it was incubated at 37°C with 5% CO_2 for 45 minutes. After incubation, cell supernatant was discarded and cells were washed eight times with PBS to remove any residual VSV*ΔG-Luc + VSV-G. After washing, 5 ml supplemented DMEM was added to each flask. The flasks were then incubated overnight at 37°C with 5% CO_2.

After overnight incubation of ±18 hours, cell supernatants were transferred to separate centrifugal tubes and centrifuged at 1 000 × *g* at 4°C for ten minutes to pellet cell debris. The supernatants containing pseudoparticles were then transferred to sterile tubes which were stored at 4°C if used within two weeks or at -80°C for long-term storage.

2.3.4.3 Determination of pseudoparticle titres by flow cytometry

The titre of the VSV*ΔG-Luc + VSV-G stock and that of the individual pseudoparticles were determined by inoculating Vero E6 cells with the particles generated as described in section 2.3.4.4.1. This was achieved by seeding Vero E6 cells onto 6-well plates at a concentration of 2×10^5 cells/ml to reach ~70% confluence 24 hours after seeding. A 10^{-3} dilution of VSV*ΔG-Luc + VSV-G stock was prepared in DMEM; 1 ml dilutions of a 1:9 ratio of pseudoparticles to DMEM were prepared for each of the different pseudotypes (ppVSV-G. ppEV, ppMERS-S, ppNCV-S and ppSARS-S). Infection was performed in triplicate by adding 1 ml of each dilution to three separate wells. Next, the plates were agitated at 80 rpm at room temperate for half an hour, then incubated at 37°C with 5% CO_2 for 45 minutes. Thereafter, the supernatants were aspirated and supplemented DMEM was added to the cells before incubating at 37°C with 5% CO_2 for 24 hours.

Cells were subsequently fixed for flow cytometry which was performed as described in section 2.3.4.4.3. The results were analysed with FlowJo version 10.4.2 software, after which the total number of infected cells were determined by multiplying the percentage of infected cells with the number of cells in each corresponding sample, which were counted using the method in section 2.3.2.2. An average was calculated from this data using the formula below. This average was used to determine the number of recombinant VSV particles or newly generated pseudotyped viruses per ml by taking into account the dilution factors for each.

Cells/sample × % GFP expressing cells detected = GFP expressing cells in sample

2.3.4.4 Infection and analysis of pseudoparticle infections

2.3.4.4.1 Infection of various cell lines with pseudoparticles

Cell lines of various origins (table 2.20) were infected with the generated pseudoparticles to investigate the possible host range of NeoCoV and how it compares with that of MERS-CoV and SARS-CoV. NCK and Vero E6 cells were infected using the protocol that allows for analysis by fluorescence microscopy; CaKi, NCK, NCL, NCT, PipNi, Vero E6 and Vero EMK cells were infected according to the method that is used for analysis by flow cytometry as explained in the below sections.

Infection of cells with pseudoparticles was achieved by seeding the required cells in a 12-well plate (fluorescence microscopy [refer to section 2.3.4.4.2]) or a 6-well plate (flow cytometry [refer to section 2.3.4.4.3]) at a concentration of 2×10^5 cells/ml that led to 70% to 80% confluence at the time of infection (±24 hours after seeding). Cells were seeded onto coverslips with a 16 mm diameter for fluorescence microscopy and were seeded directly onto 6-well plates for flow cytometry purposes. Cell supernatant was discarded and cells were washed once with PBS before adding pseudoparticle stock in 2 ml OptiPRO Serum-Free Medium (fluorescence microscopy) or 1 ml DMEM (flow cytometry) at a ratio of 1:9 to each well. One well of cells to be analysed by flow cytometry remained uninfected for each cell line in order to act as a negative control. Infections were performed in duplicate for samples to be used in fluorescence microscopy and in triplicate for samples analysed by flow cytometry. Cells were agitated at 80 rpm at room temperature for half an hour; thereafter incubated at 37°C with 5% CO_2 for 45 minutes. The supernatant was removed and cells were washed once with PBS. Supplemented DMEM was added to the cells and incubated at 37°C with 5% CO_2 for 24 hours, after which they were prepared for analysis by fluorescence microscopy or flow cytometry.

2.3.4.4.2 Preparation of cells for fluorescence microscopy and analysis

NCK and Vero E6 cells infected with pseudoparticles (section 2.3.4.4.1) were analysed by fluorescence microscopy to determine if GFP expression indicating positive pseudoparticle infection had occurred. To achieve this, cells had to be fixed, stained and mounted before being viewed on a fluorescence microscope.

The cell supernatant of infected cells was removed after 24 hours of incubation and cells were washed thrice with PBS. Cells were fixed onto coverslips by incubating at room temperature in 4% v/v formaldehyde in 1× PBS for 20 minutes. Thereafter, the supernatant was removed and cells were washed twice with PBS. Cells were stained by adding 300 µl 4’,6-diamidino-2-phenylindole, dihydrochloride (DAPI) at a concentration of 300 nM to each coverslip and incubating in the dark for five minutes. The DAPI was removed, cells were washed twice with PBS and once with distilled water.

Coverslips were mounted using ProLong Gold antifade reagent. Coverslips with fixed and stained cells were removed from the wells, dabbed on paper to remove excess water and placed inverted on a drop of mounting media on a microscope slide. The mounted samples were allowed to dry in the dark at 4°C overnight, after which the edges of the coverslips were sealed with clear nail polish. The slides were analysed by fluorescence microscopy with an Eclipse Ci microscope, making use of the DAPI and GFP filters. Slides were photographed using Sperm

Class Analyzer software. The total number of cells and GFP expressing cells were determined by counting the visualised cells by eye. Slides were stored at 4°C when not in use.

2.3.4.4.3 Preparation of cells for flow cytometry and analysis

CaKi, NCK, NCL, NCT, PipNi, Vero E6 and Vero EMK cells infected with pseudoparticles according to the method described for analysis by flow cytometry, along with a well of uninfected cells, were prepared for flow cytometry, which was used to measure GFP expression by cells, indicating infection by pseudoparticles. Briefly, cells were fixed by washing cells once with PBS, incubating with Accutase and incubating at 37°C for ten minutes. Detached cells were then transferred to 15 ml centrifuge tubes and centrifuged at 4 000 × *g* for three minutes, after which cells were washed twice in 1 ml PBS and centrifuged at 4 000 × *g* for three minutes each time. Thereafter, 4% v/v formaldehyde in 1× PBS was added to the cells and incubated at 4°C for ten minutes. Cells were then centrifuged at 4 000 × *g* for three minutes, after which the supernatant was removed and cells were resuspended in 250 µl PBS. The cell suspensions were stored at 4°C prior to performing flow cytometry.

The data on the percentage of GFP expressing cells were acquired using the BD FACSCanto II flow cytometer along with BD FACSDiva software. Cytometer Setup and Tracking beads were processed on the machine daily to ensure that data were standardised. The uninfected cell sample of each cell line was processed first to determine the robust standard deviation value of each cell line, after which a gate was created to separate uninfected cells from ones expressing GFP when subsequently running the infected cells. Data were acquired on a total of 1×10^4 events per sample.

The results were analysed with FlowJo version 10.4.2 , after which the total number of infected cells was determined by multiplying the percentage of infected cells with the number of cells in each corresponding sample. An average was calculated from this data, which was used to determine the number of pseudoparticle-infected cells for each cell line and pseudotyped virus.

CHAPTER 3

3 Results

3.1 Screening bat faecal samples for NeoCoV

3.1.1 PCR of bat faecal samples 1 to 30

In order to determine whether any of the bat faecal samples were NeoCoV positive, samples were screened with a PCR assay targeting different regions in the RdRp region of the coronavirus genome using four different primer sets, as described in section 2.3.1.1.4. The products of the screening PCR were visualised after agarose gel electrophoresis (section 2.3.1.3).

Overall, 12 of the 30 samples screened (40%) yielded fragments of the expected sizes. Fragments of the correct sizes were obtained for samples 12, 16, 17, 18, 19 and 20 using PCR Gr1Sp (Figure 3.1 A), for samples 17, 18, 19, 23 and 25 using PCR RGU_2c (Figure 3.1 B), for samples 16, 17 and 19 using PCR SP3080 F1 (Figure 3.1 C), and for samples 2, 9, 12, 14, 17, 18, 19 and 22 using PCR SP3374 F3 (Figure 3.1 D).

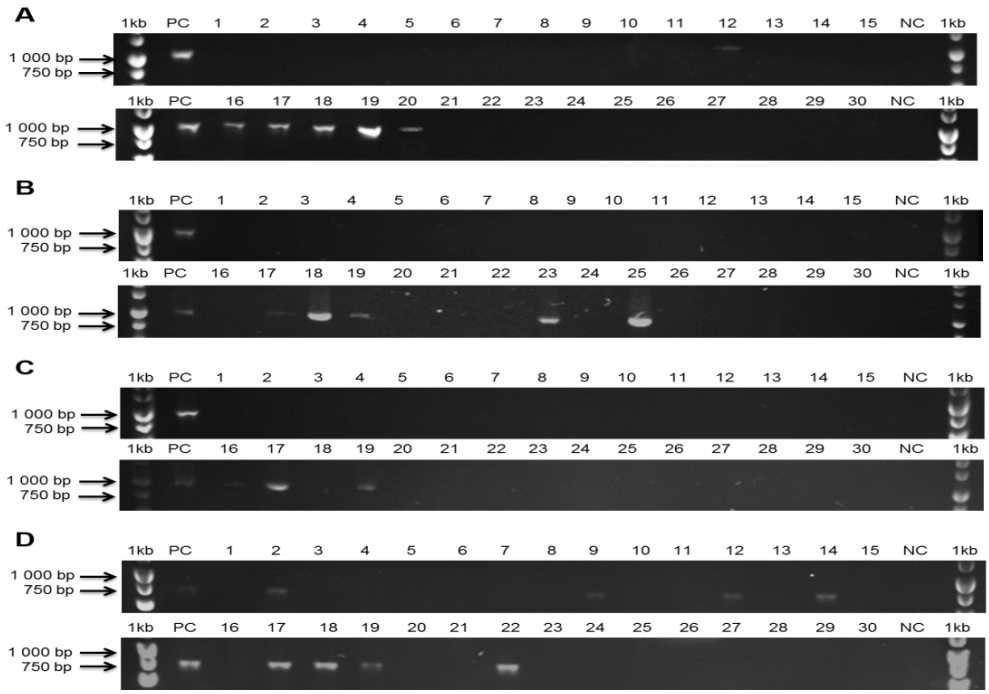

Figure 3.1. Screening for coronaviruses using four different primer sets. A) PCR Gr1Sp; fragment size = 974 bp. **B)** PCR RGU_2c; fragment size = 974 bp. **C)** PCR SP3080 F1; fragment size = 974 bp. **D)** PCR SP3374 F3; fragment size = 682. 1kb = GeneRuler 1kb DNA Ladder; PC = positive control; NC = negative control.

3.1.2 Sequencing

Amplified PCR products of the desired sizes from section 3.1.1 were purified and sequenced as described in sections 2.3.1.4 and 2.3.1.6, respectively, using the BigDye Terminator v3.1 Cycle Sequencing kit with the corresponding primers. Sequences were analysed using Geneious R10 bioinformatics software and NCBI BLAST online tool was utilised to determine genetic similarity to other coronavirus sequences available in the database. BLAST results revealed four alpha-, four beta- and four unclassified coronavirus sequences. For the purposes of this study, only sample 23 generated a 974 bp fragment by PCR RGU_2c that aligned to NeoCoV (GenBank accession number: KC869678) with 100% similarity. Sample 23 was therefore regarded as positive for NeoCoV.

3.2 Attempted isolation of NeoCoV in cell culture

3.2.1 Inoculation, passaging and monitoring for CPE

Isolation of NeoCoV in cell culture was attempted four times on NCK cells. Sample 23, of which the partial RdRp fragment shared 100% homology with that of the NeoCoV strain originally discovered by Ithete *et al*. (2013) (GenBank accession number: KC869678), was selected as the sample to be used for virus isolation on NCK cells in culture (section 2.3.3).

NCK cells were inoculated with bat faecal homogenate and monitored for signs of CPE. For attempts 1 and 2, cells were monitored visually at 24, 48, 72 and 144 hours post-inoculation with bat faecal homogenate and 24, 48, 72, 96 and 168 hours after cell passaging. For attempts 3 and 4, cells were monitored for CPE at 24, 48, 72, 92 and 144 hours post-inoculation with bat faecal homogenate, 24 and 48 hours after the first supernatant passage and 24 hours after the second virus passage. No discernible CPE was seen at any of the time points for any attempt. An RT-qPCR was done in order to assess virus growth in the case that any virus possibly isolated was non-lytic.

3.2.2 Analysis of NeoCoV replication by RT-qPCR

3.2.2.1 Generation of RT-qPCR standard

An *in vitro* transcribed RNA standard to be used as a standard with a known viral RNA concentration was generated for the RT-qPCR assay (section 2.3.1.11.1). This was done in order to quantify the viral RNA in samples with unknown concentrations. The fragment of the RdRp region of the NeoCoV genome generated by PCR RGU_2c for sample 23 was cloned into a pTZ57R/T vector. Plasmid DNA was sequenced after purification. After confirmation of the

presence of the fragment using the NCBI BLAST online tool, the plasmid was linearised and *in vitro* transcribed.

3.2.2.2 RT-qPCR for the detection of NeoCoV

The SensiFAST Probe No-ROX One-Step kit was used for RT-qPCR reactions that detected the presence of the NeoCoV RdRp region with a limit of detection of 10^5 viral RNA copies/ml (section 2.3.1.11.2). The assay was used to detect the presence of NeoCoV RNA in the supernatants removed from inoculated cell cultures and the bat faecal homogenate used for inoculation.

According to RT-qPCR analysis, the homogenate used for inoculation contained 7.72×10^5 viral RNA copies/ml. Furthermore, RT-qPCR analysis of the RNA extracted from the supernatants removed at each time point for revealed that no NeoCoV viral RNA was present in any of the extracted supernatants of attempts 1, 2 or 4. For attempt 3, 1.28×10^5 viral RNA copies/ml were detected 48 h.p.i. in the sample inoculated with DMEM containing NeoCoV-positive homogenate.

3.3 Pseudoparticle infections

3.3.1 Generation of pseudoparticles

3.3.1.1 Propagation of VSV*ΔG-Luc + VSV-G for pseudotyping

A stock of replication-incompetent, VSV-G-trans-complemented VSV (VSV*ΔG-Luc + VSV-G) was propagated according to the method described in section 2.3.4.1 to be used in the generation of pseudoparticles expressing heterologous proteins. This was done by infecting BHK-21 (G43) cells with a stock and harvesting the supernatant containing newly-generated VSV*ΔG-Luc + VSV-G.

The titre of this stock was determined by infecting Vero E6 with the stock of pseudotyped VSV particles as described in section 2.3.4.3. Flow cytometry was performed on the cells as described in section 2.3.4.4.3 to detect GFP expression.

The average titre of the VSV*ΔG-Luc + VSV-G stock was determined to be $\sim1.10\times10^7$ particles/ml.

3.3.1.2 Generation of VSV-based coronavirus pseudoparticles

Pseudoparticles expressing the VSV-G (ppVSV-G), MERS-CoV S (ppMERS-S), NeoCoV S (ppNCV-S) and SARS-CoV (ppSARS-S) proteins, as well as pseudoparticles that do not express

any heterologous proteins, namely ppEV, were generated as described in section 2.3.4.2. Briefly, BHK-21 (G43) cells were transfected with plasmids carrying the genes of interest and infected with VSV*ΔG-Luc + VSV-G, after which supernatants containing pseudotyped viruses were harvested and stored until use.

The titres of these pseudotyped viruses were determined by infecting Vero E6 cells with the pseudoparticles as described in section 2.3.4.3 and performing flow cytometry to measure GFP expression (section 2.3.4.4.3). The cells in each sample were counted (section 2.3.2.2) and pseudoparticle titres were calculated using the formula in section 2.3.4.3. The average titre calculated for each pseudotype is shown in Table 3.1.

Table 3.1. Titres of coronavirus and control pseudotypes.

Pseudotyped virus	Number of pseudoparticles/ml
ppVSV-G	6.36×10^{5}
ppEV	1.11×10^{4}
ppMERS-S	5.90×10^{5}
ppNCV-S	5.70×10^{5}
ppSARS-S	5.75×10^{5}

3.3.2 Infection of various mammalian cell lines using coronavirus pseudoparticles

3.3.2.1 Analysis of infection using fluorescence microscopy

NCK and Vero E6 cells were infected with ppEV, ppVSV-G, ppMERS-S, ppNCV-S and ppSARS-S as described in section 2.3.4.4.1. The expression of GFP was measured through fluorescence microscopy, as described in section 2.3.4.4.2, and used to infer the number of pseudoparticle infections. This was achieved by counting the total number of cells on the slide using the DAPI filter of the microscope, followed by counting the number of GFP expressing cells using the GFP filter and calculating the percentage of GFP expressing cells. A representative picture of the different fields visualised through fluorescence microscopy can be seen in Figure 3.2. The images generated for all fields captured for infection of both cell lines resulted in similar images, therefore only a representative picture is shown.

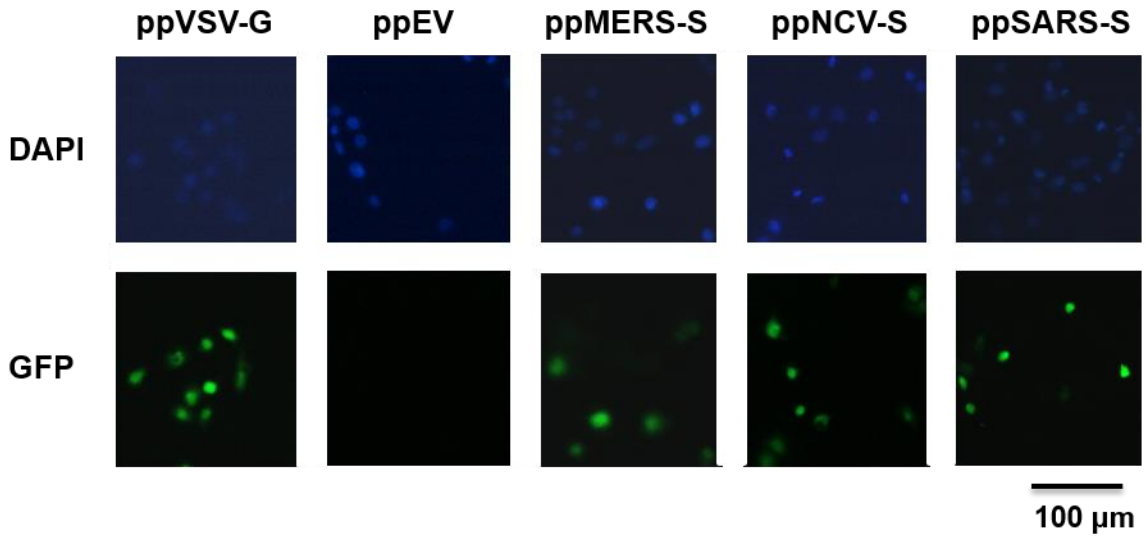

Figure 3.2. Fluorescence imaging of pseudoparticle infections. Microscopic fields were imaged at 40x magnification after infection of Vero E6 cells with pseudoparticles. Cells were stained with DAPI 24 h.p.i. The blue regions represent nuclear staining of all cells by DAPI fluorescent dye. The green regions represent cells expressing GFP due to pseudoparticle infection. Bar = 100 µm.

3.3.2.2 Analysis of infection using flow cytometry

Seven cell lines, namely CaKi, NCK, NCL, NCT, PipNi, Vero E6 and Vero EMK cells were infected with ppEV, ppVSV-G, ppMERS-S, ppNCV-S and ppSARS-S according to the protocol described in section 2.3.4.4.1. The expression of GFP was measured using flow cytometry (section 2.3.4.4.3). A representative image of flow cytometry results can be seen in Figure 3.3. The flow cytometry data generated was expressed in percentages and all produced similar graphs when visually expressed, as shown in Figure 3.3; therefore, only one representative image is shown here. All graphs generated from flow cytometry data for the cell lines can be found in Figure E.1 in Addendum E. The subsequent graphs in this section provide more information on the infections based on the number of cells infected with each pseudotyped virus.

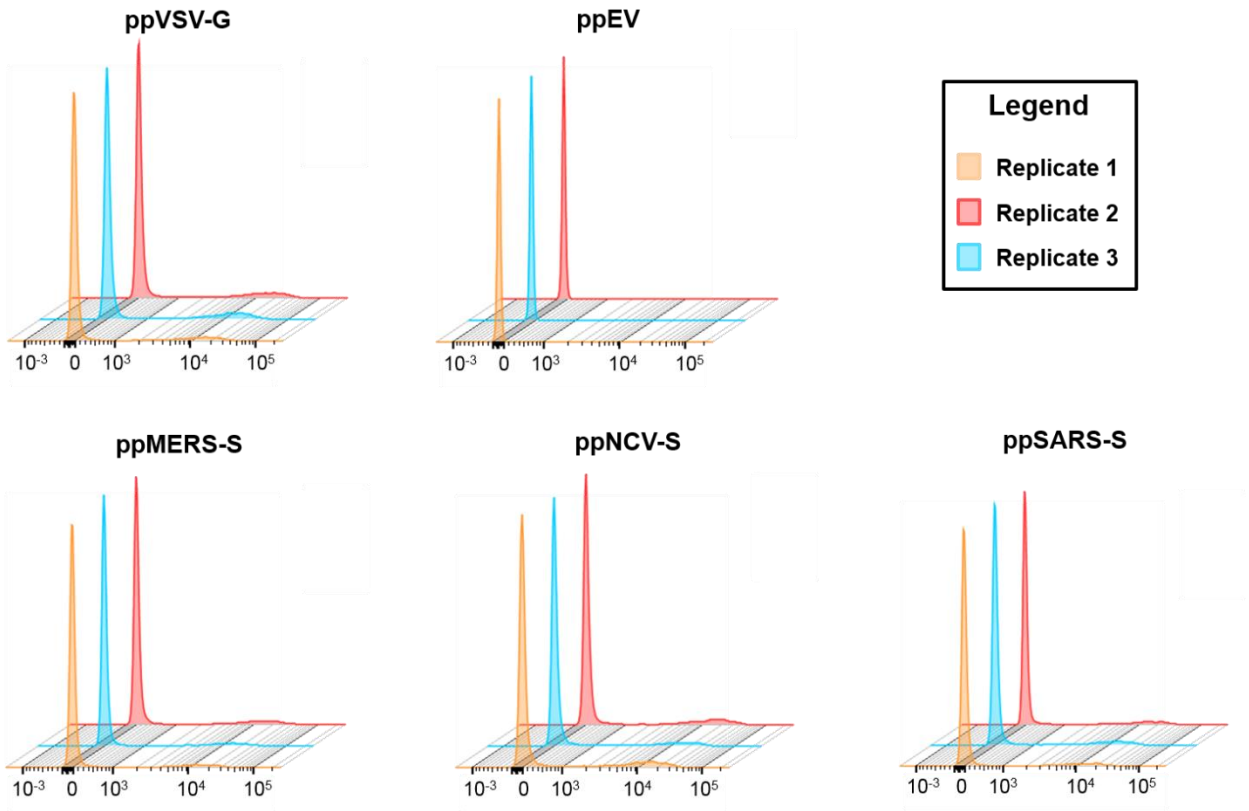

Figure 3.3. GFP expression measured through flow cytometry in NCK cells. Each graph shows the GFP measured per pseudoparticle, which was done in triplicate, therefore yielding three graphs per pseudoparticle. The first peak for each sample shows the cells that do not express GFP, with the smaller peaks (if present) showing the number of GFP expressing cells. The number of events is indicated on the y-axis, while the GFP fluorescence intensity is indicated on the x-axis.

Cells in each sample were counted as described in section 2.3.2.2 and the number of infected cells for each of the pseudoparticles in each cell line was calculated using the formula in section 2.3.4.3. Since infections were performed in triplicate for each different pseudotyped virus for each cell line, an average was determined for each.

3.3.2.2.1 Infection of NCK cells with coronavirus pseudoparticles

As can be seen in Figure 3.4, ppNCV resulted in the highest number of infected cells of the three pseudoparticles of interest when infecting NCK cells, with an average number of infections at 7.60×10^4. The ppMERS-S-infection yielded the second highest number of infected cells, with an average of 5.05×10^4 infections. Infection with ppSARS-S resulted in the lowest number of GFP expressing cells, with an average number of 4.60×10^4 GFP expressing cells.

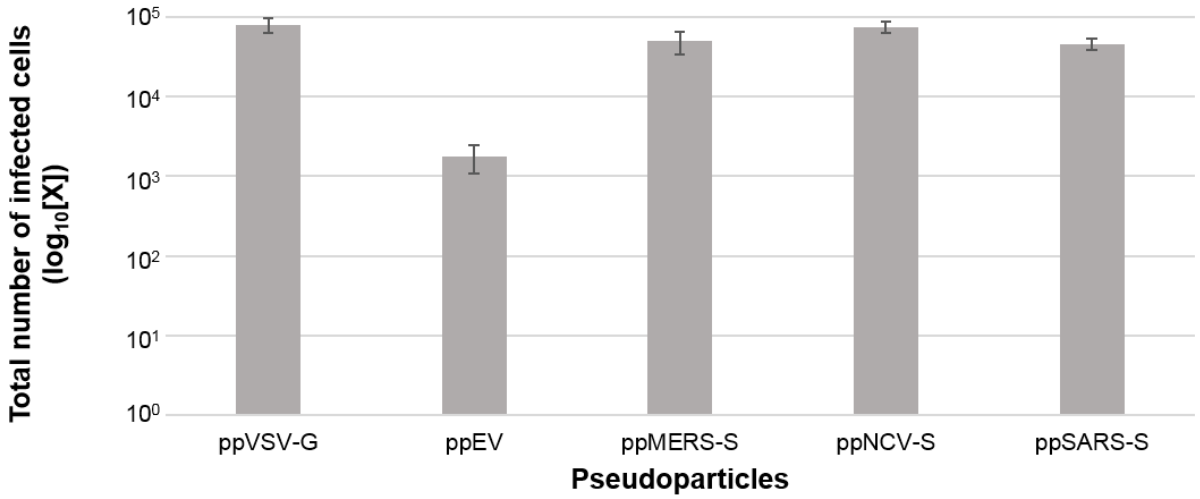

Figure 3.4. Infection of NCK cells with coronavirus pseudoparticles. Bars show the average number of infected cells for each pseudoparticle infection as determined by flow cytometry.

3.3.2.2.2 Infection of PipNi cells with coronavirus pseudoparticles

For infection of PipNi cells, it was found that ppSARS-S had the highest infection level of the three viruses being investigated (Figure 3.5). It had an average of 6.54×10^2 infected cells, with ppMERS-S and ppNCV-S having an average number of 4.71×10^2 and 3.62×10^2 infected cells, respectively.

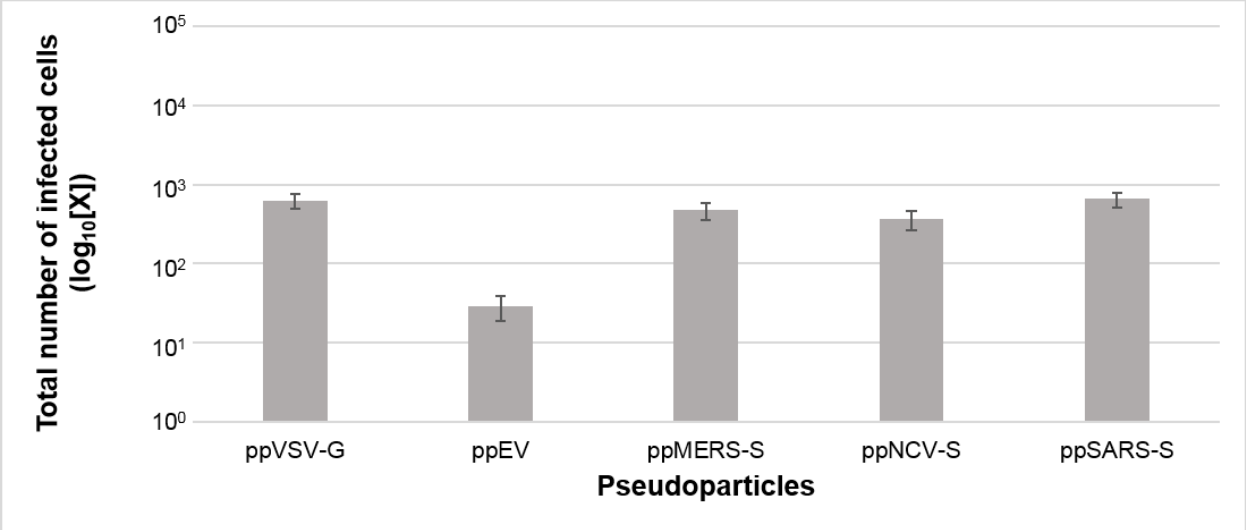

Figure 3.5. Infection of PipNi cells with coronavirus pseudoparticles. Bars show the average number of infected cells for each pseudoparticle infection as determined by flow cytometry.

3.3.2.2.3 Infection of Vero E6 cells with coronavirus pseudoparticles

Figure 3.6 shows the number of Vero E6 cells infected by each of the different pseudoparticles. The results are very similar for ppMERS-S, ppNCV-S and ppSARS-S, with average numbers of 5.91×10^4, 5.70×10^4 and 5.75×10^4 infected cells, respectively.

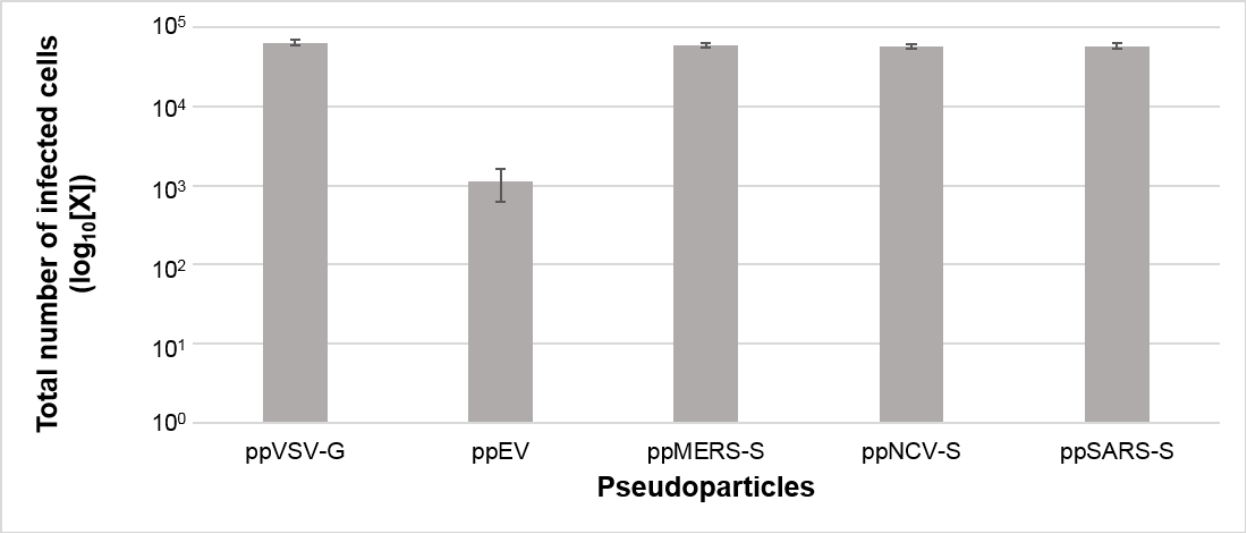

Figure 3.6. Infection of Vero E6 cells with coronavirus pseudoparticles. Bars show the average number of infected cells for each pseudoparticle infection as determined by flow cytometry.

3.3.2.2.4 Infection of Vero EMK cells with coronavirus pseudoparticles

For infection of Vero EMK cells with the three pseudoparticles of interest, ppNCV-S and ppSARS-S showed similar levels of infection, as can be seen in Figure 3.7. The number of ppMERS-S-infected cells was lower, at an average number of infections of 2.20×10^4, which is only 48% of the number of ppNCV-S-infected cells, and 46% of ppSARS-S-infected cells.

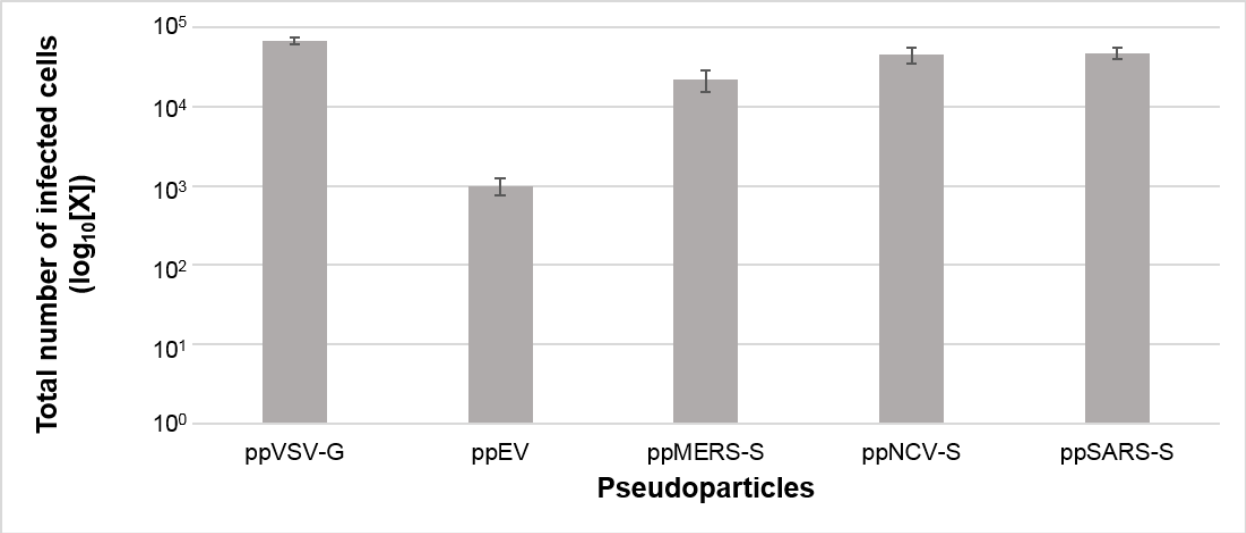

Figure 3.7. Infection of Vero EMK cells with coronavirus pseudoparticles. Bars show the average number of infected cells for each pseudoparticle infection as determined by flow cytometry.

3.3.2.2.5 Infection of CaKi, NCL and NCT cells with coronavirus pseudoparticles

Results were inconclusive for the infection of the CaKi, NCL and NCT cells. The percentages of GFP expressing cells obtained through flow cytometry were either very low and/or varied widely between the triplicates. The results of the infections of these cell lines were thus excluded from further analysis.

3.4 Screening cell cultures for *Mycoplasma* contamination

In order to determine whether the cell cultures used for the isolation of NeoCoV, propagation and preparation of pseudoparticles, and infection with pseudoparticles were not contaminated with *Mycoplasma*, the supernatants of the cell cultures were screened for *Mycoplasma* contamination with the protocol described in section 2.3.1.2. PCR products were visualised on agarose gels after electrophoresis. All cultures were negative for *Mycoplasma* contamination, except for the CaKi cells, for which a product of 500 bp was amplified and visualised through agarose gel electrophoresis. This fragment was purified and sequenced using the BigDye Terminator v3.1 Cycle Sequencing kit with the reverse *Mycoplasma* screening primers. After

analysing with Geneious R10 bioinformatics software, sequences were put through the BLAST online tool by NCBI and it was found that the amplified product aligned to *M. hyorhinis* (GenBank accession number: CP003231.1).

CHAPTER 4

4 Discussion

4.1 Detection and identification of coronaviruses

Thirty bat faecal samples were screened for the presence of coronaviruses. A two-step RT-PCR using four different primer sets was used in order to detect NeoCoV in samples, if present. Even though primers for PCRs Gr1Sp, SP3080 F1 and SP3374 F3 were initially designed for the detection of alphacoronaviruses and SARS-related coronaviruses, they have been found to successfully detect MERS-related coronaviruses if they are present in high titres (Cronjé, 2017), therefore, the aforementioned PCRs were used in this study for the detection of the MERS-related NeoCoV.

Of the 30 samples tested, 40% were positive for coronaviruses. Of the 12 positive samples, four belonged to the genus alphacoronavirus, four to betacoronavirus, and four were unclassified coronaviruses. This high proportion of positives correlates with the literature as coronaviruses have been found to be highly prevalent in bat populations (Masters, 2006; Smith & Denison, 2012; Ithete, 2013; Ithete *et al.*, 2013; Coleman & Frieman, 2014; Corman *et al.*, 2014, Cronjé, 2017; Banerjee *et al.*, 2018).

Since NeoCoV was originally found in an *N. capensis* bat (Ithete, 2013; Ithete *et al*., 2013; Corman *et al.*, 2014), it is known that the virus is able to infect *N. capensis* bats and that this virus might be present in other individuals of this bat species, as found by Cronjé (2017). It is therefore conceivable that NeoCoV was detected in sample 23, which originates from an *N. capensis* bat, using PCR RGU_2c. With sample 23 having the highest genetic similarity to NeoCoV of the sequences obtained from samples that were screened and the virus having a high titre as determined by RT-qPCR, it was chosen to be used in virus culturing and isolation attempts.

4.2 Failure to isolate NeoCoV in cell culture

Studying viruses through isolation in cell culture plays an important part in the characterisation of viruses (Lednicky & Wyatt, 2012; Dijkman *et al.*, 2013; Hoffmann *et al.*, 2013; Banerjee *et al.*, 2018), as it allows for the monitoring of cellular responses to viral infection, as well as the investigation of viral replication. Moreover, novel viruses have to be studied in cell culture in order to observe their pathogenicity and assess the possibility of spillover events that can occur

(Eckerle *et al.*, 2014). Since NeoCoV is highly related to MERS-CoV, it is important to investigate the behaviour of NeoCoV in cell culture.

In this study, four attempts were made at isolating NeoCoV. NCK cells were inoculated with inocula containing ~3.47×10^5 viral RNA copies in attempts 1 (inoculum prepared with DMEM) and 2 (inoculum prepared with OptiPRO Serum-Free Medium), and ~1.54×10^5 viral RNA copies for attempts 3 (inoculum prepared with DMEM) and 4 (inoculum prepared with OptiPRO Serum-Free Medium), respectively. Supernatant was removed from cell cultures at 24, 48, 72 and 144 h.p.i. and 24, 48, 72, 96 and 168 hours after cell passaging for the first two attempts. For attempts 3 and 4, supernatant was removed at 24, 48, 72, 92 and 144 h.p.i, 24 and 48 hours after the first virus passage and 24 hours after the second virus passage. An RT-qPCR sensitive enough to detect 10^5 viral RNA copies/ml was used to monitor the supernatant from inoculated cell cultures. During the first, second and fourth attempts, no viral RNA was detected at any of the time points. During attempt 3, ~$1{,}28\times10^5$ copies of viral RNA/ml was detected 48 h.p.i. in the supernatant from the cells inoculated with the DMEM-homogenate mixture, but no viral RNA copies were detected at any of the other time points.

Isolation of bat coronavirus has been attempted repeatedly (Lau *et al.*, 2005; Poon *et al.*, 2005; Chu *et al.*, 2006; Tang *et al.*, 2006; Woo *et al.*, 2007; Gloza-Rausch *et al.*, 2008; Drexler *et al.*, 2010; Gouilh *et al.*, 2011; Moreno *et al.*, 2017; Lau *et al.*, 2018b), but has only been successful in two cases in which SARS-CoV-like bat coronaviruses were isolated using Vero E6 cells and transgenic HeLa cells bearing the ACE2 receptors, respectively (Ge *et al.*, 2013; Yang *et al.*, 2016). Cells lines such as Vero E6 are known to be susceptible to many different viruses and have often been used in virus isolation attempts (Govorkova *et al.*, 1996; Lednicky & Wyatt, 2012; Ge *et al.*, 2013; Wei *et al.*, 2017; Banerjee *et al.*, 2018). However, numerous attempts utilising Vero E6 and other commercially-available cell lines for samples originating from bats failed (Lau *et al.*, 2005; Poon *et al.*, 2005; Chu *et al.*, 2006; Tang *et al.*, 2006; Woo *et al.*, 2007; Gloza-Rausch *et al.*, 2008; Drexler *et al.*, 2010; Gouilh *et al.*, 2011; Moreno *et al.*, 2017; Lau *et al.*, 2018b), as these cell lines do not provide conditions that are suitable for the proliferation of the virus it attempts to isolate, such as expression of receptors necessary for binding and entry (Eckerle *et al.*, 2014). Failure to isolate coronavirus from bat samples may therefore be, at least in part, due to a lack of availability of bat-derived cell lines (Crameri *et al.*, 2009; Eckerle *et al.*, 2014; Banerjee *et al.*, 2018).

In this study, a host-derived cell line, namely NCK, which was derived from *N. capensis* kidneys, was used in attempts to isolate NeoCoV. This and other *N. capensis*-derived cell lines such as

NCL and NCT developed from *N. capensis* lungs and tracheas, respectively, were developed for the purpose of isolating NeoCoV. Using host-derived cell lines is the most direct method with which to mimic virus-host interactions in a laboratory setting. In addition, supernatant was passaged in order to accommodate for virus adaptations to cell culture (Borucki *et al.*, 2013). However, no viral replication could be demonstrated. Therefore, a method to isolate NeoCoV remains to be discovered. This confirms the complexity of the issue of bat virus isolation commonly reported in the literature (Lau *et al.*, 2005; Poon *et al.*, 2005; Chu *et al.*, 2006; Tang *et al.*, 2006; Woo *et al.*, 2007; Gloza-Rausch *et al.*, 2008; Drexler *et al.*, 2010; Gouilh *et al.*, 2011; Moreno *et al.*, 2017; Banerjee *et al.*, 2018; Lau *et al.*, 2018b).

One explanation for the detection of a low level of viral RNA copies at one time point only in one of four attempts is that viral particles from the inoculum, whether viable or not, did not adsorb and enter the cells and may also not have been removed during the washing step following inoculation and adsorption. Hence the RNA detected 48 h.p.i. may have been a result of residual virus particles which failed to produce culture *in vitro* or residual RNA from lysed virus particles.

A lack of sufficient contact at the virus-cell interface may be a reason these isolation attempts did not yield a viable virus culture. There is a possibility that the virus did not enter the cells during the adsorption phase of infection, as adsorption time affects the success of viral infection in coronaviruses (Richards & Weinheimer, 1985; Schwegmann-Wessels *et al.*, 2011). According to Richards and Weinheimer (1985), static adsorption (i.e. virus incubation without agitation) leads to a decreased success of infection, which could be an explanation for the failure of these four attempts since the incubation for all four attempts did not involve agitation. Similarly, as the isolation procedure is done largely by trial and error, and assuming that viral entry did occur, it is possible that amounts of virus passaged serially were insufficient to elicit CPE or a sustained infection, and was therefore undetectable.

Maintaining the cold chain is a vital part of the sampling process, as disruption of the cold chain could lead to a loss of viable viral material in samples (Nasci *et al.*, 2002; USAID, 2013). Failure to isolate NeoCoV from the sample could be the result of virus degradation due to the disruption of the cold chain, leading to RT-qPCR-detectable viral RNA fragments but degraded viral particles in samples. Considering that the samples had to be transported from the field to the laboratory, where it needed to be processed before cryopreservation, as well as freeze-thawing when using the same sample for multiple assays, there are many different stages at which the cold chain could have been interrupted. The sample in question had been stored at -80°C for four months before use, during which time it had been freeze-thawed at least three times before

using the sample for inoculation. Interruption of the cold chain is therefore a plausible reason for the failure to isolate NeoCoV.

Furthermore, innate bat immune mechanisms are known to be an obstruction in isolation of coronaviruses, even *in vitro* (Eckerle *et al.*, 2014; Banerjee *et al.*, 2018). As attempts at virus isolation were performed on bat-derived cells, it is possible that infection by NeoCoV particles present in inocula were inhibited by innate immune mechanisms.

4.3 Pseudoparticle generation and infection

A VSV pseudotyped system that expresses GFP upon infection was used to express heterologous proteins in this study. This system, VSV*ΔG-Luc + VSV-G, was propagated on BHK-21 (G43) cells (inducible to express VSV-G) in order to obtain more particles to be used in the preparation of pseudoparticles that express foreign proteins. Vero E6 cells were infected with VSV*ΔG-Luc + VSV-G and flow cytometry, detecting GFP expression, was subsequently performed in order to determine the titre of the stock.

Vero E6 cells were successfully infected with VSV*ΔG-Luc + VSV-G stock, resulting in a titre of 1.10×10^{7} particles/ml. The titre of pseudoparticles generated was sufficient for use in the preparation of the different pseudotyped viruses, as infecting at an MOI of 3 or more has been found to yield high pseudoparticle titres (Hoffmann, 2017).

The VSV*ΔG-Luc + VSV-G system was used to infect BHK-21 (G43) cells that were transfected with vectors to express the S proteins of MERS-CoV, NeoCoV and SARS-CoV, as well as VSV-G (positive control) and no surface proteins (negative control). Infection of transfected cells with VSV*ΔG-Luc + VSV-G resulted in the formation of pseudoparticles expressing MERS-CoV, NeoCoV and SARS-CoV S proteins, VSV-G and no proteins (ppMERS-S, ppNCV-S, ppSARS-S, ppVSV-G and ppEV, respectively). Pseudoparticle titres were determined by infecting Vero E6 cells and performing flow cytometry to measure GFP expression, a method previously used to determine GFP expressing cells by infection with VSV*ΔG (Coil & Miller, 2004).

Titres of ppVSV-G, ppMERS-S, ppNCV-S and ppSARS-S were similar, indicating that transfection and budding took place in equal measures for these pseudoparticles during preparation. The ppVSV-G yielded a slightly higher titre than the three pseudotyped viruses of interest, which is anticipated, as it is likely that VSV incorporates its authentic glycoprotein, VSV-G, with the highest efficiency. The titre calculated for ppEV does not truly represent the number of ppEV particles in samples, but rather the GFP expression for infections with the VSV*ΔG-Luc + VSV-G used in the preparation of pseudotyped viruses. This ‘titre’ can be used as the

baseline; thus, if any of the other pseudotypes infect the same number of cells or less than ppEV for any given infection experiment, it is probably the result of infection by VSV*ΔG-Luc + VSV-G and not of the specific pseudotype (Giroud *et al.*, 2017; Li *et al.*, 2017).

For pseudoparticle generation, it is required to ensure that the desired spike or envelope proteins are being expressed to adequate levels in transfected cells and, more importantly, are efficiently incorporated into the budding pseudoparticles. This could be done by monitoring protein expression by using protein tags in plasmids carrying proteins of interest such as polyarginine (Arg), polyhistidine (His) or FLAG (a peptide consisting of aspartic acid, tyrosine and lysine residues) and analysing by western blot/immunofluorescence with the aid of specific antibodies (Terpe, 2003; Lau *et al.*, 2018b). However, it is known that tagging of viral surface proteins can decrease their expression, localisation and could lead to conformational changes of the proteins of interest (Terpe, 2003; Waugh, 2005; Burg *et al.*, 2016; Hoffmann, 2017; Saiz-Baggetto *et al.*, 2017; Booth *et al.*, 2018), which has been known to influence the efficiency with which the S proteins are incorporated into pseudoparticles (Hoffmann, 2017). Therefore, tagging of S proteins was not performed in this study.

NCK and Vero E6 cells were infected with pseudoparticles and fluorescence microscopy was used to detect GFP expressed by pseudopaticles once in cells. Other methods for determining the number of infected cells are available, such as antigen detection methods where fluorescent-labelled antibodies recognise the virus of interest's surface protein in the cell, or monitoring of luciferase activity when infection had taken place (Beels *et al.*, 2008; Hoffmann *et al.*, 2013).

After the NCK and Vero E6 infection experiments were analysed using fluorescence microscopy, it was found that the washing steps necessary to prepare the cells for fluorescence microscopy removed a large number of cells from slides, which could produce skewed results. Detection of GFP expression through flow cytometry was therefore regarded as the method of choice for this study, as less cells would be lost through washing. Furthermore, there was convenient access to a flow cytometry unit, sample processing was straightforward, and flow cytometry reduced the risk of errors compared to counting the total number of cells and the number of GFP expressing cells by eye when using fluorescence microscopy. In addition, the use of fluorescence microscopy introduces potential bias, since only certain fields on the slides are selected for counting while flow cytometry evaluates all cells in the sample. For one, the investigator might be tempted to select fields that represent results as hypothesised. Using flow cytometry therefore aids in determining the exact number of infected cells in the whole sample, unlike fluorescence microscopy, where some of the infected cells remain on the plate and only certain

fields on the slide are counted. The number of GFP expressing cells after infection of CaKi, NCK, NCL, NCT, PipNi, Vero E6 and Vero EMK cells were subsequently measured by flow cytometry.

For infection of NCK cells, ppVSV-G had infected the highest number of cells; infection with ppEV showed the lowest number of infected cells, as was expected. Among infections with the pseudoparticles of interest, ppNCV-S elicited the highest number of infections, with ppMERS-S scoring second. As *N. capensis* bats are the natural hosts of NeoCoV, it was expected that ppNCV-S would elicit a high number of infections in NCK cells (Ithete *et al.*, 2013; Corman *et al.*, 2014). The number of ppMERS-S-infected cells was considerably lower than that of ppNCV-S. Since the two viruses are 85.5% genetically identical, they would be expected to have the ability to infect the same host cells, though not necessarily with the same efficiency (Corman *et al.*, 2014). This difference could indicate that NeoCoV would have to undergo several genetic changes in its S protein before it could putatively infect humans (Ithete *et al.*, 2013; Corman *et al.*, 2014; Anthony *et al.*, 2017). If such changes did indeed happen to a presumptive MERS-CoV ancestral bat virus, resulting in MERS-CoV, the S proteins of the two viruses would differ in such a way as to make *N. capensis* cells less susceptible to MERS-CoV and human cells less susceptible to infection by NeoCoV (Anthony *et al.*, 2017).

The number of NCK cells infected by ppSARS-S, even though relatively high with ~$4{,}60\times10^4$ infections, were noticeably less than that infected by ppMERS-S and especially ppNCV-S, eliciting infection of only ~60% of the number of cells infected by ppNCV-S. This may be due to the fact that SARS-CoV is believed to have emerged in horseshoe bats and is less related to NeoCoV than MERS-CoV is, with their S1 and S2 subunits sharing only 20% and 42% similarity, respectively, consequently making it less probable that the SARS-CoV S protein is adapted to infect NeoCoV's original host (Corman *et al.*, 2014). Nevertheless, a high level of infection was still observed, possibly due to the fact that the virus is adapted to infecting certain bat cells (Lau *et al.*, 2005; Li *et al.*, 2005).

Infection of NCK cells resulted in the highest infection level by ppNCV-S across all the tested cell lines. Kidney cells are oftentimes the tissue in which coronaviruses replicate (de Haan & Rottier, 2005; Mossel *et al.*, 2005; Cavanagh *et al*., 2007; Pacciarini *et al.*, 2008; Mackay & Arden, 2015). With *N. capensis* bats being the natural host of NeoCoV (Ithete, 2013; Ithete *et al.*, 2013; Corman *et al*., 2014), it was hypothesised that NeoCoV would have the ability to infect and replicate in NCK cells, as discussed in section 4.2. However, this hypothesis remains to be

confirmed as there is no evidence in the literature of *N. capensis* kidney samples testing positive for NeoCoV.

The number of PipNi cells that were infected with each pseudotype is much smaller compared to the number of infected cells seen in NCK, Vero E6 and Vero EMK cells. MERS-related coronaviruses have been found in *P. hesperidus* bats (Cronjé, 2017), hence it is possible that these coronaviruses are not adapted to infect cells that originate from *Pipistrellus* species as efficiently as seen for *N. capensis* cells, but rather infect and replicate in other organs of *Pipistrellus* bats. However, MERS-related coronaviruses originating from *Pipistrellus* bats are closely related to NeoCoV and differ mainly in their S proteins (Cronjé, 2017). There is therefore a possibility that the MERS-CoV-related viruses detected in *Pipistrellus* bats are better adapted to their natural host and do replicate in the kidneys of their natural host, whereas NeoCoV is better adapted for binding and entering *N. capensis* cells.

The large number of ppSARS-S-infected cells relative to the other pseudotypes of interest indicates that SARS-CoV is better adapted to infecting PipNi cells than MERS-CoV and NeoCoV. MERS-CoV has been found to infect PipNi cells (Müller *et al.*, 2012; Raj *et al*., 2013), however the same was not reported for SARS-CoV. The findings of the current study indicate that SARS-CoV is able to bind to and enter PipNi cells; thus failure to culture SARS-CoV on PipNi cells is not due to its inability to enter the cells, but rather an inability to replicate in the cultures.

The number of infections elicited with ppSARS-S infection was higher than the number of ppVSV-G-infected cells when infecting PipNi cells. This discrepancy could be the result of events measured by the flow cytometer that were not necessarily cells expressing GFP, such as the fluorescence of cell debris in the sample (Reardon *et al.*, 2014). With the pseudoparticle infection of PipNi resulting in such low levels of infection, the proportion of autofluorescence in relation to the total fluorescence detected after PipNi infection is higher than the ratio of autofluorescence to GFP expressing cells for NCK, Vero E6 and Vero EMK cell infections, and therefore can be distinguished more prominently when analysing the results of PipNi infection. The number of cells expressing GFP after infection with ppEV was, nonetheless, lower than that for any of the other infections. It is therefore improbable that the high level of infection for ppSARS-S is only the result of fluorescence of cell debris.

Infection of Vero E6 cells yielded similar results when infecting with the pseudoparticles of interest, with ppVSV-G having infected slightly more cells than the coronavirus pseudoparticles, and ppEV eliciting a very small proportion of infections. It is known that Vero E6 cells have the

receptor DPP4 for MERS-CoV (Raj *et al.*, 2013) and the receptor ACE2 for SARS-CoV (Li *et al.*, 2003), therefore it was not unexpected that ppNCV-S is able to infect the same cell line, since NeoCoV and MERS-CoV share 87% similarity in their S2 subunits on an amino acid level. It might be reasoned that NeoCoV utilises either DPP4 or ACE2, or, if not one of these, another receptor that is present on Vero E6 cells, since the pseudotype bearing NeoCoV's surface antigen is able to infect Vero E6 cells to approximately the same level as viruses known to have the ability to infect Vero E6 cells. Furthermore, these results indicate that NeoCoV might be effectively transmitted from bats to non-human primates, where it might undergo modifications in its genome and recombine with other primate coronaviruses and increase its zoonotic potential and transmissibility (Corman *et al.*, 2014).

Lower numbers of infected cells were seen for the pseudotyped viruses of interest when infecting Vero EMK cells than were seen in the infection of Vero E6 cells. This is an unanticipated result, since the cell lines were derived from the same species. However, for infection with ppVSV-G, ~6% more Vero EMK than Vero E6 cells were successfully infected; ppEV infection of Vero EMK cells yielded a number of infected cells ~90% that of Vero E6 infected cells with the pseudotype. As the infection levels of the controls among the two Vero cell lines are quite similar, the lower numbers of infected cells observed when infecting Vero EMK cells with the coronavirus pseudotypes could be the result of adaptations the two cell lines underwent once the strains of the cells were established. Since the VSV-G receptor, a low-density lipoprotein, is conserved among several species and is present in most cell lines (Finkelshtein *et al.*, 2013), cell culture adaptations might not have influenced the expression of this protein as it possibly did that of DPP4, ACE2 and the NeoCoV receptor in Vero EMK cells.

Another interesting result is that the number of cells infected by ppNCV-S and ppSARS-S are very similar for infection of Vero EMK cells, while ppMERS-S has a much lower number of infected cells. Since the NeoCoV and MERS-CoV S proteins are more closely related than that of NeoCoV and SARS-CoV, it would be expected that ppMERS-S and ppNCV-S should elicit similar levels of infection. This could indicate that MERS-CoV has a narrower tropism than NeoCoV, leading to a lowered ability to infect the same cell lines as NeoCoV.

Very low numbers of infected cells (<10 per pseudotype) were seen when infecting CaKi, NCL and NCT cells with all the pseudoparticles. Considering the autofluorescence of cell debris when measuring GFP expression with flow cytometry, it is very likely that these minimal numbers of GFP expressing cells were in fact autofluorescence and not the presence of infected cells (Reardon *et al.*, 2014). Considering that no cells expressed GFP when infecting CaKi, NCL and

NCT cells, it can be hypothesised that CaKi, NCL and NCT cells do not express DDP4 and ACE2 receptors, nor the receptor for NeoCoV, which is yet unknown, for infection by MERS-CoV, SARS-CoV and NeoCoV, respectively.

Since NeoCoV and other MERS-related betacoronaviruses have been found in *N. capensis* bats (Ithete, 2013; Cronjé, 2017), the viruses' abilities to infect *N. capensis* cells are confirmed. Coronaviruses are often found in kidneys (de Haan & Rottier, 2005; Mossel *et al.*, 2005; Cavanagh *et al*., 2007; Pacciarini *et al.*, 2008; Mackay & Arden, 2015). Since the results of this study indicate that the three coronaviruses of interest are able to enter NCK cells, it can be hypothesised that these viruses use *N. capensis* kidneys as a site of replication and therefore do not utilise the lungs or trachea of *N. capensis*.

Interestingly, CaKi cells were not susceptible to any of the pseudoparticles. MERS-CoV and antibodies for the virus have been detected in *C. dromedarius* individuals in the Middle East (Hilgenfeld & Peiris, 2013; Perera *et al.*, 2013, Reusken *et al.*, 2013; Adney *et al.*, 2014; Coleman & Frieman, 2014; Haagmans *et al.*, 2014; Nowotny & Kolodziejek, 2014), therefore it is expected that ppMERS-S should be able to infect CaKi cells and express GFP. However, MERS-CoV has not been reported to have been detected in *C. dromedarius* kidney tissue, nor has it been used to infect CaKi cells specifically; it is therefore not known whether the virus is able to infect the kidney cells themselves or if they infect other organ(s). If this is the case, the *C. dromedarius* kidney cells may not necessarily express the MERS-CoV receptor and the MERS-CoV that has been discovered in *C. dromedarius* individuals did not originate from the kidneys.

Since infection with pseudoparticles did not yield any GFP expression for ppNCV-S or ppSARS-S, it can be hypothesised that CaKi cells do not express the receptors for NeoCoV or SARS-CoV either. It is, however, possible that the presence of *Mycoplasma* contamination in the CaKi cell cultures could have influenced the susceptibility of the cell line to the pseudoparticles. *Mycoplasma* contamination has been found to influence cell susceptibility to viral infection (Rottem & Barile, 1993) and can cause constant interferon signalling (Rinaldo *et al*., 1973), which would hinder infection. Unfortunately, no *Mycoplasma*-free CaKi cells were available for repeating the experiments to ensure that the results were reliable. It was not possible to cure the CaKi cells of *Mycoplasma* contamination in a timely manner that would have allowed for the use of cured cells that can be infected with viable pseudoparticles, since the use of a method such as antibiotic treatment, which is the most widely-used method available, is time-consuming. It could take up to two weeks to eradicate *Mycoplasma* contamination when using an appropriate antibiotic (Uphoff *et al.*, 2012), by which time the pseudoparticles would have lost their viability.

Furthermore, antibiotic treatment introduces a variable in the experiment and it would be difficult to determine whether introducing a new antibiotic in the cell culture has an effect on the cells' metabolism (Kuhlmann, 1995). For future studies, infection with pseudoparticles with a known titre needs to be repeated using *Mycoplasma*-free CaKi cells in order to determine whether *Mycoplasma* contamination influenced the susceptibility of the cells in this study. To achieve this, fresh, uncontaminated aliquots of CaKi cells either need to be obtained from the source, or cells need to be cured using antibiotics, or other methods such as treating cells with ether-chloroform, heat-treatment, microfilter filtration or addition of macrophages to the culture (Uphoff & Drexler, 2002b), followed by procedures to confirm that the cells are *Mycoplasma*-free and subsequently culturing the cured cells without the treatments for an extended period of time to ensure that the metabolism of the cells has returned to its natural state.

CHAPTER 5

5 Conclusions

Investigating potentially zoonotic coronaviruses that could lead to the emergence of important human pathogens is essential for the prevention or early detection of outbreaks. The current study has provided more information on the host range of one such virus, namely NeoCoV, through the use of viral pseudoparticles and attempts at isolating the virus in culture.

Isolation of NeoCoV from bat faecal material was not achieved, even when using a cell line derived from the bat species *N. capensis* in which the virus was discovered. Different approaches need to be tested in order to find a protocol for the isolation of NeoCoV in cell culture. Future attempts at isolation could include the use of a fresh NeoCoV-positive sample, using higher titres of NeoCoV in inocula, agitated adsorption, and the use of transgenic cell lines expressing bat cell receptors and/or lacking interferon responses in order to circumvent the issue of innate bat immune mechanisms in cell culture. Furthermore, determining the NeoCoV receptor will greatly improve the probability of isolating the virus in cell culture.

Infecting different cell lines with pseudoparticles revealed that a pseudotype carrying the S protein of NeoCoV was able to infect the kidney cells of *N. capensis* bats, in which NeoCoV was originally detected (Ithete, 2013; Ithete *et al.* 2013; Corman *et al.*, 2014). The pseudotype carrying the S protein of NeoCoV also infected a high number of Vero E6 cells, similar to that of the pseudotype carrying the MERS-CoV S protein. This result leads to the assumption that NeoCoV would be able to infect the non-human primate *C. aethiops*, from which the Vero E6 cell line was derived. Taking this into account, it is possible that certain primate species, among others, might be links in the host 'jumping' which is hypothesised to take place to allow zoonotic transmission of NeoCoV/MERS-CoV. This finding suggests that non-human primates might provide a suitable environment for the development of NeoCoV as a zoonotic agent. However, this needs to be further investigated by testing the NeoCoV S-bearing pseudoparticles on other non-human primate cell lines, as well as human cell lines such as HEK-293.

It is unlikely that *P. pipistrellus* bats are a natural host for NeoCoV, since none of the pseudoparticles of interest infected PipNi cells at levels as high as seen in the infection of NCK, Vero E6 and Vero EMK cells. This theory should be further investigated by testing the pseudoparticles on cell lines originating from different *P. pipistrellus* organs, as the viruses might be able to infect other organs and possibly replicate in them. Furthermore, the transmissibility of MERS-CoV-related viruses detected in *P. hesperidus* bats can be tested by constructing

pseudoparticles bearing the S proteins of these viruses and using it to determine whether these viruses could infect *N. capensis* and *P. pipistrellus* cells.

The lack of infections seen when inoculating the CaKi cells is surprising since it is expected that MERS-CoV should be able to infect dromedary camel kidney cells. The *Mycoplasma* infection of the CaKi cells could be the reason for seeing no infections in these cells. In future studies, pseudoparticles should be tested on CaKi cells that are *Mycoplasma*-free in order to determine whether the results observed for this cell line in the current study are reliable. As there is a possibility that the virus does not replicate in the kidney cells of *C. dromedarius*, the pseudoparticles also need to be tested on other cell lines originating from *C. dromedarius*, such as lung, trachea and pharynx cells for more conclusive findings.

To better understand the possible emergence of NeoCoV, together with phylogenetic analyses, pseudoparticles could be used to infect cell lines that were not investigated in this study. Cell lines originating from domesticated animals and animals living in close proximity with humans, such as sheep, cattle, pigs, cats, dogs and rodents should also be tested. Testing the pseudoparticles on human cell lines from different organs will also provide insight into the ability of NeoCoV to infect humans directly. Doing so will ultimately lead to improved comprehension of the often complex events giving rise to the zoonotic transmission of coronaviruses.

References

Adams, N.R. & Hofstad, M.S. 1971. Isolation of transmissible enteritis agent of turkeys in avian embryos. *Avian Diseases*, 15(3): 426 – 433.

Adney, D.R., van Doremalen, N., Brown, V.R., *et al*. 2014. Replication and shedding of MERS-CoV in upper respiratory tract of inoculated dromedary camels. *Emerging Infectious Diseases*, 20(12): 1999 – 2005.

Aiken, C. 1997. Pseudotyping human immunodeficiency virus Type 1 (HIV-1) by the glycoprotein of vesicular stomatitis virus targets HIV-1 entry to an endocytic pathway and suppresses both the requirement for Nef and the sensitivity to cyclosporin A. *Journal of Virology*, 71(8): 5871 – 5877.

Annan, A., Baldwin, H.J., Corman, V.M., *et al.* 2013. Human betacoronavirus 2c EMC/2012-related viruses in bats, Ghana and Europe. *Emerging Infectious Diseases*, 19: 456 – 459.

Anthony, S.J., Gilardi, K., Menachery, V.D., *et al*. 2017. Further evidence for bats as the evolutionary source of Middle East respiratory syndrome coronavirus. *mBio*, 8(2): 1 – 13.

Banerjee, A., Misra, V., Schountz, T. & Baker, M.L. 2018. Tools to study pathogen-host interactions in bats. *Virus Research*, 248: 5 – 12.

Banik, G.R., Khandaker, G. & Rashid, H. 2015. Middle East respiratory syndrome coronavirus ‘‘MERS-CoV’’: current knowledge gaps. *Paediatric Respiratory Reviews*, 16(3): 197 – 202.

Baron, S., Fons, M. & Albrecht, T. 1996. Viral pathogenesis, in S. Baron (ed.). *Medical microbiology, 4th edition*. Texas: University of Texas Medical Branch at Galveston.

Barr, J.A., Smith, C., Marsh, G.A., Field, H. & Wang, L.-F. 2012. Evidence of bat origin for Menangle virus, a zoonotic paramyxovirus first isolated from diseased pigs. *Journal of General Virology*, 93: 2590 – 2594.

Bartosch, B., Dubuisson, J. & Cosset, F.-L. 2003. Infectious hepatitis C pseudo-particles containing functional E1-E2 envelope protein complexes. *Journal of Experimental Medicine*, 197(5): 633 – 642.

Baseler, L., de Wit, E. & Feldmann, H. 2016. A comparative review of animal models of Middle East respiratory syndrome coronavirus infection. *Veterinary Pathology*, 53(3): 521 – 531.

Beels, D., Heyndrickx, L., Vereecken, K., *et al*. 2008. Production of human immunodeficiency virus type 1 (HIV-1) pseudoviruses using linear HIV-1 envelope expression cassettes. *Journal of Virological Methods*, 147(1): 99 – 107.

Belouzard, S., Chu, V.C. & Whittaker, G.R. 2009. Activation of the SARS coronavirus spike protein via sequential proteolytic cleavage at two distinct sites. *Proceedings of the National Academy of Sciences of the United States of America*, 106(14): 5871 – 5876.

Berger, A., Drosten, C., Doerr, H.W., Stürmer, M. & Preiser, W. 2004. Severe acute respiratory syndrome (SARS) - paradigm of an emerging viral infection. *Journal of Clinical Virology*, 29(1): 13 – 22.

Berger Rentsch, M. & Zimmer, G. 2011. A vesicular stomatitis virus replicon-based bioassay for the rapid and sensitive determination of multi-species type I interferon. *PLOS One*, 6(10): 1 – 8.

Boehm, M. & Nabel, E.G. 2002. Angiotensin-converting enzyme 2 – a new cardiac regulator. *The New England Journal of Medicine*, 347(22): 1795 – 1797.

Bolz, M., Kerber, S., Zimmer, G. & Pluschke, G. 2016. Use of recombinant virus replicon particles for vaccination against *Mycobacterium ulcerans* disease. *PLOS Neglected Tropical Diseases*, 9(8): 1 – 18.

Booth, W.T., Schlachter, C.R., Pote, S., *et al*. 2018. Impact of an N-terminal polyhistidine tag on protein thermal stability. *ACS Omega*, 3: 760 – 768.

Borucki, M., Allen, J.E., Chen-Harris, H., *et al*. 2013. The role of viral population diversity in adaptation of bovine coronavirus to new host environments. *PLOS One*, 8(1): 1 – 11.

Breiman, R.F., Evans, M.R., Preiser, W., *et al*. 2003. Role of China in the quest to define and control severe acute respiratory syndrome. *Emerging Infectious Diseases*, 9(9): 1037 – 1041.

Brody, J.R. & Kern, S.E. 2004. Sodium boric acid, a Tris-free, cooler conductive medium for DNA electrophoresis. *BioTechniques*, 36(2): 214 – 216.

Burg, L., Zhang, K., Bonawitz, T., *et al*. 2016. Internal epitope tagging informed by relative lack of sequence conservation. *Scientific Reports*, 6: 1 – 8.

Calisher, C.H., Childs, J.E., Field, H.E., Holmes, K.V. & Schountz, T. 2006. Bats: important reservoir hosts of emerging viruses. *Clinical Microbiology Reviews*, 19(3): 531 – 545.

Cavanagh, D., Casais, R., Armesto, M., *et al.* 2007. Manipulation of the infectious bronchitis coronavirus genome for vaccine development and analysis of the accessory proteins. *Vaccine*, 25: 5558 – 5562.

Centers for Disease Control and Prevention. 2017. *Human coronavirus types* [Online]. Available: https://www.cdc.gov/coronavirus/types.html [2018, November 6].

Chan, J.F.-W., Lau, S.K.-P. & Woo, P.C.-Y. 2013. The emerging novel Middle East respiratory syndrome coronavirus: the "knowns" and "unknowns". *Journal of the Formosan Medical Association*, 112: 372 – 381.

Chiu, S.S., Hung Chan, K., Wing Chu, K., *et al.* 2005. Human coronavirus NL63 infection and other coronavirus infections in children hospitalized with acute respiratory disease in Hong Kong, China. *Clinical Infectious Diseases*, 40(12): 1721 – 1729.

Chu, D.K.W., Poon, L.L.M., Chan, K.H., *et al*. 2006. Coronaviruses in bent-winged bats (*Miniopterus* spp.). *Journal of General Virology*, 87: 2461 – 2466.

Coil, D.A. & Miller, A.D. 2004. Phosphatidylserine is not the cell surface receptor for vesicular stomatitis virus. *Journal of Virology*, 78(20): 10920 – 10926.

Coleman, C.M., & Frieman, M.B. 2014. Coronaviruses: important emerging human pathogens. *Journal of Virology*, 88(10): 5209 – 5212.

Corman, V.M., Ithete, N.L., Richards, L.R., *et al*. 2014. Rooting the phylogenetic tree of Middle East respiratory syndrome coronavirus by characterization of a conspecific virus from an African bat. *Journal of Virology*, 88(19): 11297 – 11303.

Corman, V.M., Baldwin, H.J., Tateno, A.F., *et al*. 2015. Evidence for an ancestral association of human coronavirus 229E with bats. *Journal of Virology*, 89(23): 11858 – 11870.

Cosset, F.-L., Marianneau, P., Verney, G., *et al*. 2009. Characterization of Lassa virus cell entry and neutralization with Lassa virus pseudoparticles. *Journal of Virology*, 83(7): 3228 – 3237.

Cotten, M., Watson, S.J., Kellam, P., *et al*. 2013. Transmission and evolution of the Middle East respiratory syndrome coronavirus in Saudi Arabia: a descriptive genomic study. *The Lancet*, 382(9909): 1993 – 2002.

Crameri, G., Todd, S., Grimley, S., *et al*. 2009. Establishment, immortalisation and characterisation of pteropid bat cell lines. *PLOS One*, 4(12): 1 – 9.

Cronin, J., Zhang, X.-Y. & Reiser, J. 2005. Altering the tropism of lentiviral vectors through pseudotyping. *Current Gene Therapy*, 5(4): 387 – 398.

Cronjé, N. 2017. The diversity of coronaviruses in southern African bat populations. Unpublished doctoral dissertation. Cape Town, Stellenbosch University.

Cui, J., Edene, J.S., Holmes, E.C. & Wang, L.F. 2013. Adaptive evolution of bat dipeptidyl peptidase 4 (dpp4): implications for the origin and emergence of Middle East respiratory syndrome coronavirus. *Virology Journal*, 10: 1 – 5.

Danilczyk, U., Eriksson, U., Oudit, G.Y. & Penninger, J.M. 2004. Physiological roles of angiotensin-converting enzyme 2. *Cellular and Molecular Life Sciences*, 61(21): 2714 – 2719.

Dato, V.M., Campagnolo, E.R., Long, J. & Rupprecht, C.E. 2016. A systematic review of human bat rabies virus variant cases: evaluating unprotected physical contact with claws and teeth in support of accurate risk assessments. *PLOS One*, 11(7): 1 – 13.

de Groot, R.J., Baker, S.C., Baric, R., *et al*. 2012. *Virus taxonomy: classification and nomenclature of viruses. Ninth report of the International Committee on Taxonomy of Viruses*. London: Academic Press.

de Groot, R.J., Baker, S.C., Baric, R.S., *et al*. 2013. Middle East Respiratory syndrome coronavirus (MERS-CoV): announcement of the coronavirus study group. *Journal of Virology*, 87(14): 7790 – 7792.

de Haan, C.A.M. & Rottier, P.J.M. 2005. Molecular interactions in the assembly of coronaviruses. *Advances in Virus Research*, 64: 165 – 230.

de Souza Luna, L.K., Heiser, V., Regamey, N., *et al*. 2007. Generic detection of coronaviruses and differentiation at the prototype strain level by reverse transcription-PCR and nonfluorescent low-density microarray. *Journal of Clinical Microbiology*, 45(3): 1049 – 1055.

de Wit, E. & Munster, V. 2013. MERS-CoV: the intermediate host identified? *The Lancet Infectious Diseases*, 13(10): 827 – 828.

Desjardins, D., Huret, C., Dalba, C., *et al*. 2009. Recombinant retrovirus-like particle forming DNA vaccines in prime-boost immunization and their use for hepatitis C virus vaccine development. *The Journal of Gene Medicine*, 11: 313 – 325.

Desmarets, L.M.B., Vermeulen, B.L., Theuns, S., *et al*. 2016. Experimental feline enteric coronavirus infection reveals an aberrant infection pattern and shedding of mutants with impaired infectivity in enterocytes cultures. *Scientific Reports*, 6: 1 – 11.

Dijkman, R., Jebbink, M.F., Koekkoek, S.M., *et al*. 2013. Isolation and characterization of current human coronavirus strains in primary human epithelia cultures reveals differences in target cell tropism. *Journal of Virology*, 87(11): 6081 – 6090.

Doyle,L.P. & Hutchings, L.M. 1946. A transmissible gastroenteritis in pigs. *Journal of the American Veterinary Medical Association,* 108: 257 – 259.

Drexler, J.F., Gloza-Rausch, F., Glende, J., *et al*. 2010. Genomic characterization of severe acute respiratory syndrome-related coronavirus in European bats and classification of coronaviruses based on partial RNA-dependent RNA polymerase gene sequences. *Journal of Virology*, 84(21): 11336 – 11349.

Drosten, C., Günther, S., Preiser, W., *et al.* 2003. Identification of a novel coronavirus in patients with severe acute respiratory syndrome. *The New England Journal of Medicine*, 348(20): 1967 – 1976.

Eckerle, I., Ehlen, L., Kallies, R., *et al*. 2013. Bat airway epithelial cells: a novel tool for the study of zoonotic viruses. *PLOS One*, 9(1): 1 – 9.

Eckerle, I., Corman, V.M., Müller, M.A., Lenk, M., Ulrich, R.G. & Drosten, C. 2014. Replicative capacity of MERS coronavirus in livestock cell lines. *Emerging Infectious Diseases*, 20(2): 276 – 279.

Erles, K., Toomey, C., Brooks, H.W. & Brownlie, J. 2003. Detection of a group 2 coronavirus in dogs with canine infectious respiratory disease. *Virology*, 310(2): 216 – 223.

Finkelshtein, D., Werman, A., Novick, D., Barak, S. & Rubinstein, M. 2013. LDL receptor and its family members serve as the cellular receptors for vesicular stomatitis virus. *Proceedings of the National Academy of Sciences of the United States of America*, 110(18): 7306 – 7311.

Fischer, W.B. & Sansom, M.S. 2002. Viral ion channels: structure and function. *Biochimica et Biophysica Acta*, 1561(1): 27 – 45.

Fisher, R. 2016. Next generation sequencing demonstrates minor variant HIV drug resistance mutations. Unpublished doctoral dissertation. Cape Town, Stellenbosch University.

Garrone, P., Fluckiger, A.-C., Mangeot, P.E., *et al*. 2011. A prime-boost strategy using virus-like particles pseudotyped for HCV proteins triggers broadly neutralizing antibodies in macaques. *Science Translational Medicine*, 3(94).

Ge, X.-Y., Li, J.-L., Yang, X.-L., *et al*. 2013. Isolation and characterization of a bat SARS-like coronavirus that uses the ACE2 receptor. *Nature*, 503(7477): 535 – 538.

Geldenhuys, M., Mortlock, M., Weyer, J., *et al*. 2018. A metagenomic viral discovery approach identifies potential zoonotic and novel mammalian viruses in *Neoromicia* bats within South Africa. *PLOS One*, 13(3): 1 – 27.

Giroglou, T., Cinatl, J.Jr., Rabenau, H., *et al*. 2004. Retroviral vectors pseudotyped with severe acute respiratory syndrome coronavirus S protein. *Journal of Virology*, 78(17): 9007 – 9015.

Giroud, C., Du, Y., Marin, M., *et al*. 2017. Screening and functional profiling of small-molecule HIV-1 entry and fusion inhibitors. *ASSAY and Drug Development Technologies*, 15(2): 53 – 63.

Gloza-Rausch, F., Ipsen, A., Seebens, A., *et al*. 2008. Detection and prevalence patterns of group I coronaviruses in bats, northern Germany. *Emerging Infectious Diseases*, 14(4): 626 – 631.

Gouilh, M.A., Puechmaille, S.J., Gonzalez, J.-P., Teeling, E., Kittayapong, P. & Manuguerra, J.-C. 2011. *SARS-coronavirus* ancestor's foot-prints in South-East Asian bat colonies and the refuge theory. *Infection, Genetics and Evolution*, 11: 1690 – 1702.

Govorkova, E.A., Murti, G., Meignier, B., de Taisne, C. & Webster, R.G. 1996. African green monkey kidney (Vero) cells provide an alternative host cell system for influenza A and B viruses. *Journal of Virology*, 70(8): 5519 – 5524.

Graham, R.L., Donaldson, E.F. & Baric, R.S. 2013. A decade after SARS: strategies for controlling emerging coronaviruses. *Nature Reviews Microbiology*, 11(12): 836 – 848.

Guan, Y., Zheng, B.J., He, Y.Q., *et al.* 2003. Isolation and characterization of viruses related to the SARS coronavirus from animals in southern China. *Science*, 302: 276 – 278.

Haagmans, B.L., Al Dhahiry, S.H.S., Reusken, C.B.E.M., *et al.* 2014. Middle East respiratory syndrome coronavirus in dromedary camels: an outbreak investigation. *The Lancet Infectious Diseases*, 14(2): 140 – 145.

Hamre, D. & Procknow, J.J. 1966. A new virus isolated from the human respiratory tract. *Proceedings of the Society for Experimental Biology and Medicine*, 121(1): 190 – 193.

Hanika, A., Larisch, B., Steinmann, E., Schwegmann-Weßels, C., Herrler, G. & Zimmer, G. 2005. Use of influenza C virus glycoprotein HEF for generation of vesicular stomatitis virus pseudotypes. *Journal of General Virology*, 86: 1455 – 1465.

Herrewegh, A.A., De Groot, R.J., Cepica, A., Egberink, H.F., Horzinek, M.C. & Rottier, P.J.M. 1995. Detection of feline coronavirus RNA in feces, tissues, and body fluids of naturally infected cats by reverse transcriptase PCR. *Journal of Clinical Microbiology*, 33(3): 684 – 689.

Hilgenfeld, R. & Peiris, M. 2013. From SARS to MERS: 10 years of research on highly pathogenic human coronaviruses. *Antiviral Research*, 100(1): 286 – 295.

Hoffmann, M., Müller, M.A., Drexler, J.F., *et al*. 2013. Differential sensitivity of bat cells to infection by enveloped RNA viruses: coronaviruses, paramyxoviruses, filoviruses, and influenza viruses. *PLOS One*, 8(8): 1 – 12.

Hoffmann, M. 2017. Question re pseudoparticles, e-mail to A. Kotzé & T. Suliman [Online]. Available e-mail: mhoffmann@dpz.eu.

Huynh, J., Li, S., Yount, B., *et al*. 2012. Evidence supporting a zoonotic origin of human coronavirus strain NL63. *Journal of Virology*, 86(23): 12816 – 12825.

Ithete, N.L. 2013. Investigation of small mammal-borne viruses with zoonotic potential in South Africa. Unpublished doctoral dissertation. Cape Town, Stellenbosch University.

Ithete, N.L., Stoffberg, S., Corman, V.M., *et al*. 2013. Close relative of human Middle East respiratory syndrome coronavirus in bat, South Africa. *Emerging Infectious Diseases*, 19(10): 1697 - 1699.

Kanwar, A., Selvaraju, S. & Esper, F. 2017. Human cronavirus-HKU1 infection among adults in Cleveland, Ohio. *Open Forum Infectious Diseases*, 4(2): 1 – 6.

Kennedy, D.A. & Johnson-Lussenburg, C.M. 1975. Isolation and morphology of the internal component of human coronavirus, strain 229E. *Intervirology*, 6: 197 – 206.

Kuhlmann, I. 1995. The prophylactic use of antibiotics in cell culture. *Cytotechnology*, 19(2): 95 – 105.

La Monica, N., Yokomori, K. & Lai, M.M. 1992. Coronavirus mRNA synthesis: identification of novel transcription initiation signals which are differentially regulated by different leader sequences. *Virology*, 188: 402 – 407.

Lai, M.M., Liao, C.L., Lin, Y.J. & Zhang, X. 1994. Coronavirus: how a large RNA viral genome is replicated and transcribed. *Infectious Agents in Disease*, 3: 98 – 105.

Lau, S.K.P., Woo, P.C.Y., Li, K.S.M., *et al.* 2005. Severe acute respiratory syndrome coronavirus-like virus in Chinese horseshoe bats. *Proceedings of the National Academy of Sciences of the United States of America*, 102(39): 14040 – 14045.

Lau, S.K.P., Fan, R.Y.Y., Luk, H.K.H, *et al.* 2018a. *Replication of MERS and SARS coronaviruses in bat cells offers insights to their ancestral origins* [Online]. Available: https://www.biorxiv.org/content/early/2018/05/20/326538 [2018, July 23].

Lau, S.K.P., Zhang, L., Luk, H.K.H., *et al*. 2018b. Receptor usage of a novel bat lineage C betacoronavirus reveals evolution of Middle East respiratory syndrome-related coronavirus spike proteins for human dipeptidyl peptidase 4 binding. *The Journal of Infectious Diseases*, 218(2): 197 – 207.

Lednicky, J.A. & Wyatt, D.E. 2012. The art of animal cell culture for virus isolation, in Ceccherini-Nelli, L. & Matteoli, B. (eds.). *Biomedical Tissue Culture*. London: IntechOpen Limited. 151 – 178.

Leroy, E.M., Epelboin, A., Mondonge, V., *et al*. 2009. Human Ebola outbreak resulting from direct exposure to fruit bats in Luebo, Democratic Republic of Congo, 2007. *Vector-Borne and Zoonotic Diseases*, 9(6): 723 – 728.

Li, W., Moore, M.J., Vasilieva, N., *et al*. 2003. Angiotensin-converting enzyme 2 is a functional receptor for the SARS coronavirus. *Nature*, 426: 450 – 454.

Li, W., Shi, Z., Yu, M., *et al.* 2005. Bats are natural reservoirs of SARS-like coronaviruses. *Science*, 310: 676 – 679.

Li, Q., Liu, Q., Huang, W., Li, X. & Wang, Y. 2017. Current status on the development of pseudoviruses for enveloped viruses. *Reviews in Medical Virology*, 28(1).

Lim, P.L., Kurup, A., Gopalakrishna, G., *et al*. 2004. Laboratory-acquired severe acute respiratory syndrome. *The New England Journal of Medicine*, 350(17): 1740 – 1745.

Machamer, C.E. & Youn, S. 2006. The transmembrane domain of the infectious bronchitis virus E protein is required for efficient virus release. *Advances in Experimental Medicine and Biology*, 581: 193 – 198.

Mackay, I.M. & Arden, K.E. 2015. Middle East respiratory syndrome: an emerging coronavirus infection tracked by the crowd. *Virus Research*, 202: 60 – 88.

Masters, P.S. 2006. The molecular biology of coronaviruses. *Advances in Virus Research*, 66: 193 – 292.

McIntosh, K., Becker, W.B. & Chanock, R.M. 1967. Growth in suckling-mouse brain of "IBV-like" viruses from patients with upper respiratory tract disease. *Proceedings of the National Academy of Sciences of the United States of America*, 58(6): 2268 – 2273.

Memish, Z.A., Mishra, N., Olival, K.J., *et al*. 2013. Middle East respiratory syndrome coronavirus in bats, Saudi Arabia. *Emerging Infectious Diseases*, 19(11): 1819 – 1823.

Meyer, B., García-Bocanegra, I., Wernery, U., *et al*. 2015. Serologic assessment of possibility for MERS-CoV infection in equids. *Emerging Infectious Diseases*, 21(1): 181 – 182.

Milne-Price, S., Miazgowicz, K.L. & Munster V.J. 2014. The emergence of the Middle East respiratory syndrome coronavirus. *Pathogens and Disease*, 71(2): 121 – 136.

Moratelli, R. & Calisher, C.H. 2015. Bats and zoonotic viruses: can we confidently link bats with emerging deadly viruses? *Memórias do Instituto Oswaldo Cruz*, 110(1): 1 – 22.

Moreno, A., Lelli, D., de Sabato, L., *et al*. 2017. Detection and full genome characterization of two beta CoV viruses related to Middle East respiratory syndrome from bats in Italy. *Virology Journal*, 14: 1 – 11.

Mortola, E. & Roy, P. 2004. Efficient assembly and release of SARS coronavirus-like particles by a heterologous expression system. *FEBS Letters*, 576(1-2): 174 – 178.

Mossel, E.C., Huang, C., Narayanan, K., Makino, S., Tesh, R.B. & Peters, C.J. 2005. Exogenous ACE2 expression allows refractory cell lines to support severe acute respiratory syndrome coronavirus replication. *Journal of Virology*, 79(6): 3846 – 3850.

Müller, M.A., Raj, V.S., Muth, D., *et al*. 2012. Human coronavirus EMC does not require the SARS-coronavirus receptor and maintains broad replicative capability in mammalian cell lines. *mBio*, 3(6): 1 – 5.

Nasci, R.S., Gottfried, K.L., Burkhalter, K.L., *et al*. 2002. Comparison of vero cell plaque assay, TaqMan reverse transcriptase polymerase chain reaction RNA assay, and VecTest antigen assay for detection of West Nile virus in field-collected mosquitoes. *Journal of the American Mosquito Control Association*, 18(4): 294 – 300.

Navas-Martín, S. & Weiss, S. R. 2004. Coronavirus replication and pathogenesis: implications for the recent outbreak of severe acute respiratory syndrome (SARS), and the challenge for vaccine development. *Journal of NeuroVirology*, 10(2): 75 – 85.

Nowotny, N. & Kolodziejek, J. 2014. Middle East respiratory syndrome coronavirus (MERS-CoV) in dromedary camels, Oman, 2013. *Eurosurveillance*, 19(16): 20781.

Otter, J.A., Donskey, C., Yezli, S., Douthwaite, S., Goldenberg, S.D. & Weber, D.J. 2016. Transmission of SARS and MERS coronaviruses and influenza virus in healthcare settings: the possible role of dry surface contamination. *Journal of Hospital Infection*, 92(3): 235 – 250.

Pacciarini, F., Chezzi, S., Canducci, F., *et al*. 2008. Persistent replication of severe acute respiratory syndrome coronavirus in human tubular kidney cells selects for adaptive mutations in the membrane protein. *Journal of Virology*, 82(11): 5137 – 5144.

Perera, R.A., Wang, P., Gomaa, M.R., *et al*. 2013. Seroepidemiology for MERS coronavirus using microneutralisation and pseudoparticle virus neutralisation assays reveal a high prevalence of antibody in dromedary camels in Egypt, June 2013. *Eurosurveillance*, 18(36): 20574.

Pernet, O., Schneider, B.S., Beaty, S.M., *et al*. 2014. Evidence for henipavirus spillover into human populations in Africa. *Nature Communications*, 5: 1 – 10.

Pfefferle, S., Oppong, S., Drexler, J.F., *et al*. 2009. Distant relatives of severe acute respiratory syndrome coronavirus and close relatives of human coronavirus 229E in bats, Ghana. *Emerging Infectious Diseases*, 15(9): 1377 – 1384.

Poon, L.L.M., Chu, D.K.W., Chan, K.H., *et al.* 2005. Identification of a novel coronavirus in bats. *Journal of Virology*, 79(4): 2001 – 2009.

Qiu, C., Huang, Y., Zhang, A., *et al*. 2013. Safe pseudovirus-based assay for neutralization antibodies against influenza A (H7N9) virus. *Emerging Infectious Diseases*, 19(10): 1685 – 1687.

Raamsman, M.J.B., Krijnse Locker, J., de Hooge, A., *et al*. 2000. Characterization of the coronavirus mouse hepatitis virus strain A59 small membrane protein E. *Journal of Virology*, 74: 2333 – 2342.

Raj, V.S., Mou, H., Smits, S.L., *et al*. 2013. Dipeptidyl peptidase 4 is a functional receptor for the emerging human coronavirus-EMC. *Nature*, 495: 251 – 256.

Raj, V.S., Osterhaus, A.D.M.E., Fouchier, R.A.M. & Haagmans, B.L. 2014. MERS: emergence of a novel human coronavirus. *Current Opinion in Virology*, 5: 58 – 62.

Reardon, A.J.F., Elliott, J.A.W. & McGann, L.E. 2014. Fluorescence as an alternative to light-scatter gating strategies to identify frozen–thawed cells with flow cytometry. *Cryobiology*, 69(1): 91 – 99.

Reusken, C.B.E.M., Haagmans, B.L., Müller, M.A., *et al.* 2013. Middle East respiratory syndrome coronavirus neutralising serum antibodies in dromedary camels: a comparative serological study. *The Lancet Infectious Diseases*, 13(10): 859 – 866.

Reusken, C.B.E.M., Raj, V.S., Koopmans, M.P. & Haagmans, B.L. 2016. Cross host transmission in the emergence of MERS coronavirus. *Current Opinion in Virology*, 16: 55 – 62.

Richards, G.P. & Weinheimer, D.A. 1985. Influence of adsorption time, rocking, and soluble proteins on the plaque assay of monodispersed poliovirus. *Applied and Environmental Microbiology*, 49(4): 744 – 748.

Rinaldo, C.R., Overall, J.C., Cole, B.C. & Glasgow, L.A. 1973. Mycoplasma-associated induction of interferon in ovine leukocytes. *Infection and Immunity*, 8(5): 796 – 803.

Rottem, S. & Barile, F. 1993. Beware of mycoplasmas. *Current Trends in Biotechnology and Pharmacy*, 11(4): 143 – 151.

Rottier, P.J.M., Nakamura, K., Schellen, P., Volders, H. & Haijema, B.J. 2005. Acquisition of macrophage tropism during the pathogenesis of feline infectious peritonitis is determined by mutations in the feline coronavirus spike protein. *Journal of Virology*, 79(22): 14122 – 14130.

Saif, L.J. & Heckert, R.A. 1990. Enteropathogenic coronaviruses, in L.J. Saif & K.W. Theil (eds.). *Viral diarrheas of man and animals*. Boca Raton: CRC Press Inc. 185 – 252.

Saiz-Baggetto, S., Méndez, E., Quilis, I., Igual, J.C. & Bañó, M.C. 2017. Chimeric proteins tagged with specific 3×HA cassettes may present instability and functional problems. *PLOS One*, 12(8): 1 – 12.

Schultz, A., Koch, S., Fuss, M., *et al*. 2012. An automated HIV-1 Env-pseudotyped virus production for global HIV vaccine trials. *PLOS One*, 7(12): 1 – 10.

Schwegmann-Wessels, C., Bauer, S., Winter, C., Enjuanes, L., Laude, H. & Herrler, G. 2011. The sialic acid binding activity of the S protein facilitates infection by porcine transmissible gastroenteritis coronavirus. *Virology Journal*, 8: 1 – 7.

Scully, C. & Samaranayake, L.P. 2016. Emerging and changing viral diseases in the new millennium. *Oral Diseases*, 22(3): 171 – 179.

Sharif, S., Arshad, S.S., Hair-Bejo, M., *et al*. 2011. Evaluation of feline coronavirus viraemia in clinically healthy and ill cats with feline infectious peritonitis. *Journal of Animal and Veterinary Advances*, 10(1): 18 – 22.

Shi, Z.-L., Guo, D. & Rottier, P.J.M. 2016. Coronavirus: epidemiology, genome replication and the interactions with their hosts. *Virologica Sinica*, 31(1): 1 – 2.

Shirato, K., Kawase, M. & Matsuyama, S. 2013. Middle East respiratory syndrome coronavirus (MERS-CoV) infection mediated by the transmembrane serine protease TMPRSS2. *Journal of Virology*, 87(23): 12552 – 12561.

Simmons, G., Reeves, J.D., Rennekamp, A.J., Amberg, S.M., Piefer, A.J. & Bates, P. 2004. Characterization of sever acute respiratory syndrome-associated coronavirus (SARS-CoV) spike glycoprotein-mediated viral entry. *Proceedings of the National Academy of Sciences of the United States of America*, 101(12): 4240 – 4245.

Smith, E.C. & Denison, M.R. 2012. Implications of altered replication fidelity on the evolution and pathogenesis of coronaviruses. *Current Opinion in Virology*, 2(5): 519 – 524.

Tang, X.C., Zhang, J.X., Zhang, S.Y., *et al*. 2006. Prevalence and genetic diversity of coronaviruses in bats from China. *Journal of Virology*, 80(15): 7481 – 7490.

Tani, H., Morikawa, S. & Matsuura, Y. 2012. Development and applications of VSV vectors based on cell tropism. *Frontiers in Microbiology*, 2: 1 – 7.

Terpe, K. 2003. Overview of tag protein fusions: from molecular and biochemical fundamentals to commercial systems. *Applied Microbiology and Biotechnology*, 60: 523 – 533.

The Oxford English Dictionary. 2018. Oxford: Oxford University Press.

Thermo Fisher Scientific. 2016. *Product information: Thermo Scientific InsTAclone PCR Cloning Kit, #K1213, #K1214*.

Tsunemitsu, H., El-Kanawati, Z.R., Smith, D.R., Reed, H.R. & Saif, L.J. 1995. Isolation of coronaviruses antigenically indistinguishable from bovine coronavirus from wild ruminants with diarrhea. *Journal of Clinical Microbiology*, 33(12): 3264 – 3269.

Uphoff, C.C. & Drexler, H.G. 2002a. Comparative PCR analysis for detection of Mycoplasma infections in continuous cell lines. *In Vitro Cellular & Developmental Biology – Animal*, 38: 79 – 85.

Uphoff, C.C. & Drexler, H.G. 2002b. Mycoplasma contamination of cell cultures: incidence, sources, effects, detection, elimination, prevention. *Cytotechnology*, 39(2): 75 – 90.

Uphoff, C.C. & Drexler, H.G. 2004. Detecting Mycoplasma contamination in cell cultures by polymerase chain reaction. *Methods in Molecular Medicine*, 88: 319 – 326.

Uphoff, C.C., Denkmann, S.-A. & Drexler, H.G. 2012. Treatment of Mycoplasma contamination in cell cultures with plasmocin. *Journal of Biomedicine and Biotechnology*, 2012: 1 – 8.

USAID. 2013. *Guide: implementing a cold chain for safe sample transport and storage* [Online]. Available: http://ibbea.fcen.uba.ar/wp-content/uploads/2017/05/Freezer_predict_guide_coldchain_22jul13.pdf [2018, July 20].

Vabret, A., Mourez, T., Gouarin, S., Petitjean, J. & Freymuth, F. 2003. An outbreak of coronavirus OC43 respiratory infection in Normandy, France. *Clinical Infectious Diseases*, 36(8): 985 – 989.

van den Brand, J.M.A., Smits, S.L. & Haagmans, B.L. 2015. Pathogenesis of Middle East respiratory syndrome coronavirus. *Journal of Pathology*, 235: 175 – 184.

van der Hoek, L., Pyrc, K., Jebbink, M.J., *et al.* 2004. Identification of a new human coronavirus. *Nature Medicine*, 10(4): 368 – 373.

Vlieger, G. & De Meester, I. 2018. DPPIV/CD26 as a target in anti-inflammatory therapy, in S. Chatterjee, W. Jungraithmayr & D. Bagchi (eds.). *Immunity and inflammation in health and*

disease: emerging roles of nutraceuticals and functional foods in immune support. Cambridge: Academic Press. 133 – 147.

Wang, P., Chen, J., Zheng, A., *et al*. 2004. Expression cloning of functional receptor used by SARS coronavirus. *Biochemical and Biophysical Research Communications*, 315: 439 – 444.

Wang, Q., Jianxun, Q., Yuan, Y., *et al*. 2014. Bat origins of MERS-CoV supported by bat coronavirus HKU4 usage of human receptor CD26. *Cell Host & Microbe*, 16(3): 328 – 337.

Wang, J., Deng, F., Ye, G., *et al*. 2016. Comparison of lentiviruses pseudotyped with S proteins from coronaviruses and cell tropisms of porcine coronaviruses. *Virologica Sinica*, 31(1): 49 – 56.

Wang, X., Dong, K., Long, M., *et al*. 2018. Induction of a high‐titered antibody response using HIV gag‐EV71 VP1‐based virus‐like particles with the capacity to protect newborn mice challenged with a lethal dose of enterovirus 71. *Archives of Virology*, 163(7): 1851 – 1861.

Warner, F.J., Lew, R.A., Smith, A.I., Lambert, D.W., Hooper, N.M. & Turner, A.J. 2005. Angiotensin-converting enzyme 2 (ACE2), but not ACE, is preferentially localized to the apical surface of polarized kidney cells. *The Journal of Biological Chemistry*, 280(47): 39353 – 39362.

Waugh, D.S. 2005. Making the most of affinity tags. *Trends in Biotechnology*, 23(6): 316 – 320.

Wei, H., Audet, J., Wong, G., *et al*. 2017. Deep-sequencing of Marburg virus genome during sequential mouse passaging and cell-culture adaptation reveals extensive changes over time. *Scientific Reports*, 7(1): 1 – 8.

Williams, B.H., Kiupel, M., West, K.H., Raymond, J.T., Grant, C.K. & Glickman, L.T. 2000. Coronavirus-associated epizootic catarrhal enteritis in ferrets. *Journal of the American Veterinary Medical Association*, 217(4): 526 – 530.

Wirth, M., Berthold, E., Grashoff, M., Pfützner, H., Schubert, U. & Hauser, H. 1994. Detection of mycoplasma contamination by the polymerase chain reaction. *Cytotechnology*, 16: 67 – 77.

Wise, A.G., Kiupel, M. & Maes, R.K. 2006. Molecular characterization of a novel coronavirus associated with epizootic catarrhal enteritis (ECE) in ferrets. *Virology*, 349(1): 164 – 174.

Woo, P.C.Y., Lau, S.K.P., Chu, C.-M., *et al.* 2005. Characterization and complete genome sequence of a novel coronavirus, coronavirus HKU1, from patients with pneumonia. *Journal of Virology*, 79(2): 884 – 895.

Woo, P.C.Y., Wang, M., Lau, S.K.P., *et al*. 2007. Comparative analysis of twelve genomes of three novel group 2c and group 2d coronaviruses reveals unique group and subgroup features. *Journal of Virology*, 81(4): 1574 – 1585.

Wool-Lewis, R.J. & Bates, P. 1998. Characterization of Ebola virus entry by using pseudotyped viruses: identification of receptor-deficient cell lines. *Journal of Virology*, 72(4): 3155 – 3160.

World Health Organization. 2003. *Severe acute respiratory syndrome (SARS) in Taiwan, China.* [Online]. Available: http://www.who.int/csr/don/2003_12_17/en/ [2018, August 16].

World Health Organization. 2018. *Middle East respiratory syndrome coronavirus (MERS-CoV)*. [Online]. Available: http://www.who.int/emergencies/mers-cov/en/ [2018, November 6].

Yang, Y., Du, L., Liu, C., *et al*. 2014. Receptor usage and cell entry of bat coronavirus HKU4 provide insight into bat-to-human transmission of MERS coronavirus. *Proceedings of the National Academy of Sciences of the United States of America*, 111(34): 12516 – 12521.

Yang, Z.-L., Hu, B., Wang, B., *et al*. 2016. Isolation and characterization of a novel bat coronavirus closely related to the direct progenitor of severe acute respiratory syndrome coronavirus. *Journal of Virology*, 90(6): 3253 – 3256.

Yuan, J., Hon, C.-C., Li, Y., *et al.* 2010. Intraspecies diversity of SARS-like coronaviruses in *Rhinolophus sinicus* and its implications for the origin of SARS coronaviruses in humans. *Journal of General Virology*, 91: 1058 – 1062.

Zaki, A.M., van Boheemen, S., Bestebroer, T.M., Osterhaus, A.D. & Fouchier, R.A. 2012. Isolation of a novel coronavirus from a man with pneumonia in Saudi Arabia. *The New England Journal of Medicine*. 367: 1814 – 1820.

ADDENDUM A
Ethical clearance

UNIVERSITEIT•STELLENBOSCH•UNIVERSITY
jou kennisvennoot • your knowledge partner

Protocol Approval

Date: 15-Jun-2016

PI Name: Ithete, Ndapewa L

Protocol #: SU-ACUD16-00008

Title: Investigation of novel bat-borne viruses with zoonotic potential in South Africa

Dear Ndapewa Ithete, the Notification, was reviewed on 06-Jun-2016 by the Research Ethics Committee: Animal Care and Use via committee review procedures and was approved. Please note that this clearance is only valid for a period of twelve months. Ethics clearance of protocols spanning more than one year must be renewed annually through submission of a progress report, up to a maximum of three years.

Applicants are reminded that they are expected to comply with accepted standards for the use of animals in research and teaching as reflected in the South African National Standards 10386: 2008. The SANS 10386: 2008 document is available on the Division for Research Developments website www.sun.ac.za/research.

As provided for in the Veterinary and Para-Veterinary Professions Act, 1982. It is the principal investigator's responsibility to ensure that all study participants are registered with or have been authorised by the South African Veterinary Council (SAVC) to perform the procedures on animals, or will be performing the procedures under the direct and continuous supervision of a SAVC-registered veterinary professional or SAVC-registered para-veterinary professional, who are acting within the scope of practice for their profession.

Please remember to use your protocol number, SU-ACUD16-00008 on any documents or correspondence with the REC: ACU concerning your research protocol.

Please note that the REC: ACU has the prerogative and authority to ask further questions, seek additional information, require further modifications or monitor the conduct of your research.

Any event not consistent with routine expected outcomes that results in any unexpected animal welfare issue (death, disease, or prolonged distress) or human health risks (zoonotic disease or exposure, injuries) must be reported to the committee, by creating an Adverse Event submission within the system.

We wish you the best as you conduct your research.

If you have any questions or need further help, please contact the REC: ACU secretariat at or .

Sincerely,

REC: ACU Secretariat

Research Ethics Committee: Animal Care and Us

ADDENDUM B

Consumables, equipment and software

Table B.1. List of consumables, equipment and software used in the current study.

Consumables			
Consumable	**Catalogue number**	**Company**	**Country**
1.5 ml microcentrifuge tube	0030 125.150	Eppendorf	Germany
2.0 ml microcentrifuge tube	0030 120.094	Eppendorf	Germany
2.4 mm RNase & DNase free metal beads	10032-370	Omni International	USA
10 µl low binding barrier pipette tips	89136-155	Corning Incorporated	USA
100 µl low binding barrier pipette tips	89136-159	Corning Incorporated	USA
1000 µl low binding barrier pipette tips	89136-165	Corning Incorporated	USA
0.2 ml PCR 8-strip tubes	404001	Nest Biotechnology Co., Ltd	China
15 ml centrifuge tubes	601002	Nest Biotechnology Co., Ltd	China
50 ml centrifuge tubes	602002	Nest Biotechnology Co., Ltd	China
100×15 mm Petri Dishes	753001	Nest Biotechnology Co., Ltd	China
Qubit assay tubes	Q32856	Thermo Fisher Scientific	USA
Hard-shell PCR plates	HSP9601	Bio-Rad Laboratories, Inc.	USA
25 cm² cell culture flasks	707003	Nest Biotechnology Co., Ltd	China
75 cm² cell culture flasks	708003	Nest Biotechnology Co., Ltd	China
175 cm² cell culture flasks	709003	Nest Biotechnology Co., Ltd	China
6-well cell culture plates	703001	Nest Biotechnology Co., Ltd	China
12-well cell culture plates	712001	Nest Biotechnology Co., Ltd	China
1 ml serological pipettes	324001	Nest Biotechnology Co., Ltd	China
2 ml serological pipettes	325001	Nest Biotechnology Co., Ltd	China
5 ml serological pipettes	326001	Nest Biotechnology Co., Ltd	China
10 ml serological pipettes	327001	Nest Biotechnology Co., Ltd	China

25 ml serological pipettes	328001	Nest Biotechnology Co., Ltd	China
50 ml serological pipettes	329001	Nest Biotechnology Co., Ltd	China
0.2 µm filter	CLS431218	Corning Incorporated	USA
2.0 ml cryogenic vials	607001	Nest Biotechnology Co., Ltd	China
Labstar Frosted Microscope Slides	1000F-02-1009	Lasec SA	South Africa
16 mm Microscope Coverslips, round	0111560	Paul Marienfeld GmbH & Co. KG	Germany
5.0 ml polystyrene round-bottomed tube	352054	Corning Incorporated	USA
BD CS&T Beads	656505	BD Biosciences	USA
Equipment			
Equipment	**Catalogue number**	**Company**	**Country**
D380 fridge	D380	Defy Appliances	South Africa
EvoSafe Model VF360-86 Ultra Low Temperature Upright Freezer	VF360-86	Snijders Labs	The Netherlands
BioFlow II biological safety cabinet	N/A	Labotec	South Africa
10 µl pipette	3124000016	Eppendorf	Germany
100 µl pipette	3124000075	Eppendorf	Germany
1000 µl pipette	3124000121	Eppendorf	Germany
TissueLyser LT	69980	Qiagen	Germany
Prism microcentrifuge	C2500	Labnet International, Inc.	USA
AccuBlock digital dry bath	D1200	Labnet International, Inc.	USA
GeneAmp PCR System 9700	A24811	Thermo Fisher Scientific	USA
ENDURO Gel XL Electrophoresis System	E0160	Labnet International, Inc.	USA
UVITec Gel Documentation System	1541 3202 1	Progen Scientific	UK
NanoDrop ND-1000 Spectrophotometer V3.1	N/A	NanoDrop Technologies, Inc.	USA
Mr. Frosty Freezing Container	5100-0001	Thermo Fisher Scientific	USA
Vortex mixer	S0200	Labnet International, Inc.	USA
Shaking Incubator Model 3081U	3081U	Labcon	USA
Megafuge 2.0R	75003085	Heraeus	Germany
Qubit 2.0 Fluorometer	Q32866	Thermo Fisher Scientific	USA
CFX Connect Real-Time	185-5200	Bio-Rad Laboratories,	USA

PCR Detection System		Inc.	
MPS 1000 Mini Plate Spinner Centrifuge	C1000	Labnet International, Inc.	USA
US Autoflow Automatic CO_2 Incubator	N/A	NuAire, Inc.	USA
FastPette Pro Pipette Controller	P2002	Labnet International, Inc.	USA
Primovert Inverted Microscope	12-070-466	Carl Zeiss AG	Germany
Haemocytometer	N/A	N/A	N/A
ProBlot 25 Rocker	470126-522	Labnet International, Inc.	USA
BD FACSCanto II flow cytometer	640806	BD Biosciences	USA
Eclipse Ci microscope	N/A	Nikon	Japan

Software

Software	**Company**	**Country**
UVIproChemi software	Progen Scientific	UK
ND-1000 V3.1.0 software	NanoDrop Technologies, Inc.	USA
Geneious R10 bioinformatics software	Biomatters Ltd.	New Zealand
CFX Manager Software	Bio-Rad Laboratories, Inc.	USA
ZEN software	Carl Zeiss AG	Germany
FlowJo version 10.4.2	FlowJo, LLC	USA
Sperm Class Analyzer software	MICROPTIC S.L.	Spain
BD FACSDiva software	BD Biosciences	USA

ADDENDUM C

Sample information

Table C.1. Bat faecal sample information.

Sample number	Sample name	Bat species collected from	Date of collection
1	DC338	*Neoromicia capensis*	05/02/2017
2	DC339	*Neoromicia capensis*	06/02/2017
3	DC340	*Neoromicia capensis*	06/02/2017
4	DC341	*Neoromicia capensis*	06/02/2017
5	DC343	*Pipistrellus hesperidus*	06/02/2017
6	DC345	*Neoromicia capensis*	06/02/2017
7	DC346	*Neoromicia capensis*	06/02/2017
8	DC364	*Myotis tricolor*	08/02/2017
9	DC365	*Myotis tricolor*	08/02/2017
10	DC366	*Rhinolophus clivosus*	08/02/2017
11	DC367	*Rhinolophus clivosus*	08/02/2017
12	DC370	*Rhinolophus clivosus*	08/02/2017
13	DC373	*Rhinolophus clivosus*	08/02/2017
14	DC378	*Miniopterus natalensis*	08/02/2017
15	DC392	*Pipistrellus hesperidus*	08/02/2017
16	DC422	*Neoromicia capensis*	12/02/2017
17	DC427	*Neoromicia capensis*	12/02/2017
18	DC431	*Neoromicia capensis*	12/02/2017
19	DC432	*Neoromicia capensis*	12/02/2017
20	DC433	*Neoromicia capensis*	12/02/2017
21	DC435	*Neoromicia capensis*	13/02/2017
22	DC445	*Rhinolophus capensis*	13/02/2017
23	DC467	*Neoromicia capensis*	15/02/2017
24	DC626	*Pipistrellus hesperidus*	06/05/2017
25	DC627	*Myotis bocagii*	09/05/2017

26	DC629	*Pipistrellus hesperidus*	09/05/2017
27	DC632	*Pipistrellus hesperidus*	09/05/2017
28	DC633	*Pipistrellus hesperidus*	09/05/2017
29	DC634	*Pipistrellus hesperidus*	09/05/2017
30	DC638	*Pipistrellus hesperidus*	10/05/2017

ADDENDUM D

Cell culture images

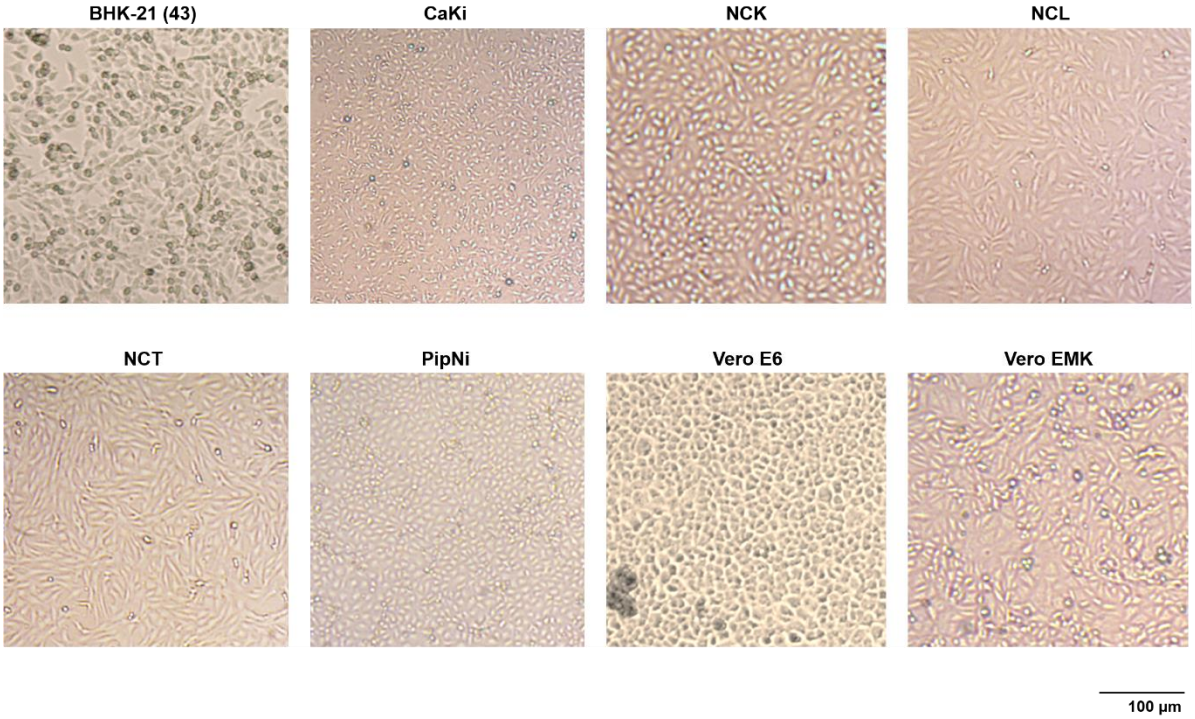

Figure D.1. Cultures of the cell lines used in this study. Culture images were captured at 40^{x} magnification. Bar = 100 µm.

ADDENDUM E

Flow cytometry graphs

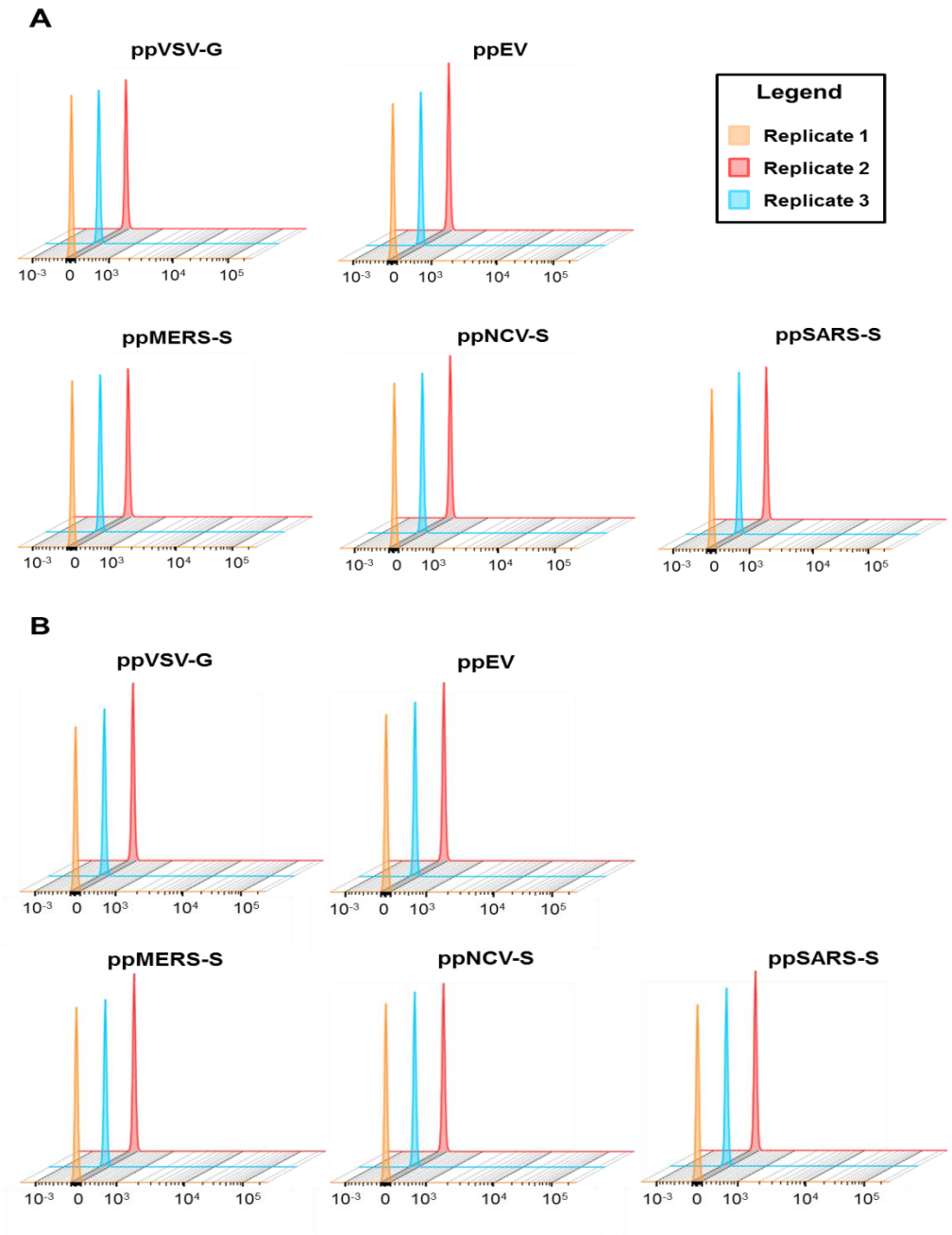

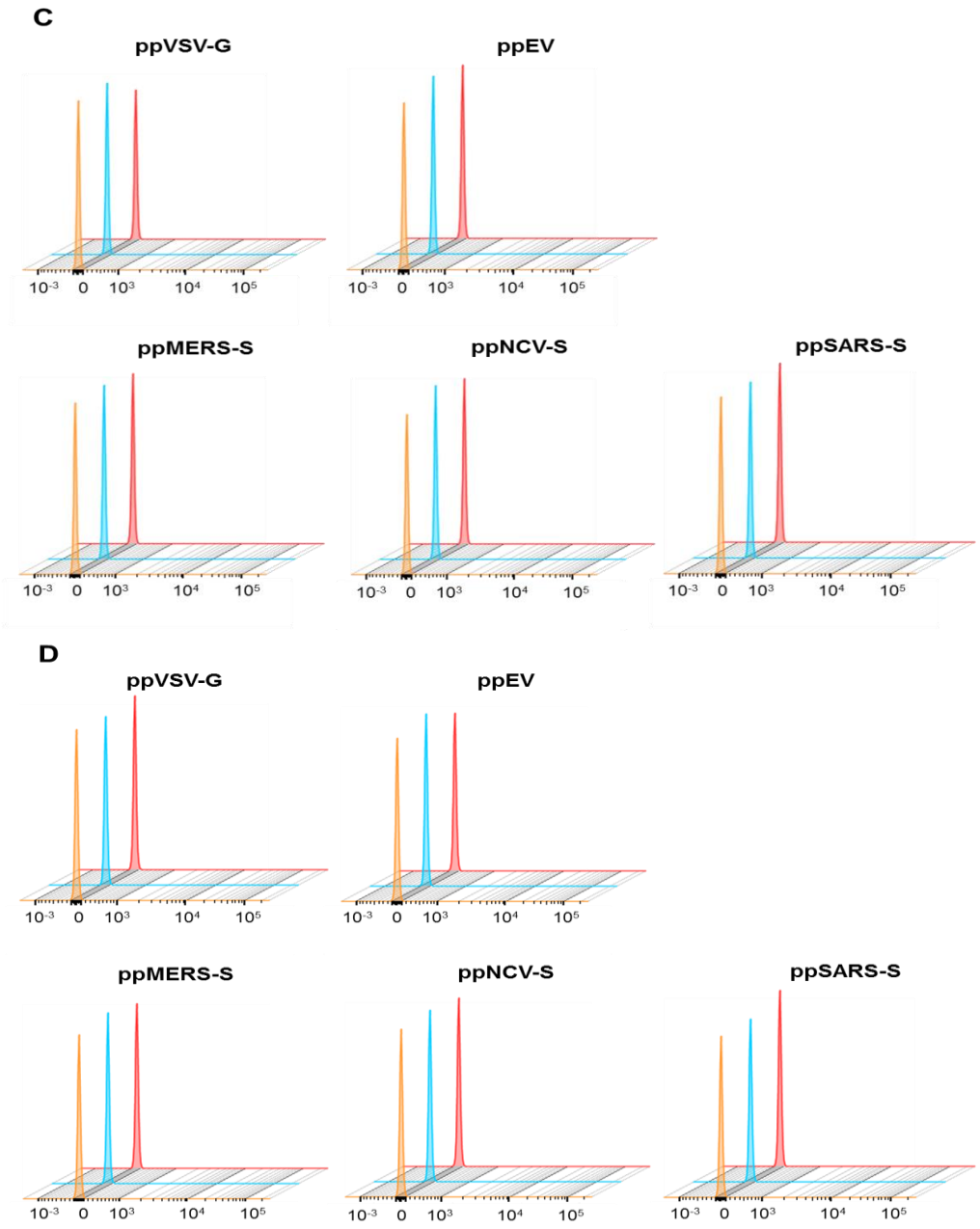

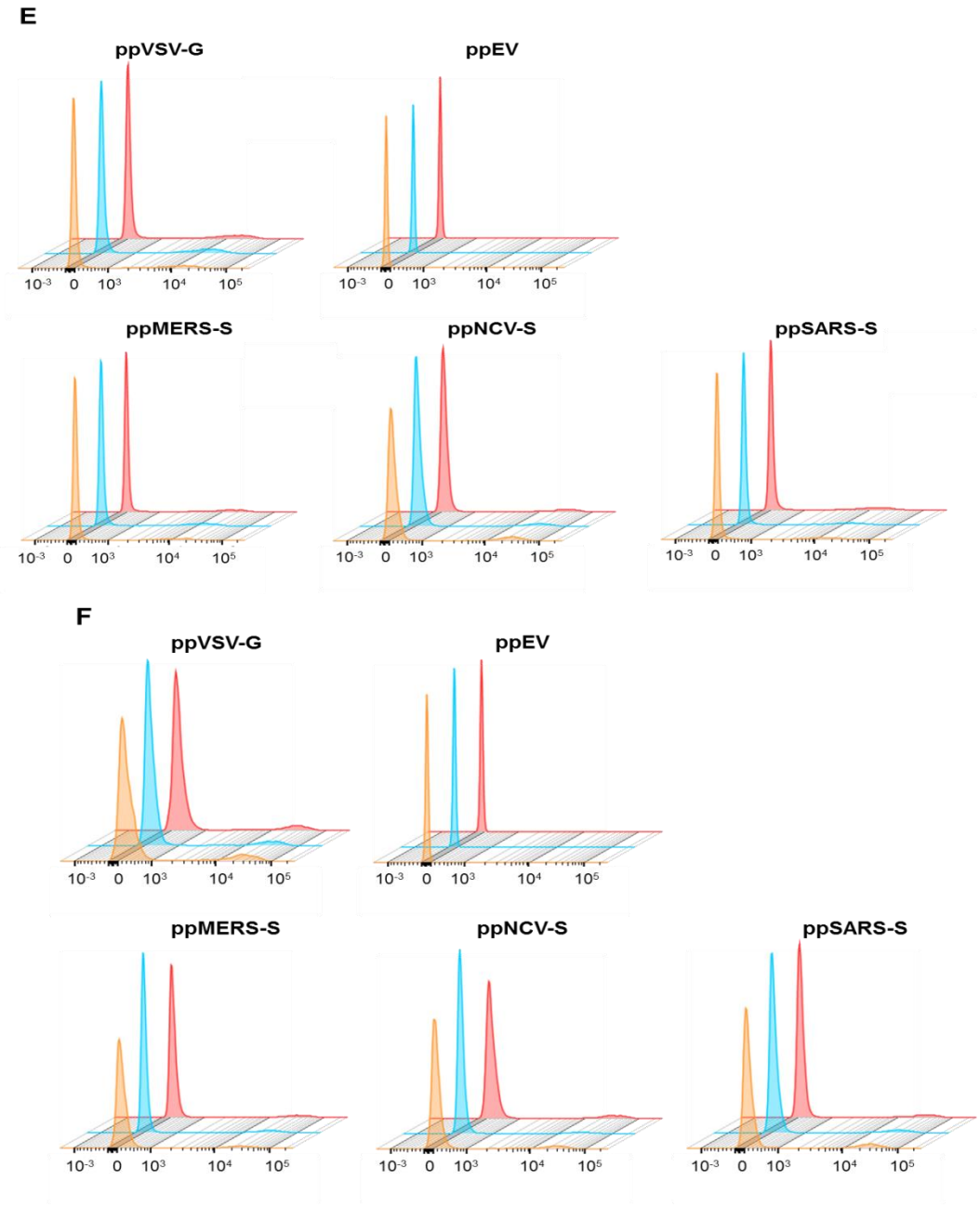

Figure E.1. GFP expression measured through flow cytometry. A) Expression in infected CaKi cells. **B)** Expression in infected NCL cells. **C)** Expression in infected NCT cells. **D)** Expression in infected PipNi cells. **E)** Expression in infected Vero E6 cells. **F)** Expression in infected Vero EMK cells. Each graph shows the GFP measured per pseudoparticle, which was done in triplicate, therefore yielding three graphs per pseudoparticle. The first peak for each sample shows the cells that do not express GFP, with the smaller peaks (if present) showing the number of GFP expressing cells. The number of events is indicated on the y-axis, while the GFP fluorescence intensity is indicated on the x-axis.